UNIVERSITY OF CALIFORNIA,
IRVINE

Transcriptional requirements of ectoderm specification and the master regulatory roles of maternal Foxi2 and Sox3

DISSERTATION

Submitted in partial satisfaction of the requirements

for the degree of

DOCTOR OF PHILOSOPHY

in Biological Sciences

by

Clark Lee Hendrickson

Dissertation Committee:
Professor Ken W.Y. Cho, Chair
Professor Tom Schilling
Professor Max Plikus
Assistant Professor Katrine Whiteson
Assistant Professor Evgeny Kvon

2025

DEDICATION

To

My parents Mark and Karin, my grandparents, Karl and Elizabeth, and my uncle Karl for always supporting me in achieving my dreams.

TABLE OF CONTENTS

LIST OF FIGURES

ACKNOWLEDGEMENTS

I would first and foremost like to sincerely thank Dr. Ken Cho for giving me the opportunity to work in his lab. Dr. Cho always supported and guided me when I needed him, but also gave me the space to explore things intellectually on my own. From the day I said I was interested in single cell sequencing, he worked extremely hard, persevering to make sure that in the end we would get data despite the tribulations we met. Importantly, Dr. Cho always met me with a good attitude and a light heart, he always reassured me when I needed it and never let me stay down on myself. I deeply appreciate our friendship and I could not be the scientist I dreamed of being without your care and guidance. Thank you for believing in me and providing me the platform to reach intellectual adulthood.

To members of the Cho Lab: I am also grateful to Dr. Ira Blitz for his instrumental mentorship on technical experimentation in frog embryos. Over the last six years we have had the most remarkable discussions about science, and you have challenged my ideas more than anyone. I appreciate our brain dance and how you pushed me to justify my scientific analyses and conclusions. Without your technical expertise several integral experiments of this dissertation would not have been possible. Thank you for your mentorship and contribution to this work, I can't imagine achieving this without you. To Dr. Jeff Zhou and Dr. Paula Pham, I thank you for your support in the early years of my Ph.D., you were both very kind and encouraging. I appreciate how much you cared about me, and rooted for me to do well during uncertain times.

To my committee, Dr. Evgeny Kvon, Dr. Tom Schilling, Dr. Max Plikus and Dr. Katrine Whiteson, thank you so much for giving me your time and support over the years. I appreciate that you always had my best interest at heart and that you held me accountable to achieve my goals. Without Dr. Whiteson taking a chance and giving me my first research opportunity eight years ago, there is a high likelihood that I would never have realized my passion for research or high throughput sequencing analysis. You always had such an amazing attitude about science, were such a nice friend to me, and were the first person to grant me the freedom to pursue my research interests hunting phage. I didn't know at the time, but joining your lab changed my life forever.

I would also like to thank my family and friends for their unwavering love and support over the years. Only through my parents, Karin and Mark, continual support, I have been able to complete this graduate school work. To my friends Fred, Kevin, Kyle, Lucas, Chase, Spencer, and Mike, with whom I share the electronic battlefield, thank you for being a part of my life for the last several years. Our Sunday congregations and guild events helped me stay balanced and motivated through tough times. And to my brother of the disc, Patrick, thank you for bringing love for the beauty of movement back into my life. You helped remove the unbearable weight of an eight year sports depression, and I cannot truly express how much it means to me.

VITA

Clark Lee Hendrickson

Education

2012-2016 A.A., Biology, A.A. Chemistry, A.A. Mathematics and Natural Sciences, A.A. Social and Behavioral Sciences, Irvine Valley College

2016-2018 B.S., Molecular Biology and Biochemistry, University of California, Irvine

2019-2023 M.S., Biological Sciences, University of California, Irvine, Project: Foxi2 and Sox3 control ectoderm specification

2023-2025 Ph.D., Biological Sciences, University of California, Irvine, Dissertation: Transcriptional requirements for ectoderm specification and the master regulatory roles of Foxi2 and Sox3

Publications

Hendrickson CL, Blitz IL, Cho KWY. Transcriptional requirements for ectoderm specification during gastrulation and the role of maternal Foxi2 (Manuscript in progress)

Cho J*, **Hendrickson CL*,** Mar N*, Blitz IL, Cho KWY. Foxh1- Ezh2 complex controls spatial patterning of H3K27me3 deposition during zygotic genome activation (Manuscript in progress)

Hendrickson CL, Blitz IL, Hussein A, Paraiso KD, Cho J, Klymkowsky MW, Kofron MJ, Cho KWY. Foxi2 and Sox3 are master regulators controlling ectoderm germ layer specification. bioRxiv [Preprint]. 2025 Jan 9:2025.01.09.632114. doi: 10.1101/2025.01.09.632114.

Wandro S, Ghatbale P, Attai H, **Hendrickson C**, Samillano C, Suh J, Dunham SJB, Pride DT, Whiteson K. Phage Cocktails Constrain the Growth of Enterococcus. mSystems. 2022 Aug 30;7(4):e0001922. doi: 10.1128/msystems.00019-22.

Oliver A, Chase AB, Weihe C, Orchanian SB, Riedel SF, **Hendrickson CL**, Lay M, Sewall JM, Martiny JBH, Whiteson K. High-Fiber, Whole-Food Dietary Intervention Alters the Human Gut Microbiome but Not Fecal Short-Chain Fatty Acids. mSystems. 2021 Mar 16;6(2):e00115-21. doi: 10.1128/mSystems.00115-21

Gallagher T, Phan J, Oliver A, Chase AB, England WE, Wandro S, **Hendrickson C**, Riedel SF, Whiteson K. Cystic Fibrosis-Associated Stenotrophomonas maltophilia Strain-Specific Adaptations and Responses to pH. J Bacteriol. 2019 Mar 13;201(7):e00478-18. doi: 10.1128/JB.00478-18.

Fellowships & Awards

Graduate Assistance in Areas of National Need (GAANN) Teaching Fellowship, University of California, Irvine, 2022-2024

Developmental and Cell Biology Teaching Excellence Award, University of California, Irvine, 2022

Dean's Award for Excellence in Undergraduate Research, University of California, Irvine, 2018

Summer Undergraduate Research Program Grant, University of California, Irvine, 2017

Undergraduate Research Opportunities Program Grant, University of California, Irvine, 2017

Presentations

Systems Biology Short Course - Single Cell Analysis in *Xenopus*, University of California, Irvine, 2022-2024

Maternal Foxi2 and Sox3 control ectoderm gene programming, 83rd Annual Meeting for the Society of Developmental Biology, July 14-17th, 2024

Maternal Foxi2 and Sox3 coordinate ectoderm gene activation, 19th International *Xenopus* Conference, August 20-24, 2023

ABSTRACT OF THE DISSERTATION

Transcriptional requirements of ectoderm specification and

the master regulatory roles of maternal Foxi2 and Sox3

by

Clark Lee Hendrickson

Doctor of Philosophy in Biological Sciences

University of California, Irvine, 2025

Professor Ken W.Y. Cho, Chair

An integral feature of early metazoan development is primary germ layer specification, reliant upon coordinated transcription factor (TF) interactions forming an epigenetic landscape permissible for transcription activation. Localized maternal TFs recruit epigenetic writers at germ layer specific cis-regulatory modules (CRMs) which deposit post-translational histone modifications to regulate lineage marker gene expression. However, the TF based gene regulatory network interactions and epigenetic state governing the specification of ectoderm remain a critical unanswered question. Foxi2 and Sox3 are maternal TFs enriched within the presumptive ectoderm to activate early marker genes implicated in ionocyte and neural development. While work demonstrates Sox3 and Pou factor cooperation during ectoderm formation, the potentially ancient relationship between the conserved Foxi and SoxB factors is unknown. Additionally, the relationship between Foxi2, Sox3 and the establishment of the ectodermal epigenetic state is not understood. Therefore, we sought to characterize the coordinated and independent roles of Foxi2 and Sox3 for gastrulation ectoderm lineage specification using high resolution sequencing and multiomic integration.

Here, I have utilized chromatin immunoprecipitation (ChIP) coupled with deep RNA

sequencing to investigate the coordinated roles of Foxi2 and Sox3 in directly regulating target gene expression during the onset of gastrulation. I identified both neural and non-neural ectoderm markers as direct gene targets for both factors jointly, as well as independently. High resolution single nucleus (sn) RNA sequencing was used to characterize inner and outer layer ectodermal cell states, demonstrating Foxi2 and Sox3 role as coordinated pan-ectodermal activators. Investigating the timing of epigenetic deposition reveals that Foxi2 and Sox3 pre-occupy ectoderm CRMs before zygotic genome activation (ZGA) and are required for recruitment of the epigenetic writer Ep300 within the ectoderm, but not endoderm. Foxi2, Sox3 and Ep300 bound CRMs become enriched with H3K27ac post-translational histone modifications, forming ectoderm specific super enhancers (SEs). Compared to other enhancers, Foxi2-Sox3 SEs facilitate increased gene expression and decreased covariation of expression of developmentally relevant ectoderm genes.

Further, through temporal snRNAseq, all ectodermal cell states arising during gastrulation were annotated. The inner and outer ectoderm was found to maintain transcriptional segregation from the early gastrula. Transcription factors defining lineage specific trajectories from the neural plate, neural plate border, as well as the inner and outer non-neural ectoderm were characterized. Temporal transcription factor expression delineated antero-posterior pre-placodal region and neural crest cell states during gastrulation. Bulk epigenetic signatures and motif presence were leveraged to build an ionocyte TF regulatory network. Finally, maternal Foxi2 knockdown was utilized in tandem with snRNAseq to reveal its control over non-neuroectoderm progenitor formation, pre-placodal region specification and the inhibition of ectopic ciliogenic signaling.

These findings indicate complex master regulatory roles of Foxi2 and Sox3 during early ectoderm specification. Both maternal factors are orientated atop the ectodermal gene programming hierarchy where they are required to establish an ectoderm specific epigenetic signature. Additionally, the temporal trajectories are useful for understanding the timing of

previously unresolved ectoderm progenitor formation and delineating models of pre-placodal and neural crest specification. Finally, the snRNAseq of Foxi2 knockdown embryos represents the first investigation of maternal TF control over gene expression at the level of a single cell, or nucleus. As Foxi and SoxB factors are deeply conserved among vertebrates, the findings presented here are impactful for discussions of embryogenesis, stem cell and ectoderm biology.

Chapter 1: Introduction

All life begins from a single-cell. Although complex organisms contain trillions of cells with diverse functions, the degree that cells have acquired specialized function inversely correlates with their ability to form new cell-types. Metazoans unify sperm and egg which are reprogrammed to form a transient totipotent cell capable of differentiating into the primary germ layers and their sub-lineages. This begs the questions; what are the initial cellular components required to form heterogeneous cell states with specialized function? And what are the cellular constraints for the timing of fate specification? Characterizing these features of early development can not only provide fundamental insights of transcription and the chromatin architecture requirements for differentiation but also help in understanding developmental diseases and organoid development.

While sperm primarily contains paternal genetic material, the egg houses additional maternal cellular components including transcription factors (TFs). In this way, the mother provides the initial regulatory environment that interacts with and reprograms the zygotic genome (Kojima et al., 2025). Incredibly, the maternal contribution is not just sufficient to reprogram zygotic nuclei. Gurdon's nuclear transplantation experiments demonstrate that maternal factors are also robust enough to reprogram fully differentiated somatic nuclei into a totipotent state (Gurdon 1958). The maternal TF initiated reprogramming and subsequent activation of zygotic gene expression is highly conserved and required for early development. This process is called the maternal to zygotic transition (MZT).

After fertilization, but before zygotic transcription, maternally deposited TF RNA becomes translated and imported into the nucleus (Nguyen et al., 2022). These maternal pioneer factors initially bind the genome and interface with epigenetic writers to induce

chromatin architecture changes, which initiate zygotic genome activation (ZGA) to facilitate germ layer specification (Zhang et al., 2022, Hu et al., 2024, Paraiso et al., 2019, 2020). Although ZGA is conserved across metazoans, its timing and the immediate environment of the zygote are not. Because of this, maternal factor asymmetries and contributions to the timing of germ layer formation vary especially between primitive metazoans and placental vertebrates. While more primitive metazoans contain asymmetrically distributed maternal TFs which specify ectoderm cell fate, placental vertebrates do not. Studying early embryogenesis in placental vertebrates poses issues because of their small size, slow internal development and low fecundity. *Xenopus tropicalis* is a non-eutherian metazoan model organism with optimal developmental characteristics to study the role of maternal TFs and cell state specification during embryogenesis. In *Xenopus*, maternal TFs are asymmetrically distributed within the egg cytoplasm (Sindelka et al., 2018). After fertilization, through cleavage divisions, these maternal factors become compartmentalized into different regions of the developing embryo. Due to this process, unique maternal factor combinations facilitate ZGA programs which specify the formation of the primary germ layers, the ectoderm, mesoderm and endoderm.

Xenopus embryos develop quickly and externally in cohorts of hundreds to thousands of siblings which are large enough to be regionally dissected. High-throughput sequencing (HTS) approaches are available to examine the direct targets of maternal TFs, the deposition of epigenetic landscape, and zygotic gene expression at the single cell level. To date, *Xenopus* research has generated the most comprehensive hierarchical maternal TF networks governing the emergence of zygotic gene regulatory networks that facilitate germ layer specification (Charney et al., 2017, Jansen et al., 2022). Additionally, *Xenopus* was the first model organism to be temporally sequenced through embryogenesis at the single cell level, providing high resolution to the earliest cell fate bifurcations. Due to these features, *Xenopus* is an ideal system to study the maternal contribution to ectoderm formation and zygotic transcription

controlling cell-type emergence during gastrulation.

Ectoderm dysplasia represents a group of more than 200 genetic disorders which originate from abnormal development of the embryonic ectoderm (Deshmukh et al., 2012, Itin 2014). Craniofacial abnormalities like cleft lip and craniosynostosis are relatively common birth defects (Schmetz et al., 2021). While congenital brain malformations are rarer, they are also more phenotypically damaging (Sarma & Pruthi 2022). Therefore, it's crucial to understand the maternal TF inputs and zygotic gene expression controlling embryonic ectoderm formation. The Fox (Forkhead box) and Sox (SRY-related HMG-box) families of maternal TFs are anciently conserved in embryonic ectoderm formation. While there are numerous Fox and Sox family proteins, I will focus on the FoxI and SoxB subclasses, predominantly expressed within animal cranial placode ectoderm and the neuroectoderm. In this chapter, I review maternal Fox and Sox transcription factor roles in ectoderm specification, the establishment of the metazoan epigenetic state, and insights into current HTS technologies used to detect transcriptional signatures during primordial cell-state emergence.

The Fox (Forkhead box) family of transcription factors

Fox TFs were discovered in *Drosophila* when a cloned novel homeotic gene was found to be expressed in the nucleus of cells in the embryo's anterior and posterior terminal regions (Weigel et al., 1989). Although not maternal, this originally discovered Forkhead box class A gene, Fkh (Foxa1), is expressed during early development in the syncytial blastoderm throughout gastrulation. Fkh expression is required for proper head fold involution and formation of both ectoderm derived fore- and hindgut. As the sequence of Fkh DNA binding domain did not match other known homeotic regulators, these results revealed a new class of transcription factors essential to, but uncharacterized in, metazoan development. All Fox TFs contain a winged helix forkhead domain capable of physically recognizing the Fox motif to control target gene

expression. Human FOXA1 crystal structure reveals its ability to bind the Fox motif in the major groove and interact with ancillary TF binding partners (Choi et al., 2022, Zhou et al., 2024). Notably, both FoxA1 and Foxi1 can function as “bookmarking” pioneer factors, capable of opening closed chromatin, and staying bound through mitotic division (Yan et al., 2005, Caravaca et al., 2013). Continued research since the landmark paper has demonstrated the ancient conservation of Forkhead box transcription factors throughout eukaryotic evolution.

Monosiga brevicollis and *Salpingoeca rosetta* are single-celled protozoan choanoflagellates which represent the closest living metazoan relatives expressing Fox family members, FoxJ and FoxN. Recent work in *Salpingoeca rosetta* has shown Foxj1 and Rfx are required for ciliogenesis gene expression and cilia formation (Coyle et al 2023). In the invertebrate *Owenia fusiformis*, Foxj1 is maternally expressed and localized to cells forming the ciliated band, while in vertebrates it is not endowed maternally. In frogs Foxj1 and Rfx2 were found to bind chromatin loops which enable multiciliated gene expression (Quigley & Kintner 2017). In humans, heterozygous *de novo* FOXJ1 mutations can cause motile ciliopathy, resulting in hydrocephalus internus, chronic destructive airway disease and L/R body axis randomization (Wallmeier et al., 2019). These data reveal that Foxj1 is linked to the emergence of cilia and its formation across single-celled eukaryotes, pre-bilaterians, invertebrates and vertebrates (Newton et al., 2012, Vij et al., 2012). As the oldest and most deeply conserved Fox transcription factor, Foxj1 highlights the important Fox family role in eukaryotic evolution. However, Foxj1 represents only a single TF from 1 of the 22 Forkhead box TF families, which arose during evolution to support the differentiation of many eukaryotic structures (Mazet et al., 2003, Larroux et al., 2009, Shimeld et al., 2010).

Phylogenetic genomic analysis of the primitive pre-bilaterian lineages demonstrates choanoflagellates express just 2 (FoxJ, N), while porifera (*Amphimedon queenslandica*) express 8 (FoxD,G,L,J,K,N,O,P), and cnidaria (*Nematostella vectensis*) express 15

(FoxA,B,C,D,E,F,G,L,Q,J,K,M,N,O,P), different Fox families classes of transcription factors (Shimeld et al., 2010). This demonstrates that the number of pre-bilaterian Fox family classes expanded rapidly according to increasing cell type and body plan complexity. Bilaterian, and especially chordate, evolution coincides with the expression of just 2 additional families (FoxH and I). Fox family TFs are involved in formation of the digestive (FoxA), nervous (FoxG), cardiovascular (FoxC), immune (FoxP) systems, as well as sensory organ progenitor (FoxI) formation and muscle differentiation (FoxO,M), among others. Even within bilateria, deuterostomes uniquely express the FoxH and I families compared to protostomes (ecdysozoans and most lophotrochozoans) (Mazet et al., 2003, Larroux et al., 2008, Schimeld et al., 2010). In particular, the FoxI family was originally reported in *Xenopus laevis* (vertebrate) and has only been found in a single protostome, spiralia *C. teleta*, presumably a close relative of the ancestral FoxI before its expansion in deuterostomia (Yang et al., 2014). The first FoxI studies in *Xenopus* identified three FoxI family homologues, Foxi1, Foxi2 and Foxi3. These FoxI family members were found to be locally expressed within the ectoderm during early development and later in either ionocytes or posterior derivatives of the pre-placodal ectoderm including the epibranchial and otic domains (Lef et al., 1994, Scheucher et al., 1995, Pohl et al., 2002, Suri et al., 2005).

The evolutionary significance of FoxI family TFs

The most primitive deuterostomes which express FoxI factors are *Stronglyocentrotus purpuratus* (echinoderm) and *Saccoglossus kowalevskii* (hemichordate) (Tu et al., 2006, Fritzenwalker et al., 2014). However, in stark contrast to vertebrates, neither of these more primitive deuterostomes, nor protostomes, develop cranial placodes as embryos. Connected through the wiring of the vertebrate central nervous system, cranial placode evolution helped establish the most complex neurosensory system found in the animal kingdom. During early

development, the pre-placodal region originates from ectodermal thickenings of the non-neural ectoderm surrounding the neural plate border. Over time, this pre-placodal region antero-posteriorly segregates into adenohypophyseal, olfactory, lens, otic and epibranchial placode progenitor domains (Saint-Jeannet & Moody 2014). More primitive deuterostome clades, like echinoderms and hemichordates, lack bonafide cranial placodes and complex anterior sensory organs. However, their FoxI factor expression lends clues as to how features of cranial placode evolution may have been co-opted in vertebrates.

In *S. kowalevskii* (hemichordate), but not *S. purpuratus* (echinoderm), FoxI expression is localized to the gill bud, a primitive placodal-like structure, and continues in a region near the center of the pharyngeal gill pouch (Tu et al., 2006, Fritzenwalker et al., 2014). This is significant because pharyngeal gills are conserved across hemichordates, chordates, and vertebrates, but structurally absent in echinoderms, like *S. purpuratus*, who instead utilize peristomial gills. In vertebrates the pharyngeal gill structures have been outsourced to placodes, like the epibranchial placodes, which form derivatives of the ear, jaw and craniosensory ganglia. As FoxI factors are known as ion regulators, the question remains whether their primary role is associated with ion regulation in the primordial pharyngeal gill. Although vertebrate pharyngeal gills are a main source of ion transport, it is unknown whether this function was gained alongside oxygen exchange or later. To date, only a single *S. kowalevskii* study exists to characterize ion regulation in primitive hemichordate gills. Although FoxI expression was found to be a magnitude higher in gills than skin, the ATPase activity associated with ion regulation was not significantly different between skin and gills (Sackville 2020). Taken together, FoxI TFs are locally expressed in primordial pharyngeal gill buds found in hemichordates, but not echinoderms, where they may facilitate ion regulation.

Further investigations of the vertebrate cranial placode network have characterized the role of FoxI factors in pharyngeal gill development of non-vertebrate chordates including *Ciona*

intestinalis, *Botryllus schlosseri* and *Branchiostoma floridae* (amphioxus). Vertebrate cranial placodes are specified at early neural plate stages of embryogenesis by expression of a core group of TFs, namely Six and Eya factors (Gasparini et al., 2013). *Ciona intestinalis* develops two placodal-like domains from which their sensory organs derive. FoxI members, Foxi1b and Foxi1c were found initially expressed in lateral ectoderm during early development and later in the gill slits and atrium invaginations which expand to enclose most of the pharynx (Mazet et al., 2005). Interestingly, they are co-expressed with Six and Eya. During both blastogenesis and larval development of *Botryllus schlosseri*, FoxI is expressed in the bud rudiment and epibranchial chambers, also alongside Six1/2 and Eya factors (Manni et al., 2005, Gasparini et al., 2013). Amphioxus also shows FoxI expression in the pharyngeal gills. Studies in *B. floridae* confirm that its gills function in ion regulation as well as gas exchange (Sackville 2020). Therefore, in non-vertebrate chordates, FoxI factors are implicated in the formation of the first placode-like epibranchial structures which pattern the primordial chordate pharyngeal gill where animals first outsourced ion regulation from the skin.

The roles of vertebrate FoxI family TFs

Duplication events in vertebrates facilitated the formation of three FoxI members, Foxi1, Foxi2 and Foxi3. Due to the differences in the order of FoxI homologue discovery across vertebrates, naming conventions have been imprecise and changed over-time. Nonetheless, these factors are expressed similarly, localized to ion regulating cells as well as the posterior region of the cranial placode forming either the epibranchial or otic placodal domains. Currently, Foxi1 in *H. sapiens* (human), *M. musculus* (mouse), *R. rattus* (rat) and *X. tropicalis* (frog) are most closely related to *D. rerio* (zebrafish) Foxi3, whereas fish Foxi1 is more closely related to frog Foxi2 and Foxi3, than mouse and rat (Soloman et al., 2003). Therefore, I will refer to fish Foxi3 as Foxi1, and Foxi1 as Foxi3.

In fish and frogs Foxi1 is a master regulator of ionocyte differentiation throughout the epidermis during early embryogenesis. While in fish it is restricted to the epibranchial placodes and pharyngeal arches, in frogs it is additionally control ectoderm germ layer boundary formation and is expressed later in the otocyst (Suri et al., 2005, Hsiao et al., 2007, Yan et al., 2015). In human and mouse, Foxi1 is expressed in the endolymphatic duct of the developing otocyst where it regulates ion transport. Foxi1 mutations in mice lead to enlarged endolymphatic compartments, and cause Pendred syndrome (deafness) in both mice and humans (Hulander et al., 2003, Vidarsson et al., 2009, Lorente-canovas et al., 2012, Ohyama & Groves 2014, Raft et al., 2014). These studies demonstrate the conserved role of Foxi1 in ionocyte differentiation and epibranchial and otic placode formation.

Foxi3 has been extensively characterized during early development where it's expressed throughout the pre-placodal ectoderm, however it is not ionocyte specific and does not activate genes associated with ion regulation. From frogs and fish to mammals, Foxi3 is initially expressed within the non-neural ectoderm surrounding the neural plate border (Lee et al., 2003, Khatri and Groves 2013, Khatri et al., 2014). Its non-neural ectoderm expression initially overlaps with Dlx and Ap2a factors, and is later restricted with Six, Eya and Pax factors as the pre-placodal region forms. Studies in fish have provided evidence that a self-sustaining network of Foxi3, Tfap2a and Gata3 expression is required for PPE competence (Bhat et al., 2013). Additionally, formation of the fish otic-epibranchial placodes requires Foxi3 and Dlx3b/4b dependent induction of FGF signaling (Hans et al., 2013). In chick, Foxi3 knockdown attenuates Pax2 expression in the pre-placodal region (Khatri et al., 2014). Foxi3 is also expressed within the branchial arches of frogs, fish and mice (Nissen et al., 2003, Soloman et al., 2003, Pohl et al., 2003). Foxi3 mutant zebrafish and mice both display defects in ear, epibranchial and jaw development (Edlund et al., 2014). In both humans and dogs, Foxi3 heterozygote mutants have mandibular asymmetry as well as tooth and outer ear malformations (Drogemuller et al., 2008,

Tassano et al., 2015). While Foxi3 has been shown to bind methyl-cytosines of Fgf15 promoter, which are linked to transcriptional repression, all other data suggest its role as an activator (Iurlaro et al., 2013, Jussila et al., 2015). Taken together, Foxi3 is a conserved vertebrate factor involved in the formation of the pre-placodal ectoderm and its posterior derivatives.

Despite its unique roles, Foxi2 is the least studied FoxI factor. In fish Foxi2 is expressed in the chordamesoderm but later restricted to the branchial arches and retina (Soloman et al., 2003). The only reported case of maternal Foxi2 expression is in *Xenopus laevis* and *tropicalis*, where it is ectodermally enriched and lies upstream of Foxi1, the ionocyte regulator during ZGA (Cha et al., 2012, Paraiso et al., 2019). It is zygotically expressed in the epibranchial placodes and later in the branchial arches and the jaw (Harland Lab photos in Xenbase). In amniotes, chick and mouse, Foxi2 is also initially expressed in the non-neural ectoderm and continues in the pharyngeal arch ectoderm but is restricted from the region forming the otic placode (Ohyama et al., 2006, Freter et al., 2008, Jayasena et al., 2008, Urness et al. 2010). These results imply that while the Foxi1, Foxi2 and Foxi3 factors have maintained shared roles in their early pre-placodal ectoderm and downstream pharyngeal/branchial arch expression, they have also co-opted unique roles in ionocyte regulation, ear and jaw formation as well as maternal expression.

Sox (HMG-related SRY box) transcription factors

Like Fox transcription factors, the Sox family of transcription factors exist within the most primordial animal lineages. In the first landmark paper, five homologous Sox genes were identified in mice, and through careful genotyping, Sry, was implicated as the testis-determining factor (Gubbay et al., 1990). Sox TFs are defined by their high-mobility group (HMG) DNA binding domain which recognizes the conserved Sox motif to bind and slightly kink the DNA minor groove, similarly to other HMG subfamily members, namely LEF/TCF (Bowles et al.,

2000, Hou et al., 2017). The Sox family of transcription factors has 8 subgroups SoxA-H (Bowles et al., 2000). While SoxA and G-I are typically vertebrate specific, SoxB-F are widespread among metazoa. Notably, all Sox subfamilies besides SoxF play a role in neural development. SoxF factors are uniquely expressed in the mesendoderm and participate in cardiovascular development (Lilly et al., 2017, Nobuhisa et al., 2024). Despite being deeply connected to neural development, the Sox family of TFs, namely Sox2 of the SoxB subfamily, is also remarkable for its genetic reprogramming potential.

Together with Oct4, Klf4 and Myc, Sox2 is a Yamanaka factor capable of inducing terminally differentiated somatic cells into a pluripotent state (Takahashi & Yamanaka 2006). This experiment was powerful in the sense that it brought to light a TF driven mechanism for Gurdon's earlier nuclear transplantation results. Interestingly, only other SoxB factors are functionally capable of replacing Sox2 during reprogramming experiments (Nakagawa et al., 2007). The results of reprogramming experiments suggest SoxB factor ability to bind chromatin and facilitate epigenetic changes associated with pluripotency. Thus, they are often deemed pluripotency factors. Additionally, SoxB factors are known to be maternally expressed in many metazoans, including chordates and humans (Keramari et al., 2010, Cattell et al., 2012). Sox1, Sox2 and Sox3 are members of the SoxB1 subgroup containing transactivation domains, whereas Sox14, and Sox21 are members of the SoxB2 subgroup containing repressor domains. Examining the role of homologous SoxB TF expression from primitive unicellular animals to complex metazoans lends clues to their evolutionary significance.

The evolutionary significance of SoxB family TFs

SoxB TFs are the most ancestral clade of transcription factors linked to stemness in metazoa. SoxB homologues have been found to be expressed in choanoflagellates, like *Salpingoeca helianthica* and *Mylnosida fluctuans*. Amazingly, these ancient SoxB homologues can

functionally replace mammalian Sox2 as a Yamanaka factor and induce pluripotency in mouse somatic cells, despite more than 800 million years of species evolutionary divergence (Gao et al., 2024). However, neither other choanoflagellate Sox-like, nor more primitive filasterean Sox or choanoflagellate Pou factors are functionally capable of replacing mouse Sox2 (Gao et al., 2024). Notably, even the ancient SoxB homologue was found to cooperate with mammalian Pou (Oct4) on DNA. As choanoflagellates do not possess a neural cell type equivalent, these results demonstrate the SoxB-Pou TF DNA binding cooperativity is even more ancestral and deeply conserved than the formation of neural progenitors or cell types. Future experiments which knockdown or inhibit the expression of choanoflagellate SoxB homologue are required to reveal SoxB TF primordial role in the choanoflagellate lifecycle.

The sponge, *Amphimedon queenslandica*, expresses SoxB1/2 factors based on their sequence similarity, though their function has not been described (Larroux et al., 2006, 2008). In another sponge, *Sycon ciliatum*, a maternally endowed SoxB factor was found strongly expressed in the oocyte, during cleavage and in neuronal-like cells at the pre-inversion stage by protein staining (Fortunato et al., 2012, 2015). Studies in *Nematostella vectensis* and *Acropora millepora* (cnidaria) reveal that, while not maternal, the Sox2 homologue is expressed throughout the blastula ectoderm, but is then restricted to neural progenitor cells during the planula stages (Shinzato et al., 2008, Richards & Rentzsch 2014, 2015). Notably, Sox2 is not expressed in differentiating neurons. Furthermore, Sox2 knockdown inhibits the expression of sensory neuron, ganglion neuron and nematocyte differentiation markers. These results were the first to implicate a TF controlled progenitor specification state in pre-bilateria. Therefore, SoxB TFs are intrinsically linked to neural stemness and represent master regulators of the first neuronal progenitor cell states.

Studies in the echinoderm *S. purpuratus* reveal that maternal SoxB TFs have similar and expanded roles. SoxB knockdown experiments show its requirement for body axis

establishment, oral ectoderm formation and neuronal specification until the early pluteus stage (Kenny et al., 2003, Zheng et al., 2011, Anishchenko et al., 2018). Similar to their role in cnidaria, SoxB factors are expressed throughout the early ectoderm in the animal pole domain, but are then restricted to progenitors of serotonergic and oral adjacent neurons (Garner et al., 2015). Surprisingly, SoxB factors are also expressed in endoderm cells which form neurons as their ectoderm neuronal cells do not migrate *in situ*. Likewise, in both the cephalochordate, *Branchiostoma belcheri*, and hemichordate, *Ptychodera flava*, SoxB is expressed in the foregut neuroprogenitors, as well as in blastula ectoderm and later in apical oral ectoderm (Taguchi et al., 2002, Lin et al., 2009). In the case of cephalochordate, the most basal group of living chordates which form a dorsal hollow nerve cord, SoxB TF are inherited maternally, expressed through neurulation, and later in the adult nerve cord. Compared to more primitive metazoans, bilateria acquired apical ectoderm, foregut neuron and maternal SoxB TF expression. Finally, SoxB TFs control neural progenitor formation from primitive neuron-like cells in porifera, to the simplest tubular central nervous system arrangements found in cephalochordates. Taken together, SoxB TFs are the most ancient and evolutionarily conserved factors maintaining pluripotency and controlling neural cell state formation.

The roles of vertebrate SoxB family TFs

The vertebrate lineage has acquired the SoxB1 family of activators, Sox1, Sox2 and Sox3 as well as the SoxB2 family of repressors, Sox14 and Sox21 (Popovic & Stvanovic 2009). In fish, all six SoxB family members are expressed in the brain and within the ectoderm during early development (Gao et al, 2014, 2015, Wei et al., 2016). Sox3 and Sox19 (a fish specific SoxB homologue) are maternally expressed throughout the zebrafish blastula ectoderm, but are restricted to unique antero-posterior neural plate domains during tailbud and somite stages. While Sox19 is pan-neurally expressed during the 12-somite stage, Sox3 is restricted from the

forebrain-midbrain boundary and midbrain-hindbrain boundary. Sox1 expression begins lens restricted during somite stages (Okuda et al., 2006). Although single SoxB factor knockdowns do not phenotypically affect CNS development, combined SoxB factor knockdowns cause significant CNS defects, demonstrating their redundancy (Okuda et al., 2010). These combined SoxB knockdowns phenotypically resemble Oct4 knockdowns indicating their overlapping function, and ancestral conservation with Pou factors. The SoxB2 TF, Sox21, is maternally expressed and later restricted to specific forebrain and hindbrain regions, but devoid from structures like the eye primordium and brain boundary regions (Argenton et al., 2004, Lan et al., 2011). Importantly, in glioblastoma stem cells, Sox21 was shown to bind AP1 gene chromatin and facilitate epigenetic silencing, functioning as a tumor suppressor (Rrapaj et al., 2024). These studies demonstrate Sox21 overexpression or inhibition represses for neural differentiation, suggesting Sox21 role in maintaining a neuroprogenitor state. These studies in zebrafish indicate that within the vertebrate lineage, SoxB factors first broadly define neural lineages and later become restricted either within progenitors or specified cell types.

In *Xenopus*, only Sox3 is maternally expressed, while Sox2 is expressed in the blastula and Sox1 later in the neurula. Sox14 and Sox21 are both highly expressed in the brain and sparingly in the posterior CNS during tailbud stages. Although maternal Sox3 is initially expressed throughout the ectoderm, it is restricted to the neural plate alongside Sox2 during gastrulation and neurulation. Experiments overexpressing SoxE factors, typically expressed only later during neurulation, inhibited gastrulation pluripotency markers, however overexpression of the SoxB pan-ectoderm activators Sox2 and Sox3 did not interfere with their expression (Buitrago-Delgado et al., 2018). In addition, experiments removing SoxB factors and substituting SoxE factors could not maintain animal cap pluripotency or induce neuron progenitor formation. In line with data from choanoflagellates, *Xenopus* Sox3 colocalizes with the Oct4 homologue, Pou5f3, and controls the chromatin landscape for more than half of the

genes activated during ZGA (Gentsch et al., 2019).

Along with the cranial placodes, the neural crest is a vertebrate specific cell-type arising from the neural plate border. Neural crest cells are important for craniofacial development, forming the skeletal and other connective tissues of the face, jaws, as well as peripheral neurons. In *Xenopus*, SoxB factors play key roles in neural crest formation and differentiation. Knocking down Sox2 blocks all neuroectoderm formation, including the neural plate border and subsequent neural crest (Kishi et al., 2000, Luo et al., 2003, Wakamatsu et al., 2021). However, Sox2 inhibition is also required for downstream neural crest induction alongside NC marker activation in both frog, chick, mice and ES cells (Luo et al., 2003, Cimadomore et al., 2011, Adameyko et al., 2012, Wakamatsu et al., 2021). This is consistent with evidence that constitutive expression of Sox2 inhibits the exit from neuroprogenitor differentiation into neural crest or neural plate derivatives (Graham et al., 2003). Taken together, these experiments demonstrate that throughout metazoan evolution, SoxB factors play conserved roles in the maintenance of pluripotency and neuroectoderm progenitor formation.

Early vertebrate epigenetic states

During gamete creation terminally differentiated cells give rise to sperm and egg which unite to form a totipotent progenitor cell. This requires a general erasure and reprogramming of the epigenome (Kojima et al., 2024). Within the zygote regions of open and closed chromatin conformation must be appropriately re-established for developmentally regulated gene activation and repression (Akkers et al., 2009, 2013, Gupta et al., 2014, Kruijsbergan et al., 2016, Wang et al., 2022). During early development, before zygotic transcription is activated, histones of the naive genome gain post-translational modifications that prevent ectopic or precocious gene expression (Hontelez et al., 2015, Hug et al., 2017, Zenk et al., 2017, Hickey et al., 2022). Despite timing and environmental differences in placental and non-mammalian

vertebrate development, the hierarchical principles of epigenetic inheritance are conserved. Taken together, what are the role of maternal factors in establishing the first epigenetic signatures required for gene transcription and ectoderm development?

Maternal PRC1/2 establish a repressive epigenetic potential

H2Aub (H2 ubiquitination) is a robustly detected repressive histone modification occurring in early vertebrate embryogenesis (Blackledge et al., 2014, 2020, Fursova et al., 2019, Mochizuki et al., 2021, Hickey et al., 2022). H2Aub marks are catalyzed by the RING1A/B components of the maternally inherited polycomb repressive complex1 (PRC1) which can bind nucleosomal DNA non-specifically and interact with an acidic patch of H4 (Bentley et al., 2011). Interestingly, neither PRC nor its PCGF cofactors have DNA binding domains, but can bind H3K27me3, or other moieties, or be recruited by TFs (Shoeftner et al., 2006, Yu et al., 2012, Endoh et al., 2017, Scelfo et al., 2019, Sugishita et al., 2021). In placental vertebrates, inherited H2Aub and H3K27me3 marks in the early zygote, as well as methylated CpG islands, serve as PRC1 binding moieties for H2Aub deposition (Mei et al., 2021). Although the repressive mark H3K27me3 is erased from the early zygote and re-established after implantation, H2Aub persists on developmentally regulated genes through implantation.

In non-mammalian vertebrates, H2Aub marks are established well before H3K27me3 detection (Akkers et al., 2009, Hickey et al., 2022). Paternally inherited H2Aub has been shown to contribute to silencing during genome activation, potentially serving as a scaffold for PRC1 binding (Francois-Campion et al., 2025). PRC1 can recognize and bind H2Aub mark~~ings~~s via maternally endowed RYBP and YY1 (Arrigoni et al., 2006, Lee et al., 2021). As methylated CpG islands are not inherited in non-mammalian vertebrates, H2Aub mark may deposit on unmethylated CpG islands, or polycomb response elements through intrinsic RING cofactor interactions with nucleosomal DNA (Bentley et al., 2011, Blackledge et al., 2014, Kahn et al.,

2016, Stielow et al., 2018). In these ways, maternal PRC1 initiates H2Aub-mediated regulation of the zygotic genome.

The H3K27me3 histone modification closes the DNA conformation and creates facultative heterochromatin associated with gene silencing essential for tissue specification. Components of the maternal PRC2 complex recognize and bind H2Aub where the catalytic subunit Ezh2 deposits H3K27me3 (Matsuwaka et al., 2024). While PRC2 recognizes H2Aub, PRC1 recognizes H3K27me3, facilitating an autoregulatory repressive loop. Additionally, PRC2 components can be recruited to the DNA by TFs who recognize sequence specific motifs. In this way, the mother endows both broadly co-propagated PRC1 and 2 repression mechanisms, as well as a modulatory mechanism of TF directed repression.

Maternal TFs and Ep300 override the repressive epigenetic potential

H3K27ac and H3K27me3 are mutually exclusive histone modifications that occur on the same lysine residue of H3. Despite their functional antagonism, these modifications are essential coordinators of gene activation and repression during germ layer formation. Trimethyl H3 PTMs sterically inhibit DNA accessibility, while in contrast acetyl PTMs promote accessibility through quenching the positive charge of histone tail residues. EP300, the main epigenetic writer of H3K27ac modifications, does not possess a DNA binding domain and relies on ancillary TF interactions for both site-specific recruitment and acetyltransferase activity (Benveniste et al., 2014, Fuglerud et al., 2018, Ma et al., 2021, Ferrie et al., 2024). Pioneer transcription factors with DNA-binding domains recognize enhancer sequences and initiate EP300 recruitment for H3K27ac deposition in H2Aub marked regions. EP300 derived H3K27ac markings of enhancer regions and their nearby genes are essential for ZGA (Wang et al., 2022, Yu et al., 2023).

Establishment of early epigenetic states relative to the timing of cellular divisions, ZGA and implantation differs slightly in placental mammals as compared with all other vertebrates. In

the former, H3K27me3 present at developmental genes in gametes is erased from the 1 cell stage (zygote) until implantation, while H2Aub remains (Raas et al., 2022). In this way, inherited H3K27me3 markings can potentially initiate H2Aub deposition. In contrast, H3K27ac is mostly absent in the egg, but becomes widespread after fertilization coinciding with H3K4me3 deposition, TF binding and ZGA (Wang et al., 2022, Wu et al., 2023). Histone deacetylases (HDACs) play an important role titrating the H3K27ac landscape to prevent precocious gene expression during preimplantation development. Notably, inhibition of early zygotic transcription prevents HDAC function, but preserves the maternally deposited H3K27ac landscape in naive hESCs. This demonstrates H3K27ac deposition is maternally controlled, but HDAC activity is not. Despite early H2Aub and H3K27ac conservation, non-mammalian vertebrates express maternal HDAC1 appreciably, and do not inherit H3K27me3 marking to establish the epigenetic state pre-ZGA (Zhou et al., 2023).

In non-mammalian vertebrates maternally inherited TFs are cytoplasmically localized along the animal-vegetal axis before fertilization. After fertilization, several nuclear divisions must occur before spatially compartmentalized TFs are imported into the nucleus where they gain access to the genome (Nguyen et al., 2022). Although H3K27me3 does not appear appreciably until major ZGA has begun, experiments inhibiting zygotic transcription demonstrate maternal control over H3K27me3 deposition during gastrulation (Akkers et al., 2009). While the timing of H2Aub, H3K27ac deposition and TF binding is not completely understood, in both *Xenopus* and *Danio* H2Aub is maternally and/or paternally established in gametes and before ZGA and maternal control over H3K27ac deposition also begins before ZGA (Gupta et al., 2014, Zhang et al., 2018, Sato et al., 2019, Hickey et al., 2022, Parast et al., 2023, Francois-Campion et al., 2025, Oak et al., 2025). In zebrafish, pre-ZGA promoters are bivalently marked by H2Aub and H3K27ac but not H3K27me3. While the very earliest locations of H3K27ac deposition are uncharacterized in *Xenopus*, it is detected at least by the 256-cell stage. Early H3K27ac

marking and the paternal influence of H2Aub in *Xenopus* (Francois-Campion et al., 2025) imply pre-ZGA bivalent epigenetic marking conservation between non-mammalian vertebrates, though more research is warranted.

Over time, regions that maintain high H3K27ac deposition become transcribed, lose H2Aub and do not accumulate H3K27me3. However, without sufficient Ep300 recruitment and H3K27ac deposition, H2Aub marked regions recruit PRC2 during ZGA and accumulate H3K27me3 to become silenced. These data suggest a hierarchy of H2Aub, H3K27ac and H3K27me3 acquisition, where maternal TFs recruit acetyltransferases, which establish H3K27ac domains to counteract the repressive potential of H2Aub. Conversely, H2Aub inherited regions without acetyltransferase recruitment are sufficient for H3K27me3 associated repression. Despite this knowledge of epigenetic signatures, the breadth of maternal factors required for recruiting Ep300 and overriding the repressive potential are not well characterized. Additionally, in the case of non-mammalian vertebrates, the window in which the epigenetic signal is propagated is also not entirely understood. While pioneer maternal TFs bind the genome first, and epigenetic signals accumulate by ZGA, we do not know if this accumulation occurs gradually or via a more punctuated event.

Maternal TFs and EP300 coordinate to establish H3K27ac

Tfap2c can bind the genome as early as the 2-cell stage and premark developmentally regulated genes which later gain H3K27ac deposition in the 4-8 cell stages and in the trophectoderm (Li et al., 2024). Tfap2c is critical for opening developmentally relevant enhancers in naive hESCs, suggesting a model where it interacts with CITED cofactors which recruit EP300 and facilitate early H3K27ac deposition (Braganca et al., 2002, 2003, Pastor et al., 2018). New research shows that Tfap2c also interacts with HDAC machinery to titrate H3K27ac levels (Abeywardana et al., 2024). Zygotic Cdx2 and Sox2 are later recruited by

Tfap2c for downstream trophectoderm differentiation and transition from toti- to pluripotency (Li et al., 2023). In this way, maternal Tfap2c is an early pioneer factor interfacing with the genome to establish the H3K27ac landscape and recruit zygotic factors required for the first ectoderm-like embryonic lineage bifurcation. While direct proof for maternal control over H3K27ac deposition is lacking in mammals, there is no practical way to specifically inhibit early zygotic transcription and confirm this. Because mammalian vertebrate zygotic transcription begins at the 1 to 2-cell stage, it is extremely difficult to tease apart maternal and zygotic contributions to the epigenetic state.

Non-mammalian vertebrate embryos develop externally and undergo several cleavage divisions before zygotic transcription occurs, allowing more sophisticated studies concerning maternal TF control over the early epigenetic state. Alpha-amanitin treatment during early embryogenesis inhibits RNA pol II function and disrupts zygotic transcription initiation. In *Xenopus* alpha-amanitin treatments of mid-gastrula embryos demonstrate that 85% of H3K27me3 deposition and 15% of Ep300 binding is maternally derived (Hontelez et al., 2015). However, as tissue specification and divergence are well underway by the mid-gastrula, it is worth noting that the ratio of maternally controlled Ep300 peaks is likely higher during earlier development. The endodermally active maternal TF, Foxh1, premarks regions which recruit EP300 or HDAC1 to establish functional cis-regulatory modules (CRMs), independently of Nodal signaling (Chiu et al., 2014, Charney et al., 2017, Zhou et al., 2023). These regions are enriched with Fox and Sox motifs, and can recruit Sox3 in the context of HDAC1 (Gentsch et al., 2019, Zhou et al., 2023). Foxh1 also colocalizes with other essential endodermal TFs, Vegt and Otx1, where together they shape the endoderm enhancer landscape (Paraiso et al., 2019). Albeit, this landscape is defined by H3K4me1, a marking highly colocalized with H3K27ac on poised enhancers (Bae et al., 2020, Kubo et al., 2024). Maternal Ascl1 is ectodermally localized and interacts with HDACs, but not EP300, to repress H3K27ac levels of endodermally

expressed genes in the ectoderm (Gao et al., 2015). Maternal Sox3 and Pou5f3 are ectodermally enriched factors which may be responsible for opening 41% of the CRMs required for ZGA (Gentsch et al., 2019). This implies that they can recruit Ep300 and facilitate acetylation. Despite these findings in *Xenopus*, there is a lack of understanding of the direct contributions of ectoderm-localized maternal transcription factors in Ep300 recruitment and H3K27ac deposition.

Studies in zebrafish have yielded the most information about maternal control over the early activating epigenetic state. H3K27ac is dynamically regulated during early zebrafish embryogenesis where it controls RNA Pol II localization. Live imaging RNA Pol II and H3K27ac reveals that H3K27ac marking precedes RNA Pol II recruitment and transcription initiation in the 256-cell stage (Chan et al., 2019, Sato et al., 2019). Nanog, Pou5f3 and Sox19b (Sox3) (NPS) are maternal pioneer factors with mammalian homologues (Lee et al., 2013, Leisenring et al., 2013, Falfy et al., 2020). Triple NPS knockdown gastrula embryos have significantly decreased H3K27ac markings and recruitment of EP300 and Brd4 to co-bound regions (Miao et al., 2022). H3K4me1 marking and chromatin accessibility were also significantly decreased, suggesting a closure of poised enhancers. Additionally, many other acetylation based epigenetic modifications with similar genomic profiles to H3K27ac were also reduced, demonstrating the master regulatory role of NPS maternal factors shaping the acetylation landscape. NPS factors co-bind regions in different combinations, and independently, depending on motif presence and nucleosome occupancy. In terms of localization, all three factors are expressed in both enveloping and deep cells, however Sox19b and Pou5f3 knockdowns in particular regulate ventral and ectoderm genes (Gao et al., 2022). Notably, in a single TF family knockdown, Sox19b required an additional SoxB factor to induce ectoderm malformations, suggesting redundancy in the TF family. Taken together these data demonstrate that maternal factors, expressed in presumptive ectoderm, combinatorially access the genome, recruit Ep300 and

facilitate H3K27ac deposition required for ZGA. However, more studies are needed to examine the potential contributions of other maternal factors exclusively enriched in the ectoderm, especially in *Xenopus* which does not express Nanog.

1.4: High resolution genomic techniques and ectoderm specification

Cellular differentiation is functionally dependent on the ability of TFs to bind CRMs which regulate gene targets through physical looping interactions, forming gene regulatory networks (GRNs). Heterogeneous spatiotemporal GRN activation is required for ectoderm, mesoderm and endoderm cellular fate acquisition through unique gene expression programs. Bulk RNA sequencing (RNA-seq) masks gene expression spatial heterogeneity by concurrently homogenizing cytoplasmic and/or nuclear contents of many cells. Single cell RNA-seq (scRNA-seq) sequencing technologies can detect transcripts from several thousand, or more, individual cells, without transcript homogenization. This allows for the (pseudo)-spatial and -temporal (if collected at different stages) elucidation of gene expression on a cell-by-cell basis during germ layer fate acquisitions. In this way, scRNA-seq technology has yielded sufficient resolution to survey spatiotemporal gene expression programs coordinating germ layer and sub-lineage specification in primitive bilateria, ecdysozoa, frog, fish and mice (Karaiskos et al., 2017, Farrell et al., 2018, Briggs et al., 2018, Wagner et al., 2018, Packer et al., 2019, Cao et al., 2019, Pijuan-Sala et al., 2019, Sladitschek et al., 2020) .

Integrating the epigenetic landscape at single cell resolution

Although scRNA-seq reveals transcriptional cell states at high resolution, a caveat of this approach for building GRNs is the lack of epigenetic information required. Computational strategies that leverage existing bulk epigenetic data and DNA sequence information alongside scRNA-seq data can predict GRNs. For example, SCENIC software uses scRNA-seq

expression profiles in each cell to predict a TF-target gene interaction (Aibar et al., 2017). This interaction prediction is weighted by the presence of TF motifs detected in the DNA sequence surrounding predicted target genes. Similarly, CellOracle creates TF-target gene predictions by initially utilizing bulk ATAC-seq to predict regulatory connections before integrating these with scRNA-seq data to interpret potential regulatory connection strengths (Kamimoto et al., 2020, 2023). These tools take advantage of bulk epigenetic signatures and the DNA sequence to further interrogate the relationship of TFs and target genes co-expressed in the same cell. In this way, scRNA-seq can be leveraged for GRN prediction which cannot be recapitulated by expression data alone.

Single cell multiomics is an emerging technology which combines single cell transcriptomic sequencing with epigenetic profiling, most commonly measuring regions of open chromatin using ATAC-seq. An inherent sequencing difficulty arises from the fact that RNA and DNA template copy numbers in each cell are potentially magnitudes apart. While some genes may be expressed with hundreds of mRNA copies, all genes have two genomic loci per cell. However, cells with similar transcriptional profiles can be clustered together, and their ATAC-seq profiles merged to generate a more robust epigenetic signal shared across cells with shared identity. These combined cell-type specific pseudo-bulk ATAC profiles offer the highest resolution of epigenetic detection. Utilizing the highest resolution transcriptomic and epigenetic signatures acquired from the same cell can offer the most robust GRN inference possible.

In recent years many different software packages, including CellOracle and SCENIC+, have become available for integrating multiomic scRNA-seq and ATAC-seq data to understand the relationship between TFs, their targets, and epigenetic states (Pliner et al., 2018, Hao et al., 2021, Gonzales-Blas et al., 2023, Kamimoto et al., 2023). Despite these technological advances, single cell sequencing has not been used in conjunction with maternal TF knockdown to reveal maternal contributions to zygotic gene expression, the epigenetic state, or GRN

formation during embryogenesis. Therefore, several outstanding questions remain: 1) Do maternal TFs localized to ectoderm activate the same GRN across different ectodermal lineages? 2) Do they facilitate different epigenetic states during different stages of ectodermal fate acquisition? 3) Do they activate or repress genes in other germ layers? Single cell associated sequencing technologies offer avenues to lineage specific TF-target interactions and understand maternal contribution to early gene expression at the highest resolution available.

Summary

In this dissertation work, I uncover the role of ectoderm localized maternal TFs controlling *Xenopus* ectoderm gene expression through the formation of developmentally relevant CRMs. I propose a mechanism in which maternal Foxi2 and Sox3 function as master regulators coordinating gene expression across inner and outer layer ectoderm sub-lineages through ectoderm specific EP300 interactions and H3K27ac enrichment during early gastrulation (Chapter 2). Utilizing temporal snRNA-seq, I uncover the delineation of all inner and outer neural and non-neural ectoderm sub-cell types, as well as the role of maternal Foxi2 in ectoderm progenitor formation and cranial ectoderm specification (Chapter 3). These temporal trajectories represent the highest resolution map to date of ectoderm specification during gastrulation. This work reveals novel insights into the master regulatory roles of maternal Foxi2 and Sox3 at the earliest stages of ectoderm development. They also reveal fundamental principles about maternal TF regulation of ectoderm identity and sub-lineage formation, and will be useful both for those who study general mechanisms of TF-directed epigenetic regulation, as well as those interested in cell-fate determination and GRNs specific to early vertebrate embryogenesis.

Chapter 2: Foxi2 and Sox3 are master regulators controlling ectoderm germ layer specification

---

Abstract:

Germ layer specification represents a critical transition where pluripotent cells acquire lineage-specific identities. We identify the maternal transcription factors Foxi2 and Sox3 to be pivotal master regulators of ectodermal germ layer specification in *Xenopus*. Ectopic co-expression of Foxi2 and Sox3 in prospective endodermal tissue induces the expression of ectodermal markers while suppressing mesendodermal markers. Transcriptomics analyses reveal that Foxi2 and Sox3 jointly and independently regulate hundreds of ectodermal target genes. During early cleavage stages, Foxi2 and Sox3 pre-bind to key cis-regulatory modules (CRMs), marking sites that later recruit Ep300 and facilitate H3K27ac deposition, thereby shaping the epigenetic landscape of the ectodermal genome. These CRMs are highly enriched within ectoderm-specific super-enhancers (SEs). Our findings highlight the pivotal role of ectodermal SE-associated CRMs in precise and robust ectodermal gene activation, establishing Foxi2 and Sox3 as central architects of inner and outer ectodermal lineage specification.

Introduction:

A major breakthrough in biology was the first animal (*Xenopus laevis*) cloning experiment, which proved that differentiated cells retain the full genetic potential to develop into an entire organism (Gurdon et al., 1958). This result demonstrated the concept of genomic equivalence, where cellular differentiation is governed by gene regulation rather than by irreversible modifications to the genome, such as differential loss of subsets of genes in cell lineages. These experiments further revealed that the egg cytoplasm contains necessary maternal regulators to reprogram the epigenetic memory of the differentiated cell nuclei to a totipotent state. Subsequently it was

shown in mammalian cells that networks of master regulator transcription factors (TFs), including most notably Klf4, Myc, Pou5f1, and Sox2, are critical for embryonic pluripotency (Takahashi and Yamanaka, 2006). This highlights the essential role of multiple TFs working in concert to orchestrate cellular identity, lineage specification, and reprogramming.

Additionally, discovery of these pluripotency TFs among many permutations highlights that not all TFs hold equal importance in development. TFs are considered master regulators when they play a more critical role in regulating specific differentiation pathways because they occupy a higher position within a gene regulatory program controlling downstream events in differentiation and maintaining pluripotency. One of the earliest TFs to support the concept of master regulators was Myod1, which was shown to drive fibroblasts into a muscle cell differentiation path (Davis et al., 1987). Other examples include Spi1 (Pu.1), which specifies myeloid and B-cell lineages in hematopoiesis (Fisher and Scott 1998), Gata1 in erythroid lineage specification (Moriguchi and Yamamoto, 2007), and Pdx1 for pancreas organogenesis (Horb et al., 2003). These master regulatory TFs play a pivotal role in determining the identity and function of specific cell types. Identifying master regulatory TFs in developmental biology is fundamentally important for comprehending the mechanisms of cell lineage segregation and advancing regenerative medicine to facilitate direct cell lineage conversion.

Our goal in this study is to determine the primary master regulators initiating ectodermal cell lineage differentiation at the highest positions in the programming of cell lineages. In vertebrates, germ layer specification is one of the earliest developmental decisions that pluripotent cells make. In amphibians, the three germ layers are organized along the animal-vegetal axis, where the ectoderm forms in the animal pole, the endoderm vegetally, and the mesoderm in the equator. The ectoderm comprises progenitor cell populations giving rise to the skin, nervous system, sensory organs and the numerous neural crest derivatives. Several experiments have demonstrated that *Xenopus* ectodermal cells of the blastula stage are pluripotent. Transplantation of blastula prospective ectodermal cells into the vegetal endoderm

converts the ectodermal cells to endodermal fates (Snape et al., 1987). In addition, explanted blastula ectodermal tissue ("animal caps") can be converted to mesendodermal cells *ex vivo* (organoids), by soaking them in activin, a TGFβ-superfamily ligand (Smith et al., 1990; Asashima et al.,1990; van den Eijnden-Van Raaij, et al., 1990). With specific combinations of growth factors and/or small molecules, blastula ectodermal explants can be programmed to differentiate into a wide range of cell types, including neural tissue, muscle cells, blood, heart and endoderm primordia (Ariizumi et al., 2017; Green et al., 1990). Although this ectodermal pluripotency persists through blastula stages, it is autonomously lost by early gastrula (Gurdon et al., 1985; Jones et al., 1987). Therefore, ectodermal germ layer and sub-lineage specification is an ideal system to study the dynamic processes controlling cellular potency and differentiation.

Previous epigenetic studies have shown that the early embryonic genome lacks significant histone modifications before the blastula stage and therefore remains epigenetically naïve (reviewed in Blitz and Cho, 2021). Histone modifications associated with active enhancers first appear during blastula stage, coinciding with major zygotic genome activation (ZGA) and the segregation of the pluripotent embryonic cells into specialized ectoderm, mesoderm, and endodermal lineages. We hypothesize that maternal, locally expressed master TFs bind to specific cis-regulatory modules (CRMs) to activate or repress the transcription of the first wave of zygotic target genes, thus orchestrating the gene regulatory programs required for cell lineage specification.

Here we reveal that the ectodermal gene regulatory program is orchestrated by maternally expressed, and ectodermally enriched master regulatory TFs, Foxi2 and Sox3. These TFs prebind to the CRMs of the naïve embryonic genome prior to ZGA, preceding the appearance of major histone modifications and transcription. This prebinding event coordinates the subsequent ectodermal cell differentiation program. The CRMs bound by Foxi2 and Sox3 are associated with ectodermal super enhancers (SEs), which ensure robust target gene

expression. Our findings are consistent with the view that Foxi2 and Sox3 function as master regulators of the ectodermal germ layer.

RESULTS

Different epigenetic states accrue on ectoderm- and endoderm-expressed genes during ZGA

Epigenetic analyses of *Xenopus* blastula stage embryos show that the embryonic genome is largely devoid of the major histone tail modifications H3K27ac, H3K27me3, and H3K4me1 (Gupta et al., 2014, van Heeringen et al., 2014). These marks begin to accrue during blastula stages, becoming widespread in the genome during gastrulation (van Heeringen et al., 2014; Hontelez et al., 2015; Charney et al., 2017; Paraiso et al., 2019). However, a limitation of whole-embryo epigenetic experiments, which homogenize the data from cells from all three germ layers, is the inability to determine whether these histone modifications occur in a spatially restricted manner.

To gain spatial information about histone modification states in different germ layers, early gastrulae (stage 10.5) were dissected into ectoderm and endoderm fragments, approximately 3 hours after the onset of ZGA (stage 8.5) (Figure 2.1A,B). Histone modifications H3K27ac and H3K27me3 were then examined (Figure 2.1C) around enhancers and promoters to understand their role in regulating the transcription of associated genes. Using early embryonic time course (Owens et al. 2016), and early gastrula embryo dissection (Blitz et al. 2017) RNA-seq data, we determined the top 250 zygotically expressed genes specifically enriched in either the ectoderm or endoderm.

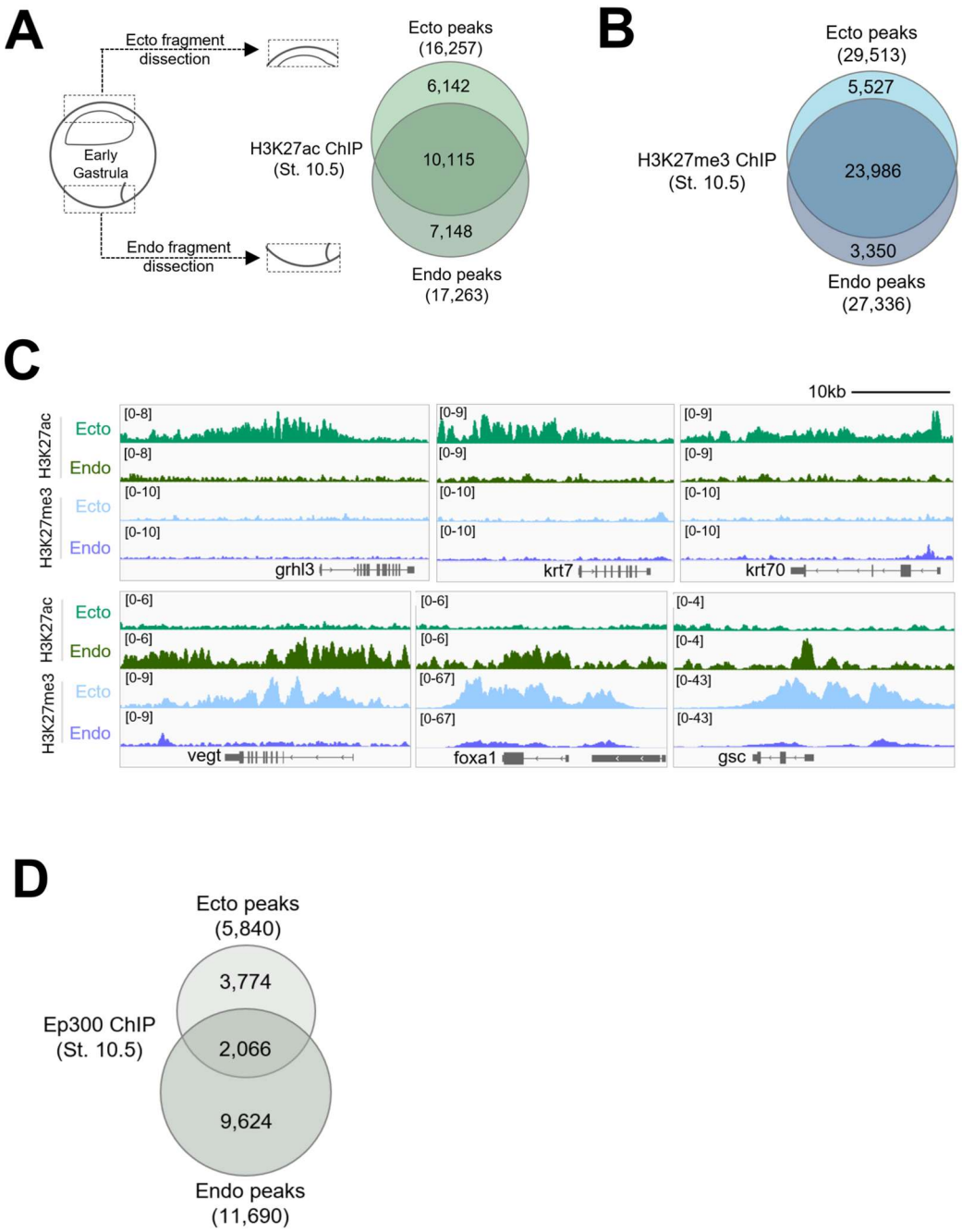

Figure 2.1: ***Differential epigenetic marking of ectodermal and endodermal cells.*** **(A)** H3K27ac ChIP-seq analysis of ectodermal and endodermal explants reveals both lineage-specific and shared peaks, indicating distinct and overlapping enhancer activity. **(B)** H3K27me3 peak distribution in ectodermal and endodermal tissues. **(C)** Genome browser views showing H3K27ac and H3K27me3 peaks at ectodermally expressed genes (grhl3, krt7, krt70) and endodermally expressed genes (vegt, foxa1, gsc). **(D)** Distribution of Ep300 peaks in ectodermal and endodermal explants.

The germ layer specific histone mark deposition of H3K27ac and H3K27me3 was plotted within a 25kb region upstream and downstream of the genes (Figure 2.2A). The mesoderm was excluded from the analysis due to contamination issues occurring across tissue boundaries.

Ectodermally expressed genes, including their up and downstream regions, are more highly decorated with the activating H3K27ac mark in the ectoderm compared to the endoderm (Figure 2.2A,B, Figure 2.1C). On the other hand, endodermally expressed genes are more highly marked by H3K27ac in the endoderm compared to the ectoderm. We also examined the distribution of the repressive mark H3K27me3 across both ectodermally and endodermally expressed genes. Endodermally-expressed genes are strongly marked by H3K27me3 in ectoderm, but remain relatively unmarked by H3K27me3 in endoderm (Figure 2.2A,B, Figure 2.1C). This H3K27me3 deposition suggests a mechanism of active repression of endodermally expressed genes in the ectoderm, which prevents their inappropriate expression outside their endodermal environment. In contrast, H3K27me3 marking of ectodermally expressed genes in both endoderm and ectoderm cells is low. Notably, Akkers et al. (2009) also examined H3K27me3 enrichment on a subset of lineage-enriched marker genes but did not analyze dissected tissue fragments. Our findings, based on dissected tissues from early gastrula embryos, reveal tissue-specific accumulation of H3K27me3 at endodermal gene loci in the ectoderm, a pattern not mirrored for ectodermal genes in the endoderm.

Since H3K27ac marking of ectodermal and endodermal genes correlates well with their region-specific expression in developing embryos, we examined the binding of the histone acetyl transferase Ep300 (Figure 2.2C; Figure 2.1D), which is a commonly used marker to identify functional enhancers (Heintzman et al., 2009). In ectoderm explants, Ep300 binding is high in ectodermally expressed genes, while in endoderm explants it is preferentially enriched in endodermal gene binding (Figure 2.2C). Ep300 functions as a transcriptional co-activator but it does not possess a DNA binding domain. Therefore, the recruitment of Ep300 to specific genomic

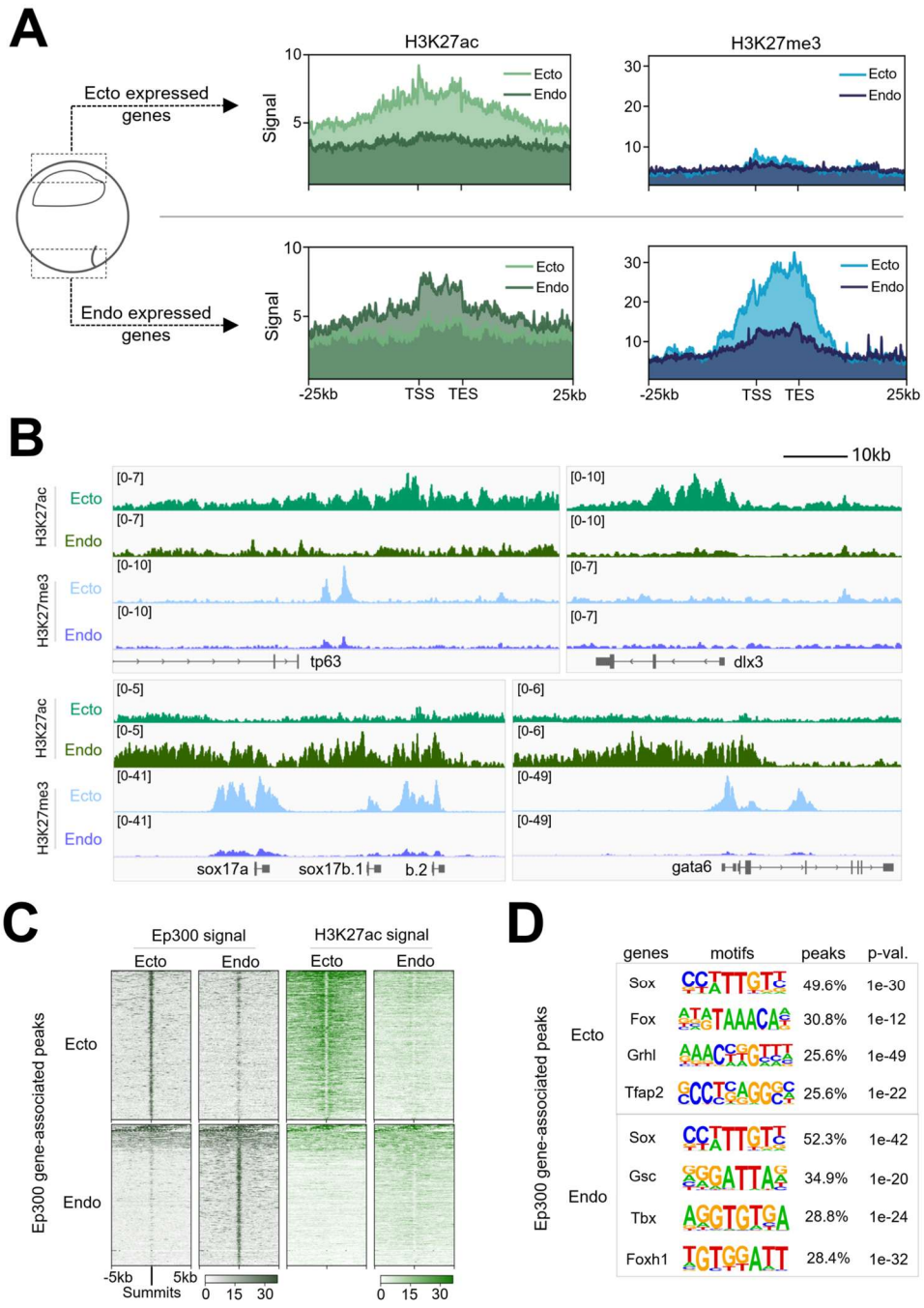

Figure 2.2. ***Differential Epigenetic Regulation of Ectodermal and Endodermal Genes in Early Gastrulae.*** **(A)** Signal deposition of H3K27ac (left, green) and H3K27me3 (right, blue) across the top 250 zygotically expressed ectodermal (top) or endodermal (bottom) gene regions obtained from early gastrula ectoderm and endoderm dissections. **(B)** Genome browser tracks showing H3K27ac and H3K27me3 marks along representative zygotically expressed ectodermal and endodermal genes. **(C)** Signal enrichment of Ep300 (left) and H3K27ac (right) across Ep300 bound regions associated with top 250 zygotically expressed ectodermal (top) and endodermal (bottom) genes from early gastrula ectoderm and endoderm dissections. **(D)** Transcription factor motifs detected within Ep300 peaks within 20kb of top 250 ectodermal (top) and endodermal (bottom) genes.

loci requires interactions with DNA-bound TFs. To identify potential Ep300 cofactors, TF motif enrichment search of Ep300-bound peaks was performed for both ectodermally and endodermally expressed gene regions. Sox, Fox, Grhl and Tfap2 family motifs were most frequently identified in Ep300 peaks associated with ectodermally expressed genes, whereas the Sox, Gsc, Tbx and Foxh1 motifs were most frequent in endodermally expressed genes (Figure 2.2D). These results suggest that gene families related to Sox and Fox TFs are critical in both ectodermal and endodermal development. Importantly, *foxi2* and *sox3* transcripts are highly expressed maternally (Figure 2.4A) and enriched in the ectoderm (Paraiso et al. 2019; Cha et al. 2012; Zhang et al., 2003; Blitz et al., 2017), implying their involvement, in not only regulating the ectodermal gene regulatory program, but also influencing epigenetic modifications of ectodermal genes.

Foxi2 and Sox3 prebind future ectodermal CRMs before Ep300 recruitment

Previous work showed that maternal Foxi2 can bind to an upstream cis-regulatory module (CRM) of the *foxi1* gene to activate its expression (Cha et al., 2012). We wished to further examine the genome-wide regulatory role of Foxi2 during early development. ChIP-seq analysis of Foxi2 was performed in mid- to late blastula (st. 8, 9) and early gastrula (st. 10.5) embryos and identified a total of 16,427 bound regions over the entire time course (Figure 2.3A). There are 13,158 high confidence Foxi2 bound regions in the mid blastula, 6,648 in the late blastula, and 6,039 in the early gastrula (Figure 2.3A). Overall, Foxi2 binding is dynamic, displaying unique (class I, III, VI), shared (class II, IV, V), as well as persistently occupied (class VII) binding patterns across stages (Figure 2.3A,B).

To characterize functionally relevant Foxi2 peaks, we examined the correlation of classified Foxi2 peaks with Ep300 and H3K27ac peaks in ectoderm and endoderm explants. Class IV, V, VI and VII regions contain more H3K27ac deposition and Ep300 binding compared

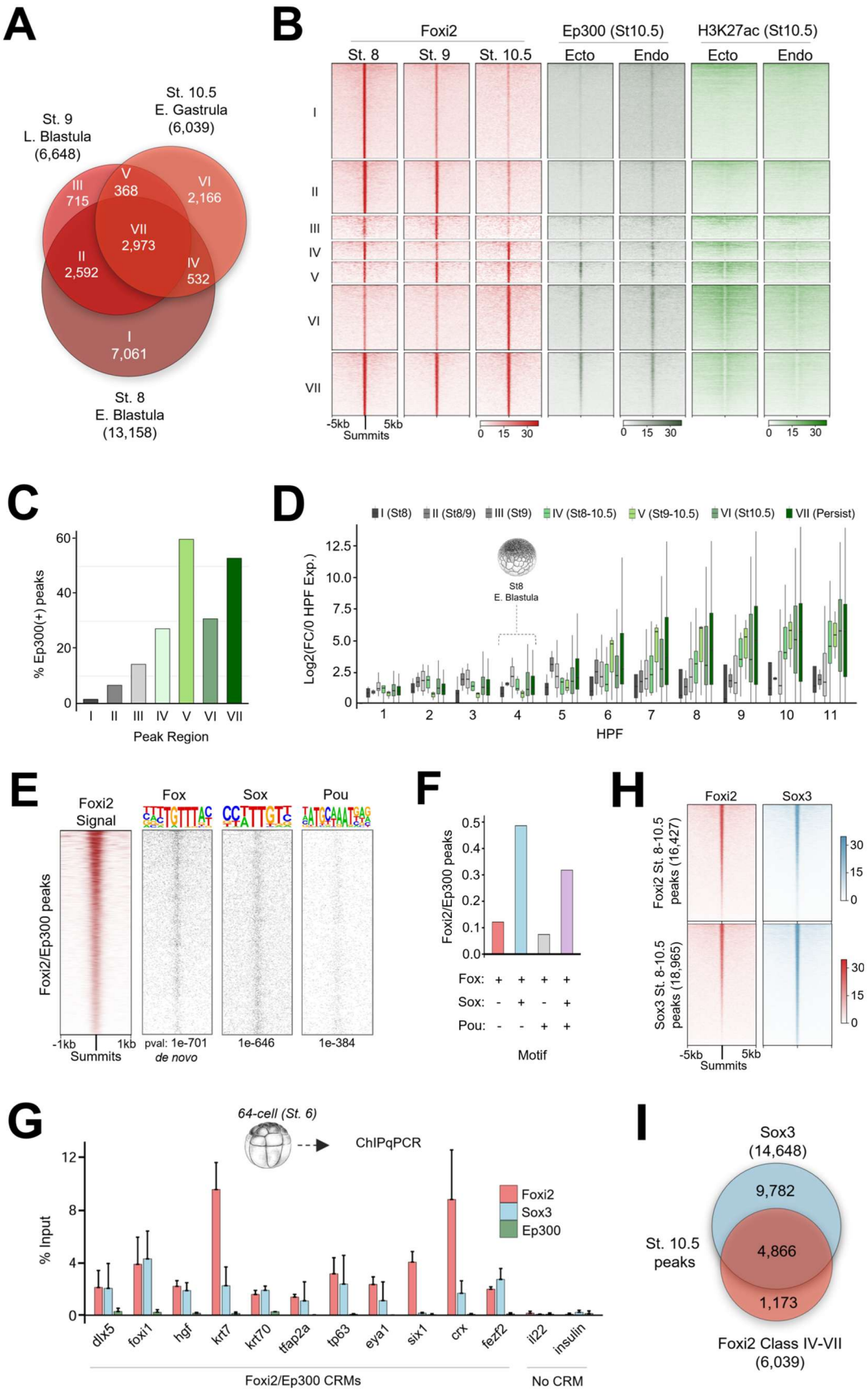
A
St. 9
L. Blastula
(6,648)
St. 10.5
E. Gastrula
(6,039)
St. 8
E. Blastula
(13,158)
III
715
V
368
VI
2,166
VII
2,973
II
2,592
IV
532
I
7,061
B
Foxi2
St. 8
St. 9
St. 10.5
Ep300 (St10.5)
Ecto
Endo
H3K27ac (St10.5)
Ecto
Endo
I
II
III
IV
V
VI
VII
-5kb
5kb
Summits
0 15 30
C
% Ep300(+) peaks
60
40
20
0
I II III IV V VI VII
Peak Region
D
I (St8) II (St8/9) III (St9) IV (St8-10.5) V (St9-10.5) VI (St10.5) VII (Persist)
Log2(FC/0 HPF Exp.)
12.5
10.0
7.5
5.0
2.5
0
St8
E. Blastula
1 2 3 4 5 6 7 8 9 10 11
HPF
E
Foxi2
Signal
Fox
Sox
Pou
Foxi2/Ep300 peaks
-1kb
1kb
Summits
pval: 1e-701
de novo
1e-646
1e-384
F
Foxi2/Ep300 peaks
0.5
0.4
0.3
0.2
0.1
0.0
Fox: + + + +
Sox: - + - +
Pou: - - + +
Motif
H
Foxi2
Sox3
Foxi2 St. 8-10.5
peaks (16,427)
Sox3 St. 8-10.5
peaks (18,965)
30
15
0
30
15
0
-5kb
5kb
Summits
G
64-cell (St. 6)
ChIPqPCR
% Input
12
8
4
0
Foxi2
Sox3
Ep300
dlx5
foxi1
hgf
krt7
krt70
tfap2a
tp63
eya1
six1
crx
fezf2
il22
insulin
Foxi2/Ep300 CRMs
No CRM
I
Sox3
(14,648)
9,782
St. 10.5
peaks
4,866
1,173
Foxi2 Class IV-VII
(6,039)

Figure 2.3: ***Temporal Dynamics and Motif Analysis of Foxi2 DNA Binding and Co-Occupancy with Sox3 and Ep300 from Blastula to Early Gastrula.*** **(A)** Venn diagram showing temporal dynamics of Foxi2 DNA binding, with ChIP-seq peaks categorized into Classes I-VII. **(B)** Analysis comparing Ep300 and H3K27ac signals from early gastrula ectoderm and endoderm dissection, within Foxi2 peak classification. **(C)** Proportion of Foxi2 class I-VII peaks overlapping Ep300 peaks from early gastrula ectoderm. **(D)** Temporal RNA expression profiles of genes within 20kb of Foxi2/Ep300 co-bound peaks in classes I-VII. **(E)** Top predicted Fox motif and best matched Sox and Pou motifs identified within Foxi2/Ep300 peaks. **(F)** Proportion of Fox, Sox and Pou motifs present in Foxi2/Ep300 peaks. **(G)** 64-cell embryo ChIP-qPCR analysis of Foxi2, Sox3 and Ep300 binding at early gastrula Foxi2/Ep300 co-bound regions. Error bars represent standard deviation from biological duplicates, ChIP samples were normalized by their percent recovery compared to input (non-pulldown) samples. **(H)** Total early blastula to early gastrula Foxi2 (top) and Sox3 (bottom) peaks with early gastrula Foxi2 and Sox3 signal. **(I)** Early gastrula Sox3 peak overlap with Foxi2 class IV-VII “active” peaks.

to classes I, II and III (Figure 2.3B, Figure 2.4B). In total, 3,050 Foxi2 regions are Ep300 co-occupied, where class IV, V, VI and VII Foxi2 peaks show the highest degree of overlap with both Ep300 and H3K27ac (Figure 2.3B,C, Figure 2.4B,C). We bioinformatically assigned nearest zygotic genes to the Foxi2 peaks marked by Ep300 and examined whether these CRMs are linked to transcriptional activity of the genes. We find that class IV, V, VI and VII genes become transcriptionally active during gastrulation, whereas class I, II and III genes remain inactive (Figure 2.3D). These results suggest that Foxi2 peaks (1) present at stage 10.5, either uniquely or overlapping with blastula stage binding, (2) are co-bound with ectodermal Ep300, (3) decorated with ectodermal H3K27ac and (4) associated with genes expressed post ZGA, thus representing active CRMs.

TFs form complexes on CRMs and typically act in combination. To predict potential co-factors that may work together with Foxi2, we characterized TF motifs enriched within Foxi2 bound regions. As expected, *de novo* motif analysis reveals Fox motifs are the most centrally enriched (Figure 2.3E). Besides the Fox motif, the next most abundantly present and centrally enriched motifs are Sox and Pou. These Fox/Sox/Pou motifs co-occur in 33% of Foxi2 peaks bound by Ep300, potentially suggesting complex formation (Fig 2.3F). Interestingly, while 48% of Foxi2 peaks contain only Fox/Sox motifs, just 7% contain only Fox/Pou motifs (Figure 2.3E,F).

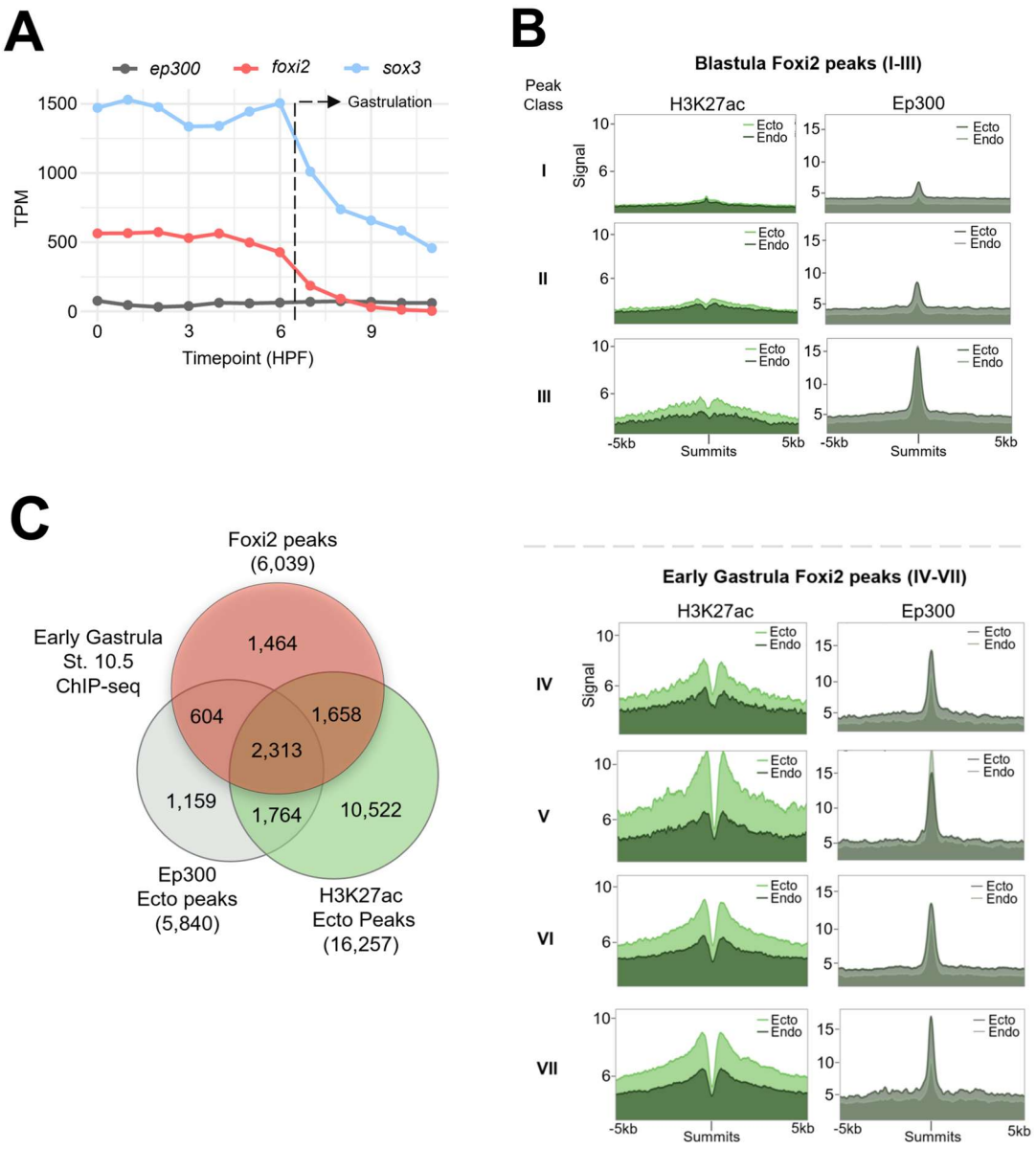

Figure 2.4: ***Temporal Foxi2 binding and epigenetic marking deposition.*** **(A)** Time course of mRNA expression for ep300, foxi2, and sox3. **(B)** Average signal density plots showing enrichment of H3K27ac and Ep300 peaks around Foxi2 binding sites in ectodermal and endodermal tissues, based on clusters I–VII defined in Figure 2A and B. **(C)** Venn diagram illustrating the overlap of peaks among Foxi2, Ep300, and H3K27ac in early gastrula-stage embryos.

Given Foxi2 and Sox3 high rate of motif co-occurrence, and their maternal expression, we assessed whether Foxi2 and Sox3 prebind functional ectoderm CRMs, before Ep300 recruitment and the onset of ZGA. Foxi2, Sox3 and Ep300 ChIP-qPCR analysis of 64-cell stage embryos (st. 6.5, ~3hpf) reveals that Foxi2 and Sox3, but not Ep300, occupy CRMs for *dlx5, foxi1, hgf, krt7, krt70, tfap2a, and tp63* (Figure 2.3G), which are expressed in the ectoderm of the early gastrula. This demonstrates that Foxi2 and Sox3 prebind to these ectodermal CRMs during cleavage stages, thus prior to ZGA (st. 8.5, ~4-4.5hpf), and before the recruitment of Ep300. Additionally, we discovered that these maternal TFs pre-mark CRMs of *eya1*, *six1, crx,* and *fezf2*, which are expressed in the preplacodal region (PPR) or anterior neural plate of neurula stage embryos (Moody et al., 2015; Maharana and Schlosser, 2018). This finding demonstrates that these maternal TFs initially recognize the CRMs of future ectodermally expressed genes during the cleavage stages.

Active ectodermal CRMs are co-occupied by Foxi2 and Sox3

Given that 64-cell stage embryos (st. 6.5, ~3hpf) have not begun zygotic gene expression, we asked if early Foxi2 and Sox3 colocalization was maintained through ZGA. Sox3 ChIP-seq during the mid- through late blastula (st. 8-9) and the early gastrula (st. 10.5), yielded a total of 18,965 peaks, which are highly co-occupied by Foxi2 (Figure 2.3H, Figure 2.5A,B). From the mid-blastula to early gastrula both factors increase reciprocal binding throughout each other's bound regions (Figure 2.5A). Sox3 signal is reciprocally enriched throughout many of the total 16,427 blastula to early gastrula Foxi2 peaks (Figure 2.3H). We examined the dynamic binding of Foxi2 and Sox3 around several ectodermally expressed genes and observed that their co-occupancy is either maintained or increases from the early blastula to the early gastrula (Figure 2.5B). By the early gastrula, Sox3 is enriched within ~81% of Foxi2 class IV, V, VI, VII peaks, which demonstrate the highest Ep300 overlap and associated

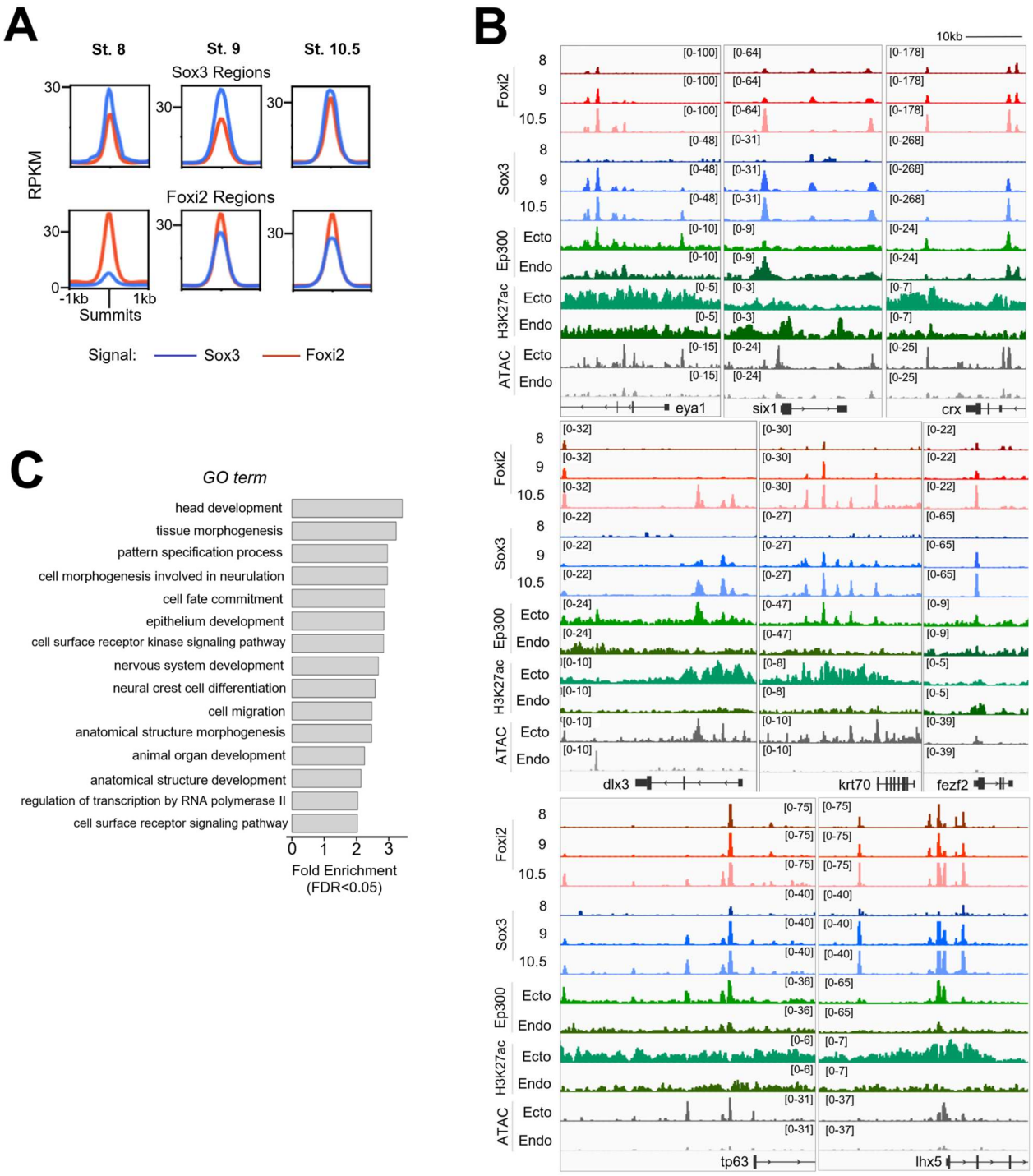

Figure 2.5: ***Co-occupancy of Foxi2 and Sox3 on the embryonic genome.*** **(A)** Overlap of Sox3 and Foxi2 ChIP-seq peaks in stage 8, 9, and 10.5 embryos, indicating dynamic co-binding across developmental timepoints. **(B)** Genome browser views showing Foxi2 and Sox3 binding near ectodermally expressed genes across multiple stages, alongside with Ep300, H3K27ac and ATAC-seq profiles from dissected ectodermal and endodermal explants. **(C)** Gene ontology (GO) enrichment analysis of Foxi2/Sox3 co-bound peaks that are also marked by Ep300.

gene expression response (Fig 2.3I). These data suggest that Foxi2 and Sox3 initiate and maintain significant colocalization on ectodermal CRMs during ZGA through the onset of gastrulation (Figure 2.5B).

Sox3 specifically binds a total of 5,828, 4,402 and 14,648 peaks in stage 8, 9, and 10.5 embryos (Figure 2.6A). To better understand Sox3 we investigated its Ep300 overlap, in line with our Foxi2 ChIP-seq analyses. Sox3 peaks display temporally unique (class I, III, VII), shared (class II, IV, VI), and persistently occupied (class V) binding patterns (Figure 2.6A,B). Class V, VI, and VII peaks all displayed higher Ep300 binding overlap and H3K27ac deposition compared to class I, II, III, and IV (Figure 2.6B,C), suggesting that class V, VI and VII associated genes are active. These results imply that, like Foxi2, Sox3 peaks that persist from stage 8-10.5 and 9-10.5, or are specifically bound at stage 10.5, are associated with Ep300 and represent active CRMs. We examined whether these CRMs are linked to transcriptional activity of the genes. Similar to Foxi2, Sox3 Class IV, V, VI and VII associated genes are expressed at higher levels compared to class I, II and III genes (Figure 2.6D).

Next, we further examined the genomic colocalization of Foxi2 and Sox3 in the context of ectoderm specific Ep300 binding. Among the 4,866 Foxi2 and Sox3 early gastrula co-bound regions (Figure 2.3I), 2,901 also overlap with ectodermal Ep300 peaks (Figure 2.6E). These overlapping regions account for 95% of the 3,050 Foxi2/Ep300 peaks and 72% of the 4,015 Sox3/Ep300 peaks (Figure 2.6E). Additionally, these CRM regions show significantly higher Ep300 binding and H3K27ac mark deposition in the ectoderm compared to endoderm, suggesting their functional importance in ectodermal gene regulation (Figure 2.6F, Figure 2.5B). Linking 2,901 Foxi2/Sox3 CRMs co-bound with Ep300 to their nearest genes, we find highly significant GO terms related to cell fate specification of neural (e.g., *fezf2, neurog3*, *zic3*), and epidermal lineages (e.g., *dlx3*, *grhl2*, *krt7*) (Figure 2.5C). This suggests that Foxi2 and Sox3 orchestrate a cis-regulatory code critical for driving both neural and non-neural ectoderm specification.

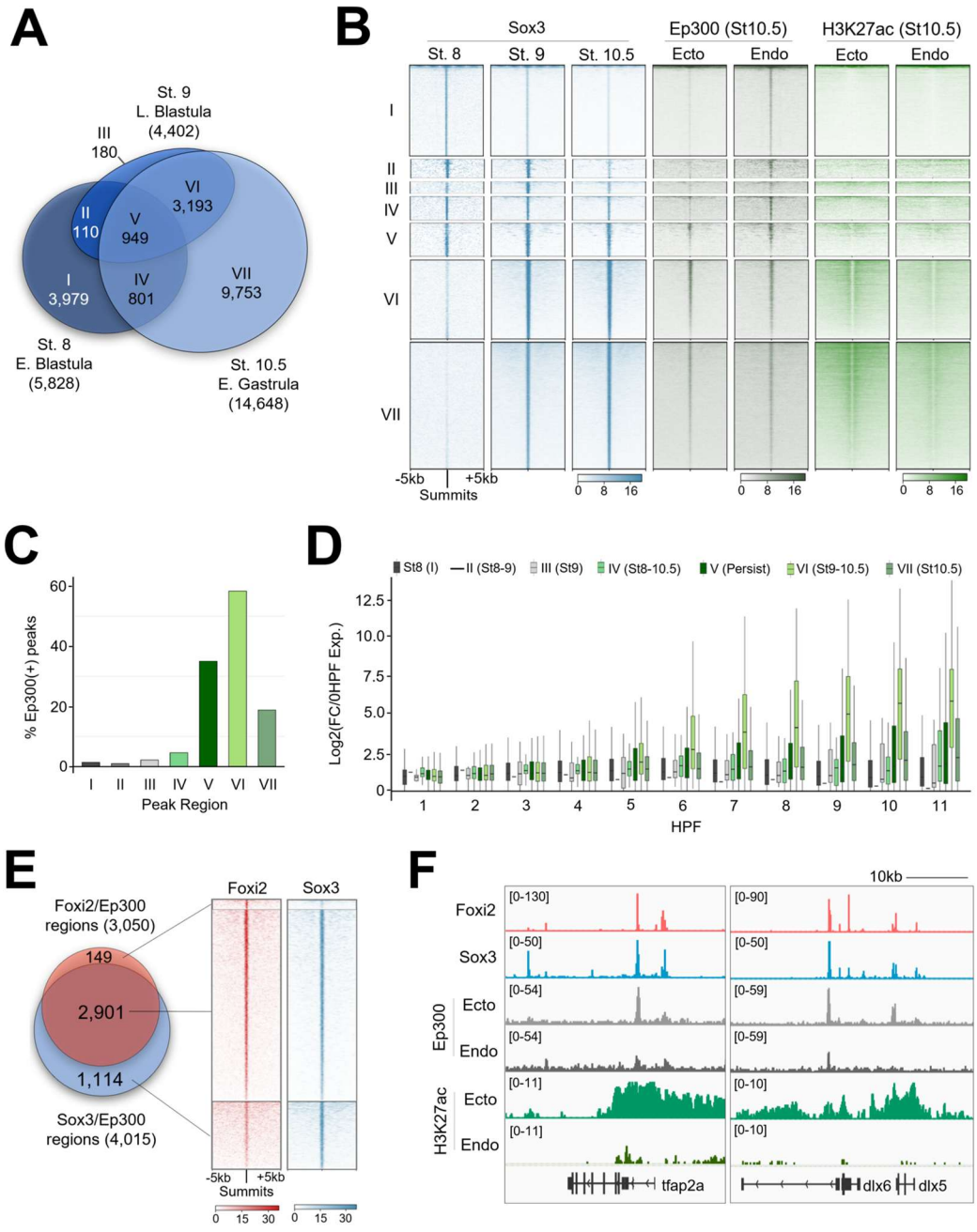

Figure 2.6: ***Foxi2 and Sox3 Preferentially Colocalize at Ectoderm CRMs in the Presence of Ep300.*** **(A**) Venn diagram illustrating the temporal dynamics of Sox3 ChIP-seq peaks, classified into categories I-VII. **(B)** Clustering analysis comparing Sox3 peak classifications with Ep300 and H3K27ac signals from early gastrula ectoderm and endoderm dissection. **(C)** Proportion of Sox3 class I-VII peaks overlapping with Ep300 peaks. **(D)** Temporal gene expression profiles of genes located within 20kb of Sox3/Ep300 co-bound peaks in Class I-VII. **(E)** Comparison of Foxi2 and Sox3 co-bound and independently bound regions overlapping with Ep300. **(F)** Genome browser tracks highlighting selected ectodermally-expressed genes with Foxi2, Sox3 and Ep300 binding.

In early gastrula stage embryos, ectodermal genes such as *dlx5*, *foxi1*, *hgf*, *krt7*, *krt70*, *tfap2a*, and *tp63*, are bound by both Foxi2 and Sox3, and overlap with Ep300 peaks (Figure 2.6F, Figure 2.5B). Interestingly, these CRMs are also premarked by Foxi2 and Sox3 by the 64-cell stage (Figure 2.3G). Given the established role of the Foxi family TFs in sensory placode formation (Solomon et al., 2003; Matsuo-Takasaki et al., 2005), we examined the key sensory placode genes, such as *eya1*, *six1*, and the anterior neural marker *fezf2,* which we found to be marked during cleavage stage (Figure 2.3G). Indeed, these genes are also co-bound by Foxi2 and Sox3 in the early gastrula stage embryos (Figure 2.5B), sharing the same CRMs pre-bound by Foxi2 and Sox3 during cleavage stages (Figure 2.3G). These findings underscore the master regulatory role of maternal TFs in pre-marking critical ectodermal CRMs for future gene expression.

Independent and cooperative roles of Foxi2 and Sox3 regulate ectodermal gene expression

To investigate the molecular function of Foxi2 and Sox3, we generated Foxi2 and Sox3 knockdown phenotypes using translation-blocking morpholino antisense oligonucleotides (MOs) (Figure 2.7A,B). Embryos injected with Foxi2 or Sox3 MOs showed substantial depletion of Foxi2 and Sox3 proteins (Figure 2.8A). While only a minority of Sox3 morphants exhibited decreases in body length and inhibited blastopore closure, Foxi2 knockdown embryos showed robust defects in both dorsoventral patterning and body length, as well as reduced head size (Figure 2.8B). RNA-seq analysis of both Foxi2 and Sox3 morphants compared to wild-type embryos identified genes activated and repressed by Foxi2 and Sox3 (Figure 2.8C,D). We intersected these data with Foxi2 and Sox3 ChIP-seq datasets to identify direct target genes, defined as those showing at least a 2-fold change in expression in the morphants and having

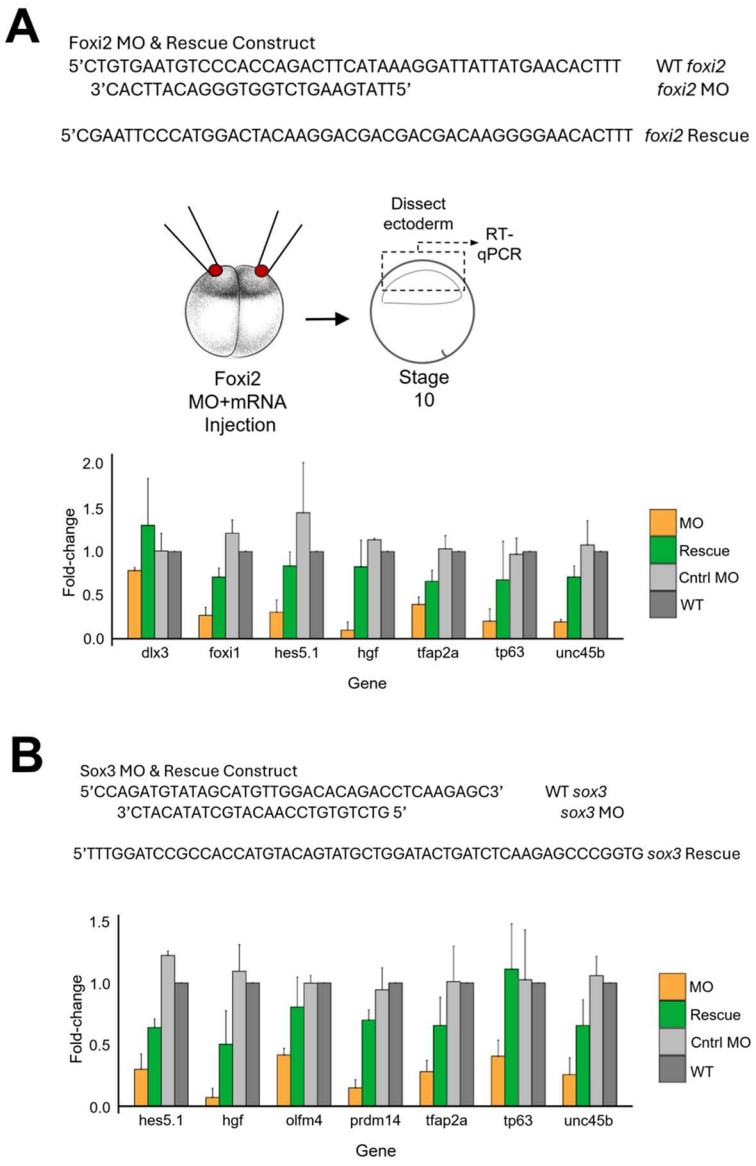

Figure 2.7*: Foxi2 and Sox3 morpholino knockdown specificity.* **(A)** Alignment of the foxi2 morpholino (MO) sequence with the wild-type target site and the rescue mRNA 5' coding sequence used in the rescue experiment. A schematic illustrates the isolation of ectodermal tissues from wild-type, morpholino-injected, and rescued embryos. The bar graph shows fold changes in the expression of Foxi2 direct target genes in foxi2 morphants. **(B)** Alignment of the sox3 MO sequence with the wild-type sox3 gene and the corresponding rescue 5' mRNA coding sequence overlapping the MO target site. The bar graph shows fold changes in the expression of Sox3 direct target genes in sox3 morphants.

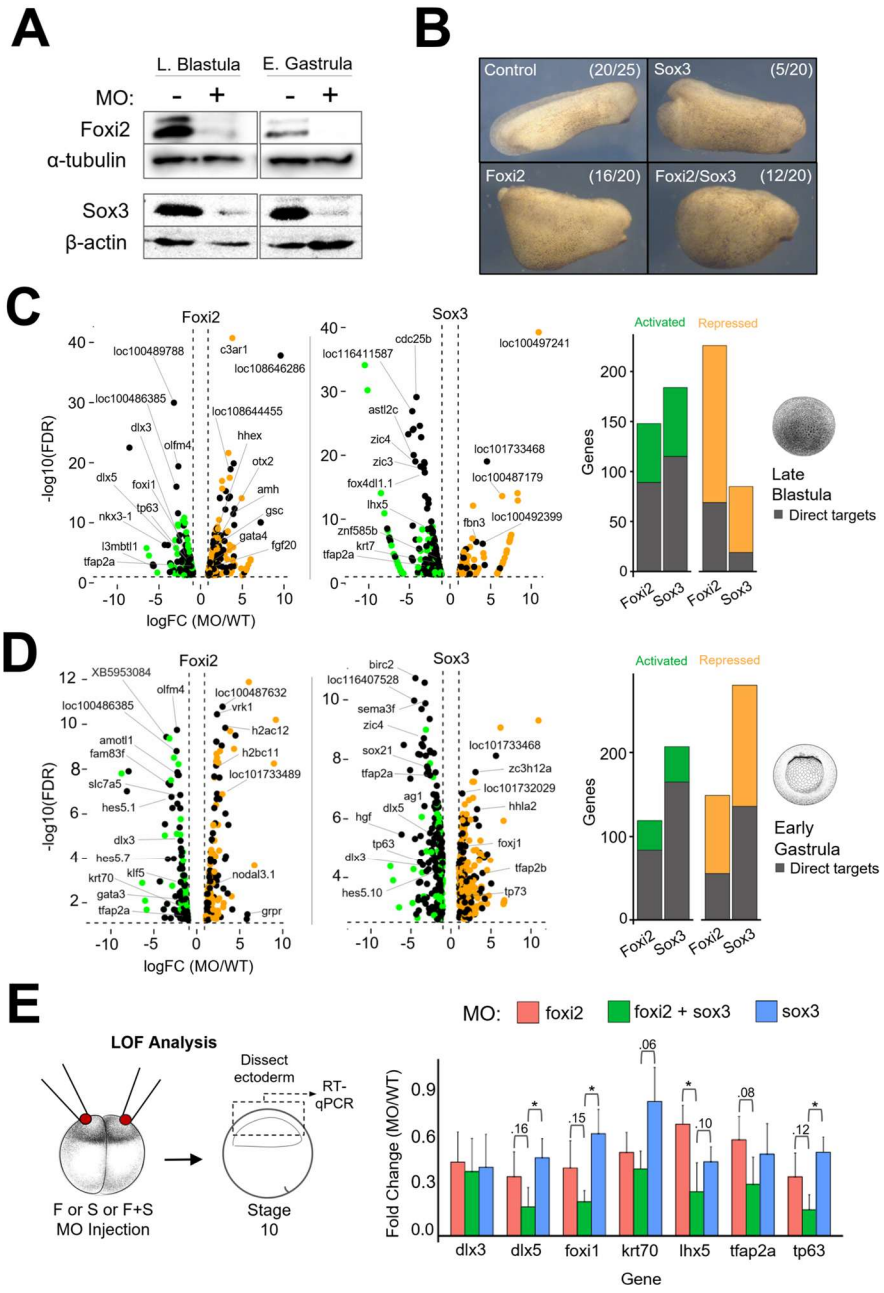

Figure 2.8 ***Independent and Cooperative Roles of Foxi2 and Sox3 in Regulating Ectodermal Gene Expression.*** **(A)** Western blot of Foxi2 and Sox3 morphant embryos at late blastula and early gastrula stages. **(B)** Phenotypic analysis of Foxi2, Sox3 and Foxi2/Sox3 morphants at the early tailbud stage. **(C,D)** RNA-seq analysis of late blastula embryos (top) and early gastrula embryos (bottom) showing activated and repressed genes within 20kb of Foxi2/Sox3 bound regions. Histograms show the total number of direct target genes affected in morphants. **(E)** Schematic diagram of loss-of-function experiment (left). RT-qPCR analysis of key ectodermally-expressed genes (right) in early gastrula ectoderm of Foxi2, Sox3 and Foxi2/Sox3 morphants. *eef1a1* expression was used for normalization. Error bars represent standard deviation from 3 biological replicates, asterisks indicate statistically significant differences ($p < 0.05$) determined by Student's t-test.

Foxi2 and/or Sox3 binding sites within 20kb of the gene (Figure 2.8C,D).

At the late blastula stage, Foxi2 and Sox3 directly activate 78 and 114 genes, and repress 68 and 18 genes, respectively (Figure 2.8C). A similar analysis in gastrula-stage embryos revealed that Foxi2 and Sox3 directly activate 72 and 164 genes and repress 54 and 136 genes, respectively (Figure 2.8D). Intersecting the lists of genes activated by Foxi2 and Sox3 identifies 34 genes co-bound and co-regulated by both factors. These genes include well-studied ectodermal transcription factors such as *dlx3, dlx5, foxi1, hes5.1, tfap2a,* and *tp63* (Moody and LaMantia, 2015; Maharana and Schlosser, 2018). RT-qPCR analysis confirms that these ectodermal TFs are jointly regulated by both factors (Figure 2.8E). Separately, 115 genes are regulated solely by Foxi2, while 243 genes are regulated solely by Sox3. Specific targets of Foxi2 include*, amotl1, dlc, gata3, kit, klf5,* and *krt70*, while direct targets of Sox3 include *cdx4, foxb1, foxd4l1.2, hes5.10, neurog3, olig4, sox21, zic3,* and *zic4.* These data suggest that Sox3 and Foxi2 regulate their specific target genes both jointly and independently, serving as master TFs that govern the early ectodermal program.

Foxi2 and Sox3 directly co-regulate spatially distinct inner and outer layer cell states

To gain a deeper understanding of gastrula ectoderm differentiation than can be provided by bulk RNA-seq analyses, we assessed nascent transcripts at the single cell level by performing single nucleus (sn) RNA-seq on stage 10.5 wild-type embryos. We then characterized the cell-type specific expression of Foxi2 and Sox3 direct target genes within this dataset. Pre-processing using a 1500 genes/cell cut-off yielded 13,711 high quality early gastrula nuclei (Figure 2.10A). *De novo* clustering and marker gene expression analysis identified a total of 13

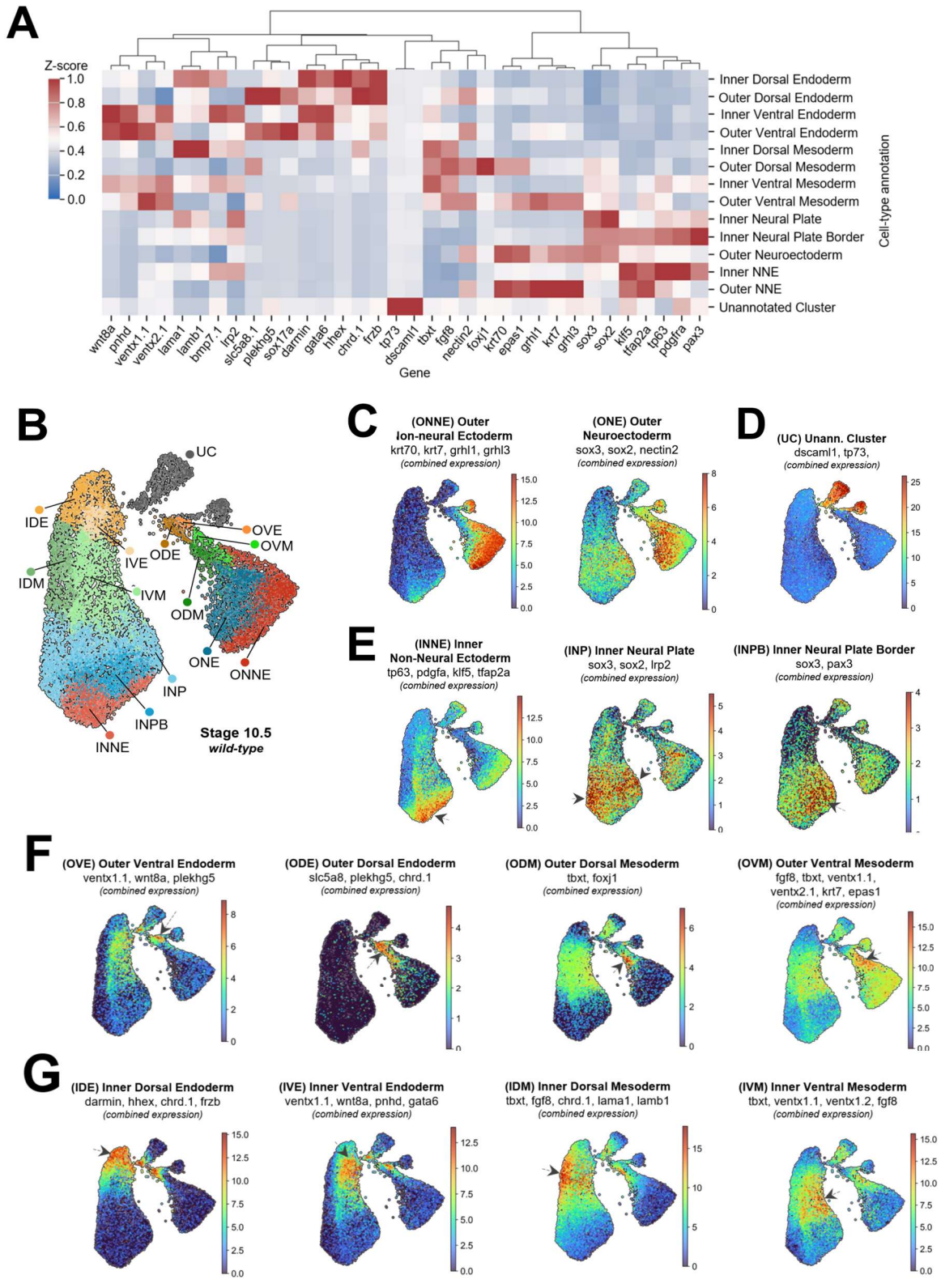
A
Z-score
1.0
0.8
0.6
0.4
0.2
0.0
Inner Dorsal Endoderm
Outer Dorsal Endoderm
Inner Ventral Endoderm
Outer Ventral Endoderm
Inner Dorsal Mesoderm
Outer Dorsal Mesoderm
Inner Ventral Mesoderm
Outer Ventral Mesoderm
Inner Neural Plate
Inner Neural Plate Border
Outer Neuroectoderm
Inner NNE
Outer NNE
Unannotated Cluster
Cell-type annotation
wnt8a
pnhd
ventx1.1
ventx2.1
lama1
lamb1
bmp7.1
lrp2
slc5a8.1
plekhg5
sox17a
darmin
gata6
hhex
chrd.1
frzb
tp73
dscaml1
tbxt
fgf8
nectin2
foxj1
krt70
epas1
grhl1
krt7
grhl3
sox3
sox2
klf5
tfap2a
tp63
pdgfra
pax3
Gene
B
UC
IDE
OVE
OVM
ODE
IVE
IDM
IVM
ODM
ONE
ONNE
INP
INPB
INNE
Stage 10.5
wild-type
C
(ONNE) Outer Non-neural Ectoderm
krt70, krt7, grhl1, grhl3
(combined expression)
(ONE) Outer Neuroectoderm
sox3, sox2, nectin2
(combined expression)
D
(UC) Unann. Cluster
dscaml1, tp73,
(combined expression)
E
(INNE) Inner Non-Neural Ectoderm
tp63, pdgfa, klf5, tfap2a
(combined expression)
(INP) Inner Neural Plate
sox3, sox2, lrp2
(combined expression)
(INPB) Inner Neural Plate Border
sox3, pax3
(combined expression)
F
(OVE) Outer Ventral Endoderm
ventx1.1, wnt8a, plekhg5
(combined expression)
(ODE) Outer Dorsal Endoderm
slc5a8, plekhg5, chrd.1
(combined expression)
(ODM) Outer Dorsal Mesoderm
tbxt, foxj1
(combined expression)
(OVM) Outer Ventral Mesoderm
fgf8, tbxt, ventx1.1, ventx2.1, krt7, epas1
(combined expression)
G
(IDE) Inner Dorsal Endoderm
darmin, hhex, chrd.1, frzb
(combined expression)
(IVE) Inner Ventral Endoderm
ventx1.1, wnt8a, pnhd, gata6
(combined expression)
(IDM) Inner Dorsal Mesoderm
tbxt, fgf8, chrd.1, lama1, lamb1
(combined expression)
(IVM) Inner Ventral Mesoderm
tbxt, ventx1.1, ventx1.2, fgf8
(combined expression)

Figure 2.9: ***De novo clustering of snRNA-seq from early gastrula embryos.*** **(A)** Heatmap showing representative marker genes across 13 identified clusters and one newly identified cluster. **(B)** UMAP representation of all cell clusters identified in stage 10.5 embryos as reference. **(C–G)** UMAP plots showing co-expression of selected genes within specific clusters, highlighting cell-type-specific transcriptional profiles and validating the locations of clusters in panel B.

defined cell states, consisting of 5 ectodermal, 4 mesodermal, and 4 endodermal cell types (Figure 2.10A, Figure 2.9A, B). The five ectodermal cell clusters map at the bottom of two major lobes in the UMAP (Figure 2.10A) and express markers that show these represent inner neural plate (INP), inner neural plate border (INPB), inner non-neural ectoderm (INNE), outer neural ectoderm (ONE), and outer non-neural ectoderm (ONNE). Notably, inner ectoderm cell clusters are positioned in the left lobe, while outer ectoderm cell clusters segregate in the right lobe (Figure 2.10A, Figure 2.9C,E). Two small lobes in the upper right (gray) contain unannotated cells (UC) that may represent a novel cell state characterized by *dscaml1* and *tp73* expression (Figure 2.9D) among others, but the identity of these cells is currently unclear.

After identifying 5 ectodermal cell clusters in stage 10.5 embryos, we mapped the expression patterns of Foxi2 and Sox3 direct target genes in the gastrula ectoderm to determine how Foxi2 and Sox3 contribute to the regional identity of this germ layer. There are 18 inner layer and 14 outer layer bound ectoderm target genes that are exclusively regulated by Foxi2, which include *amotl1, klf5, krt70, lhx3, nkx3-1 and olfm4*. Additionally, 53 inner and 49 outer layer direct ectoderm target genes are exclusively regulated by Sox3, including *foxd4l1.2, neurog3, olig3, olig4, sal3, sox21, szl, zic3, and zic4,* many of which are involved in neurogenesis. Pan-ectodermal targets (e.g., *dlx3, hes5.1, klf5, lhx5* and *tfap2a*) are expressed across all five cell states. Some of these genes are specifically regulated by Foxi2 or Sox3 alone, while others require the combinatorial input of both Foxi2 and Sox3 (Figure 2.10C). The observations suggest that Foxi2 and Sox3 regulate genes in all five distinct cell states. Interestingly, we identified target genes of Foxi2 and Sox3

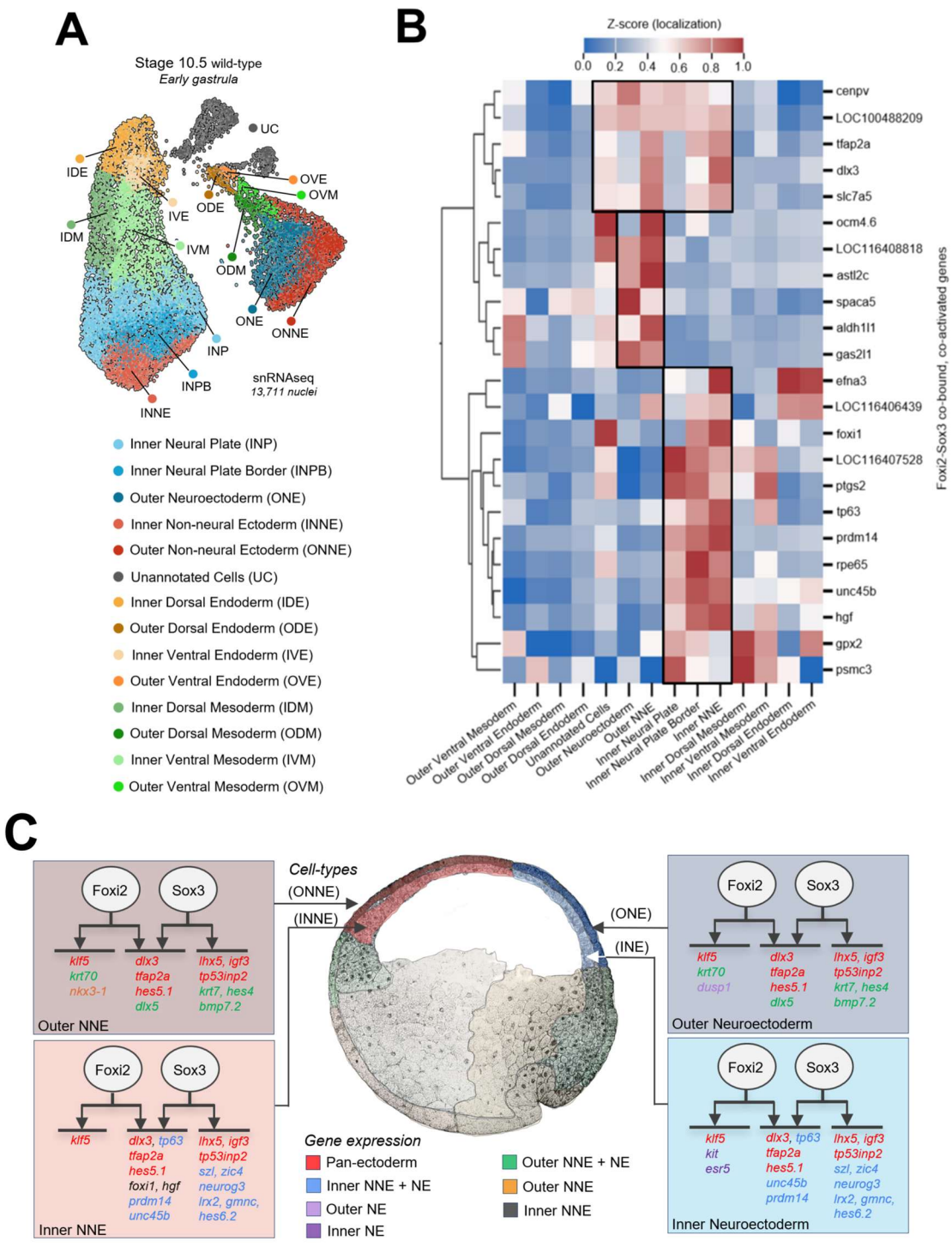
A
Stage 10.5 wild-type
Early gastrula
UC
IDE
OVE
OVM
ODE
IVE
IDM
IVM
ODM
ONE
ONNE
INP
INPB
INNE
snRNAseq
13,711 nuclei
Inner Neural Plate (INP)
Inner Neural Plate Border (INPB)
Outer Neuroectoderm (ONE)
Inner Non-neural Ectoderm (INNE)
Outer Non-neural Ectoderm (ONNE)
Unannotated Cells (UC)
Inner Dorsal Endoderm (IDE)
Outer Dorsal Endoderm (ODE)
Inner Ventral Endoderm (IVE)
Outer Ventral Endoderm (OVE)
Inner Dorsal Mesoderm (IDM)
Outer Dorsal Mesoderm (ODM)
Inner Ventral Mesoderm (IVM)
Outer Ventral Mesoderm (OVM)
B
Z-score (localization)
0.0 0.2 0.4 0.6 0.8 1.0
cenpv
LOC100488209
tfap2a
dlx3
slc7a5
ocm4.6
LOC116408818
astl2c
spaca5
aldh1l1
gas2l1
efna3
LOC116406439
foxi1
LOC116407528
ptgs2
tp63
prdm14
rpe65
unc45b
hgf
gpx2
psmc3
Foxi2-Sox3 co-bound, co-activated genes
Outer Ventral Mesoderm
Outer Ventral Endoderm
Outer Dorsal Mesoderm
Outer Dorsal Endoderm
Unannotated Cells
Outer Neuroectoderm
Outer NNE
Inner Neural Plate
Inner Neural Plate Border
Inner NNE
Inner Dorsal Mesoderm
Inner Ventral Mesoderm
Inner Dorsal Endoderm
Inner Ventral Endoderm
C
Foxi2
Sox3
klf5
krt70
nkx3-1
dlx3
tfap2a
hes5.1
dlx5
lhx5, igf3
tp53inp2
krt7, hes4
bmp7.2
Outer NNE
Cell-types
(ONNE)
(INNE)
(ONE)
(INE)
Foxi2
Sox3
klf5
krt70
dusp1
dlx3
tfap2a
hes5.1
dlx5
lhx5, igf3
tp53inp2
krt7, hes4
bmp7.2
Outer Neuroectoderm
Foxi2
Sox3
klf5
dlx3, tp63
tfap2a
hes5.1
foxi1, hgf
prdm14
unc45b
lhx5, igf3
tp53inp2
szl, zic4
neurog3
lrx2, gmnc,
hes6.2
Inner NNE
Foxi2
Sox3
klf5
kit
esr5
dlx3, tp63
tfap2a
hes5.1
unc45b
prdm14
lhx5, igf3
tp53inp2
szl, zic4
neurog3
lrx2, gmnc,
hes6.2
Inner Neuroectoderm
Gene expression
Pan-ectoderm
Inner NNE + NE
Outer NE
Inner NE
Outer NNE + NE
Outer NNE
Inner NNE

Figure 2.10: *Foxi2 and Sox3 Directly Co-regulate Genes in All Ectodermal Cell States*. (A) Single nucleus RNA-seq UMAP (uniform manifold approximation projection) identifying 14 distinct cell types in the early gastrula. **(B)** Z-score expression analysis of Foxi2/Sox3 co-bound target genes shows distinct gene expression patterns marking outer and inner ectodermal cell types. **(C)** Schematic diagram depicting the regulatory roles of Foxi2 and Sox3, either independently or jointly, in activating the expression of target genes across various ectodermal cell types.that are specifically expressed in the inner (both non-neural and neural) ectodermal layer, such as *foxi1, prdm14, szl, tp63,* and *zic4*. Similarly, genes such as *dlx5, hes4* and *krt70* are expressed in the outer (both non-neural and neural) ectodermal cell states. Since Foxi2 and/or Sox3 regulate genes across both distinct ectodermal layers, we suggest that additional factors, like Prkci and Mark3, might play a role in differential segregation of these cell layers (Chalmers et al. 2003, Ossipova et al., 2007, Tabler et al., 2010).

Foxi2 and Sox3 are master regulators shaping the ectodermal epigenetic landscape

Given the potential synergy of Foxi2 and Sox3 within the ectoderm and their distinct roles in ectoderm target gene activation, could Foxi2 and Sox3 together serve as master regulators of ectodermal differentiation? To test this hypothesis, we injected Foxi2 and/or Sox3 mRNA into the vegetal pole and assessed the endoderm cell state in dissected vegetal tissue explants at gastrula stage 10.5 (Figure 2.11A). While overexpression of Foxi2 or Sox3 alone induced modest ectoderm gene expression, coinjection of both factors robustly activated the ectodermal genes, *dlx5*, *foxi1, krt70*, *lhx5* and *tfap2a*. Moreover, expression of key endodermal genes such as *gata4*, *gsc*, *hhex* and *otx2* was significantly reduced in endodermal explants co-expressing Foxi2 and Sox3 mRNA. These findings support Foxi2 and Sox3 working together as master regulators of ectodermal identity.

In addition to the transcriptional role of Foxi2 and Sox3 in specifying the ectodermal cell state, we determined whether Foxi2 and Sox3 also shape the epigenetic landscape of ectodermal cells. Temporal analysis of H3K27ac and H3K4me1 signal deposition around 2,901 CRMs co-bound by Foxi2, Sox3, and Ep300 (FSE) (Figure 2.6E), reveals an increase from the early blastula to the early gastrula stage compared to independent Ep300 regions (Figure 2.11B). Interestingly, the repressive mark, H3K27me3 becomes gradually enriched around

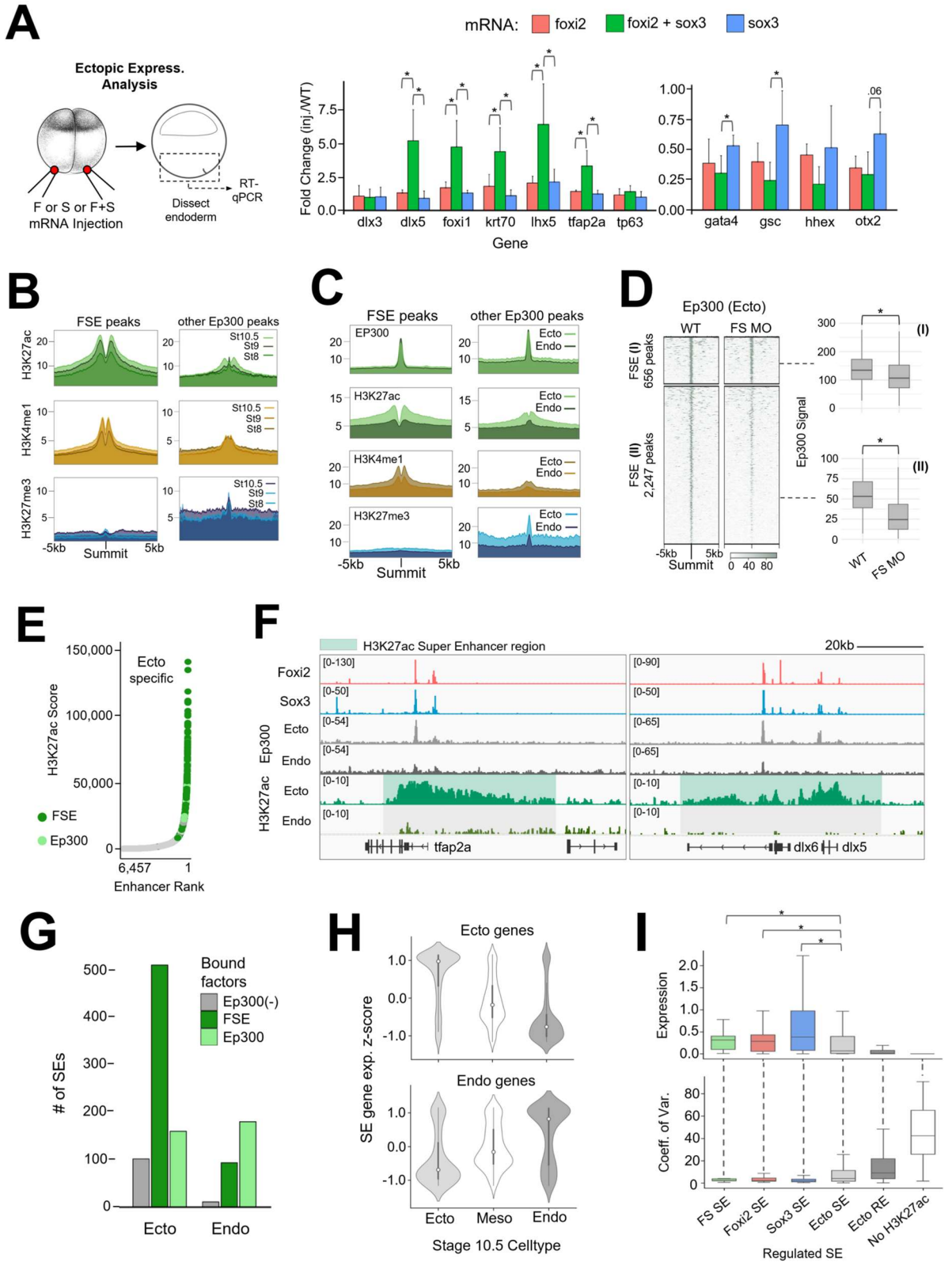
A
Ectopic Express. Analysis
F or S or F+S mRNA Injection
Dissect endoderm
RT-qPCR
mRNA: foxi2 foxi2 + sox3 sox3
Fold Change (inj./WT)
dlx3 dlx5 foxi1 krt70 lhx5 tfap2a tp63
gata4 gsc hhex otx2
Gene
B
FSE peaks
other Ep300 peaks
H3K27ac
H3K4me1
H3K27me3
St10.5 St9 St8
-5kb Summit 5kb
C
FSE peaks
other Ep300 peaks
EP300
H3K27ac
H3K4me1
H3K27me3
Ecto Endo
-5kb Summit 5kb
D
Ep300 (Ecto)
WT FS MO
FSE (I) 656 peaks
FSE (II) 2,247 peaks
Ep300 Signal
(I) (II)
-5kb Summit 5kb
0 40 80
WT FS MO
E
H3K27ac Score
150,000 100,000 50,000 0
Ecto specific
FSE
Ep300
6,457 1
Enhancer Rank
F
H3K27ac Super Enhancer region
20kb
Foxi2 Sox3 Ecto Endo
Ep300 H3K27ac
tfap2a dlx6 dlx5
G
# of SEs
500 400 300 200 100 0
Bound factors
Ep300(-)
FSE
Ep300
Ecto Endo
H
Ecto genes
Endo genes
SE gene exp. z-score
1.0 0.0 -1.0
Ecto Meso Endo
Stage 10.5 Celltype
I
Expression
Coeff. of Var.
FS SE Foxi2 SE Sox3 SE Ecto SE Ecto RE No H3K27ac
Regulated SE

Figure 2.11: ***Foxi2 and Sox3 are Master Regulators Shaping the Ectodermal Super Enhancer Landscape.*** **(A)** Schematic diagram of the experimental design (left). RT-qPCR analysis of key ectoderm and endoderm genes from early gastrula endoderm after ectopic expression of 1ng Foxi2, Sox3 or Foxi2/Sox3 mRNA. *eef1a1* expression was used for normalization. Error bars represent standard deviation from 3 biological replicates, asterisks indicate statistically significant differences ($p < 0.05$) determined by Student's t-test. **(B)** Accumulation of H3K27ac, H3K4me1 and H3K27me3 histone modifications around Foxi2/Sox3/Ep300 (FSE) co-occupied, and other solely bound Ep300 peaks. **(C)** Deposition of Ep300, H3K27ac, H3K4me1 and H3K27me3 at FSE and other Ep300 peaks present in the early gastrula ectoderm and endoderm. **(D)** Comparison of Ep300 deposition on FSE peaks between FS MO treated and WT embryo dissected ectoderm. **(E)** Total ectoderm SEs associated with FSE co-occupied peaks and Ep300 solely occupied peaks. **(F)** Genome browser views of ectodermal SEs (shaded area), which are present (highly acetylated) in ectoderm but absent in endoderm. **(G)** Histogram comparing the total number of peaks associated with super enhancers containing Foxi2/Sox3 and Ep300 (FSE), Ep300 with insignificant Foxi2/Sox3 binding (no Ep300), and without Ep300 (Ep300(-)). FSE peaks are highly associated with ectodermal SEs. **(H)** Z-score expression analysis of genes located within 20kb of ectoderm (top) and endoderm (bottom) SEs. snRNA-seq cell-type expression analysis reveals that genes associated with ectodermal SEs are preferentially expressed in ectodermal cells. **(I)** Average expression levels (top) of Foxi2- and/or Sox3-regulated ectodermal SE-associated genes compared to all enhancer associated genes. Coefficient of variation (COV) analysis (bottom) shows that Foxi2 and/or Sox3-regulated ectodermal SE-associated genes exhibit less variability in expression compared to all enhancer-associated genes using snRNA-seq. Asterisks indicate statistically significant differences ($p < 0.05$) determined by Wilcoxon Rank-Sum test.

Ep300 peaks lacking Foxi2 and Sox3 binding (Figure 2.11B). These results suggest that Foxi2/Sox3 co-binding promotes H3K27ac and H3K4me1 enrichment at the expense of H3K27me3 deposition around ectodermal CRMs.

To overcome the lack of germ layer resolution in whole-embryo histone marking studies, we also performed experiments using dissected ectodermal and endodermal tissues from the early gastrula stage. While no significant differences in Ep300 binding were observed between ectoderm and endoderm at both Foxi2-Sox3 co-bound (FSE) regions and Ep300 only peaks (lacking Foxi2/Sox3) (Figure 2.11C), we found a significant difference in histone modifications. In the ectoderm, FSE regions showed significant accumulation of H3K27ac and H3K4me1, while H3K27me3 deposition is notably absent (Figure 2.11C). In contrast, Ep300-only peaks showed modest H3K27ac and H3K4me1 accumulation but displayed strong H3K27me3 enrichment. These findings suggest that Foxi2 and Sox3 specifically regulate the epigenetic landscape of ectodermal genes within the ectodermal germ layer, but not in the endoderm.

We sought to determine the role of Foxi2 and Sox3 in establishing the ectoderm specific epigenetic landscape by measuring Ep300 genomic recruitment in the absence of both factors. To determine whether Foxi2 and Sox3 are required for tissue specific Ep300 recruitment, we performed ChIP-seq on dissected ectoderm and endoderm from FS MO injected and WT embryos. Signal based K-means clustering was performed to form FSE (I) and FSE (II) peak groups, which both display significant Ep300 deposition decreases in FS MO embryos compared to wild type (Figure 2.11D). Additionally, in FS MO embryos both non-FSE ectoderm Ep300, and vegetal Ep300 bound regions did not display significant decreases in Ep300 deposition (Figure 2.12B). Taken together these data indicate that Foxi2 and Sox3 colocalization is required to recruit Ep300 to Foxi2 and Sox3 bound CRMs, comprising 49.7% of total ectodermal Ep300 bound regions in the early gastrula.

Foxi2 and Sox3 marked regions establish ectodermal super enhancers to ensure robust gene expression

The high levels of H3K27ac modifications around Foxi2 and Sox3 co-bound sites raises the question of whether some of these regions are located within super enhancers (SEs), which are large clusters of enhancers characterized by high levels of TFs, coactivators (such as Mediator), and chromatin modifiers. SEs are typically identified by analyzing genomic regions highly marked by H3K27ac (Whyte et al., 2013). H3K27ac ChIP-seq analysis of ectodermal and endodermal explants identified 14,088 ectoderm and 15,469 endoderm enhancer peaks (“regular” enhancers, REs), with 6,962 being shared between the two germ layers (Figure 2.12C). Our investigation also identified SEs in both ectoderm and endoderm based on their increased size and H3K27ac deposition relative to the enhancer landscape (Fig. 6E, Figure 2.12C). The average size of both ectodermal and endodermal SEs is ~20kb per locus, which is significantly larger than “regular” enhancer (RE) loci, which are

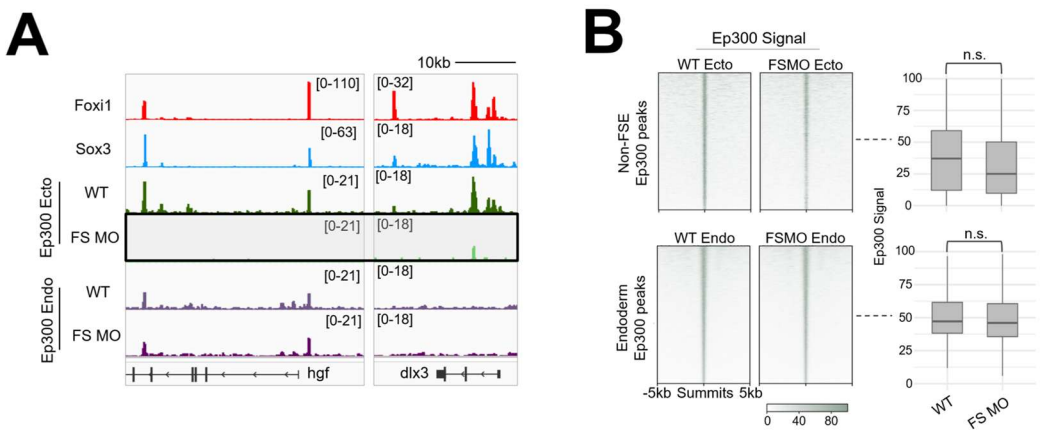
A
10kb
Foxi1
Sox3
WT
FS MO
Ep300 Ecto
Ep300 Endo
[0-110]
[0-63]
[0-32]
[0-18]
[0-21]
hgf
dlx3
B
Ep300 Signal
WT Ecto
FSMO Ecto
WT Endo
FSMO Endo
Non-FSE Ep300 peaks
Endoderm Ep300 peaks
-5kb Summits 5kb
n.s.
Ep300 Signal
WT
FS MO

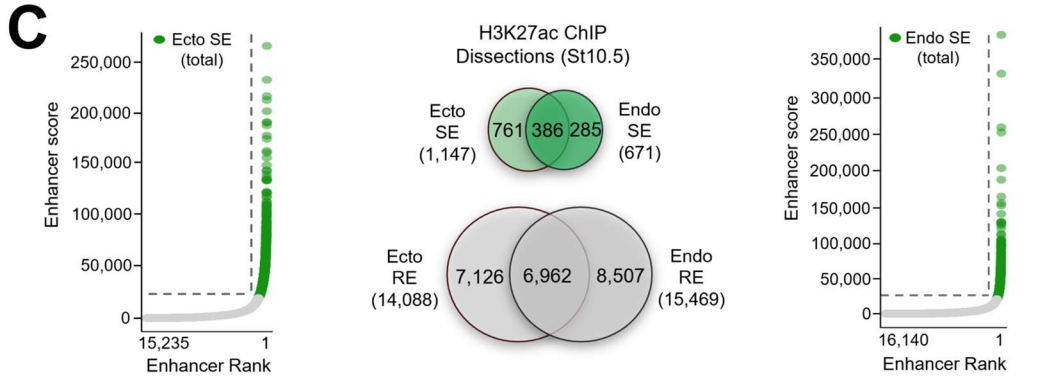
C
Ecto SE (total)
Enhancer score
Enhancer Rank
15,235
H3K27ac ChIP Dissections (St10.5)
Ecto SE (1,147)
761
386
285
Endo SE (671)
Ecto RE (14,088)
7,126
6,962
8,507
Endo RE (15,469)
Endo SE (total)
16,140

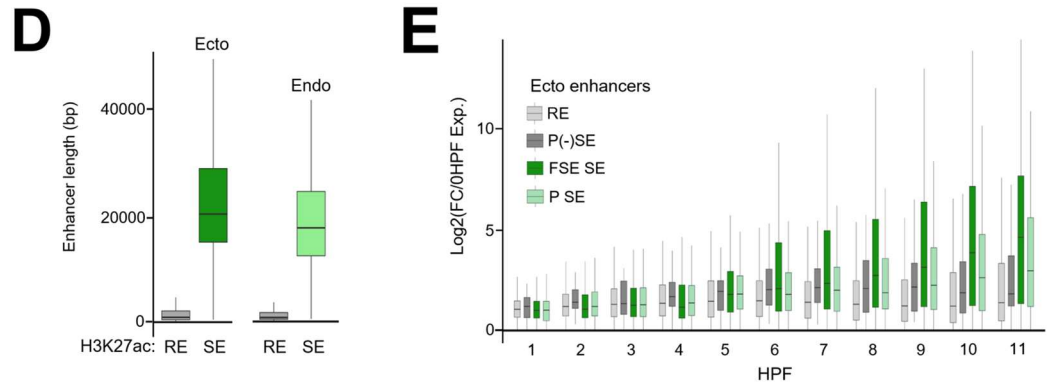
D
Ecto
Endo
Enhancer length (bp)
H3K27ac: RE SE RE SE
E
Ecto enhancers
RE
P(-)SE
FSE SE
P SE
Log2(FC/0HPF Exp.)
HPF

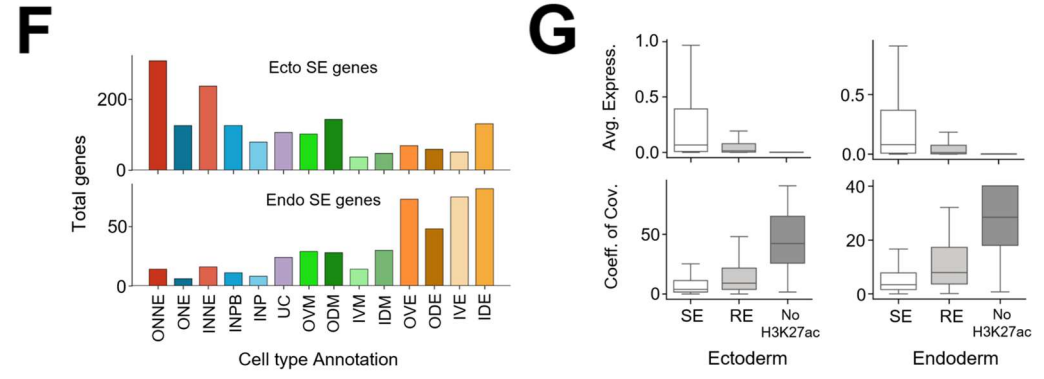
F
Ecto SE genes
Endo SE genes
Total genes
ONNE
ONE
INNE
INPB
INP
UC
OVM
ODM
IVM
IDM
OVE
ODE
IVE
IDE
Cell type Annotation
G
Avg. Express.
Coeff. of Cov.
SE
RE
No H3K27ac
Ectoderm
Endoderm

Figure 2.12: ***Foxi2 and Sox3 co-bound regions define ectodermal SEs with high and stable gene expression.*** **(A)** Genome browser views of Ep300 binding in ectodermal and endodermal tissues from foxi2/sox3 (FS) morphants, and wild-type (WT) embryos. **(B)** Ep300 signal intensity in non-FSE (Ep300 unique) peaks in dissected ectoderm (top) and Ep300 signal intensity across all Ep300 endoderm peaks in dissected endoderm (bottom). Box-and-whisker plots show signal distributions are not statistically significantly (n.s.) different between WT and FS morphants. **(C)** Identification of ectodermal and endodermal SEs using the ROSE algorithm, based on H3K27ac ChIP-seq signal enrichment. Venn diagram shows SE and RE overlaps between ectoderm and endoderm. **(D**) SE-associated genes are highly expressed in their respective germ layers compared to RE-associated genes. **(E)** FSE-associated genes display significantly higher temporal expression than SE genes lacking Ep300 (P(–)SE) or regular enhancer (RE)-associated genes. **(F)** Ectodermal and endodermal SE-associated genes are preferentially expressed in the respective ectodermal and endodermal sub-lineages. **(G)** SE associated genes exhibit higher expression levels and lower coefficient of variation (COV) compared to RE-associated genes and genes without H3K27ac enrichment.

typically less than 2kb (Figure 2.12D). While 386 SE regions overlap between ectodermal and endodermal SEs, 761 are unique to the ectoderm, and 285 are unique to the endoderm (Figure 2.12C). These findings highlight that ectodermal SEs are more abundant than endodermal SEs at stage 10.5 and the timing of accumulation of H3K27ac suggests distinct germ layer SEs arise between the onset of ZGA and early gastrulation.

Highlighting the locations of genes associated with FSE-bound regions on a super enhancer ROSE (ranked order of super enhancers) plot revealed that the Foxi2 and Sox3 regulated genes are highly enriched in ectodermal SEs relative to REs (Figure 2.11E,F,G) or endodermal SEs (Figure 2.11G). The temporal expression levels of ectoderm SE genes associated with Foxi2/Sox3 bound regions containing Ep300 (FSE) are also significantly higher than SE genes with no Ep300, and RE-associated genes (Figure 2.12E) during embryonic development. Interrogating our snRNA-seq data (Figure 2.10A), we found that ectodermal SE-associated genes are preferentially expressed in the ectodermal germ layer (Figure 2.11H), and also in ectodermal sub-lineages (Figure 2.12F). In contrast, endodermal SE-associated genes are preferentially expressed in the endodermal germ layer and its sub-lineages.

Finally, we investigated the effect of SEs on gene expression variance (transcriptional “noise”) across individual cells. To quantify differences in gene expression across genes, we

measured the coefficient of variation (COV), which reflects the extent of gene expression across individual cells within the dataset. Analysis of snRNA-seq data revealed that ectodermal SE-associated genes show higher gene expression levels and a lower COV, compared to RE genes and genes lacking H3K27ac deposition (Figure 2.12G). Additionally, we observed that SE-associated Foxi2/Sox3, Foxi2-only, and Sox3-only regulated target genes display the highest expression, and the lowest COV, compared to the entire landscape of ectoderm SEs and ectoderm REs and genes unassociated with an enhancer (Figure 2.11I). These results suggest that ectoderm SEs, enriched with Foxi2 and Sox3 binding, drive the most robust and stable expression of ectoderm-specific genes, while minimizing transcriptional noise. In sum, at the onset of gastrulation Foxi2 and Sox3-marked regions preferentially acquire Ep300 and accumulate H3K27ac to establish SEs, which ensure robust gene expression across all ectoderm sub-lineages.

DISCUSSION

In this study, we identified maternal Foxi2 and Sox3 as master regulators of the ectodermal germ layer in *Xenopus*, based on the following evidence: (1) ectopic expression of these TFs in endodermal cells confers ectodermal cell fate specification; (2) loss-of-function analysis results in the loss of key ectodermal markers; (3) bound sites for these TFs are required for with ectodermal Ep300 recruitment to CRMs, and (4) the co-bound regions include ectoderm specific H3K27ac SEs that drive a robust ectodermal gene expression program. Since Foxi2 and Sox3 prebind to many CRMs that are critical for the later activation of ectodermal developmental programs (e.g., sensory placode formation), we propose a model in which animally enriched Foxi2 and Sox3 establish early genomic occupancy at these CRMs during the cleavage stages. These interactions with the genome prefigure the accumulation of activating epigenetic

modifications around these regulatory elements by early gastrulation, driving the formation of SEs and spatially distinct gene expression programs that define ectodermal identity.

The roles of maternal Foxi2 and Sox3 in early development

In vertebrates, the Foxi subfamily comprises Foxi1, Foxi2, and Foxi3, which are pivotal in epithelial differentiation and organogenesis (Edlund et al., 2015). There are limited studies performed on the function of *foxi2* in early development. However, the available data consistently show that *foxi2* has roles at later stages, such as establishment of sensory placodes and anterior neural ectoderm. In the chick embryo, Foxi2 is crucial for craniofacial development, regulating the formation of the pharyngeal arches (Khatri and Groves, 2013). In mouse, Foxi2 is expressed in the developing forebrain, neural retina, dental and olfactory epithelium (Hulander et al., 1998, Ohyama et al., 2004, Wijchers et al., 2006). And in *Xenopus*, Foxi2 morphants similarly appear to have anterior structure defects (Figure 2.8B).

Despite these conserved roles of Foxi2 in post-gastrulation vertebrate embryos, evidence for maternally expressed Foxi2 being essential for early steps in ectodermal germ layer cell lineage development is currently limited to *Xenopus.* Maternally expressed Foxi2 directly activates *foxi1* (Figure 2.8C,E; Figure 2.7A; Cha et al., 2012), which is best characterized for its key roles in mucociliary development, ionocyte specification, and sensory placode formation in *Xenopus* (Bowden et al., 2024). This is consistent with the established roles of Foxi1 in other vertebrates. Interestingly, *Xenopus* Foxi2 pre-binds to the CRMs of *foxi1* as well as sensory placode gene *eya1* and anterior neural gene *six1* during cleavage stages (Figure 2.3G), and in early gastrulation (Figure 2.5B), perhaps priming these CRMs for subsequent activation during later stages of development.

Based on the evidence, we speculate that all three *Xenopus foxi* genes are involved in ectodermal specification, but their roles may have diverged during evolution. The maternal

function of *foxi2* in early ectoderm specification may not be unique to early *Xenopus* embryos and might exist in other species but has not yet been studied. In axolotl embryos, RNA-seq analysis shows that *foxi2* mRNA is detectable before zygotic transcription, suggesting it is maternally expressed in this urodele amphibian (Jiang et al., 2017). A zebrafish *foxi* gene referred to as *foxi1*, which our synteny analysis (unpublished observations) suggests is orthologous to both *Xenopus* and mammalian *foxi2*, is first expressed shortly after the onset of ZGA as indicated by RNA-seq profiling (White et al., 2017; https://www.ebi.ac.uk/gxa/home). This implies it might be more broadly expressed and have an early role in development in teleost fish. Finally, a single lamprey *foxi* gene is also expressed broadly in the animal pole at blastula stage (York et al., 2024). These expression patterns suggest activity in the early ectoderm, implying conserved functions that predate the divergence of fishes (York et al., 2024). In *Xenopus*, the *foxi1* and *foxi3* (formerly *foxi4*) genes are not maternally expressed but are transcribed after onset of ZGA. *foxi1* and *foxi3.2* (but not *foxi3.1*) are expressed broadly in the blastula ectoderm and later become confined to epidermal lineages, while being excluded from the neural plate (Lef et al., 1994; Pohl et al., 2002; Matsuo-Takasaki et al., 2005). Overexpression and loss-of-function experiments of various kinds suggest that these genes might have either redundant functions to *foxi2,* or more likely act as downstream effectors induced by *foxi2*. This is particularly the case with *foxi1.* Our data reveals that the early role(s) of *foxi2* in ectodermal germ layer specification includes activation of *foxi1*, however *foxi3.2* doesn't appear to be regulated by Foxi2. Similar effects on ectodermal specification in other amniotes might involve a different timing, with target genes being induced by zygotically expressed *foxi2,* but further experiments in these species are needed to confirm this model.

In *Xenopus*, *sox3* expression is both spatially and temporally dynamic during development. *sox3* mRNA is maternally supplied with expression throughout the ectoderm prior to gastrulation and becomes restricted to the presumptive neural plate by mid-gastrula (Zhang et al., 2003; Penzel et al., 1997). Sox3 represses endoderm formation to facilitate proper germ

layer formation (Zhang et al., 2003, Zhang and Klymkowsky, 2007). In later stages, *sox3* is expressed in neural progenitors along the neural tube, where it is implicated in promoting neural identity and preventing premature differentiation. Recently, Sox3 has been shown to have a role in ectoderm pluripotency, and also function as a pioneer TF affecting chromatin accessibility (Buitrago-Delgado et al., 2018; Gentsch et al., 2019; Schock et al., 2022). Our findings suggest that Sox3 has an additional role in orchestrating the ectodermal program during germ layer formation. This is supported by evidence showing that 1) several critical ectodermal genes are direct targets of Sox3, 2) Sox3 knockdown results in down-regulation of ectodermal gene expression, and 3) ectopic expression of Sox3 and Foxi2 upregulates ectodermal gene expression in the endoderm while repressing mesendodermal markers. It is plausible that Foxi2 and Sox3 prime pre-bound CRMs during early development and subsequently hand off their regulatory roles to other factors, such as *foxi1* or *soxE* family TFs (Schock et al., 2022). This handoff mechanism could maintain CRM accessibility by preventing silencing through repressive histone modifications, thereby ensuring readiness for transcriptional activation in later developmental stages.

Advantages of germ layer specific SE formation in rapidly dividing embryos

We identified germ layer-specific SEs based on H3K27ac accumulation across the *Xenopus* embryonic genome. Notably, ectodermal SEs are highly correlated with the binding of Foxi2 and Sox3 TFs (Figure 2.11D). Our findings also show that SE-associated Foxi2/Sox3 target genes exhibit higher expression levels compared to genes associated with REs, while displaying reduced expression noise (Figure 2.11I). Based on these germ layer specific SE activities, we propose that SE-linked gene expression contributes to developmental stability during cell fate specification, thereby enhancing the robustness of embryonic tissue formation.

Rapidly dividing embryos, such as those of *Xenopus* and zebrafish, undergo swift transitions from gastrulation to neurulation within a short developmental timeframe. These aquatic embryos also face varying external influences, such as temperature, that impact their development. To ensure efficient and error-free progression, these embryos must not only achieve a rapid surge in gene expression during early stages but also tightly regulate expression to avoid critical errors. SEs offer a solution by concentrating TFs and cofactors at critical genomic regions, enabling robust and precise gene expression. We propose that in these rapidly dividing embryos, a key strategy might involve pre-loading enhancers with TFs before zygotic genome activation (ZGA). While direct evidence from ChIP-seq at cleavage stages is lacking, limited ChIP-qPCR data suggests that pre-bound TFs can prime enhancers for rapid and robust activation at ZGA. At the onset of ZGA, recruitment of Ep300 and Kmt2c/d (the key histone modifying enzymes responsible for H3K4 monomethylation) to CRMs, and RNA polymerase II to promoters may enable efficient transcription, ensuring developmental success in these time-constrained systems.

Factors involved in segregating ectodermal cell clusters

The superficial (outer) and inner layer cells in *Xenopus* embryos have distinct transcriptomes in our snRNA-seq data (Figure 2.10, Figure 2.9). These differences arise due to distinct cues that are present by the 64- to 128-cell stages (Chalmers et al., 2003). The localized expression of *tp63* in the inner (basal) layer and *hes5.10* and *krt70* in the outer layer has been detected through WMISH (Chalmers et al., 2002; 2006). Additionally, our snRNA-seq analysis revealed enrichment of new markers, such as *col18a1* and *zeb2* in the inner layer, and *atp1b2, epas1,* and *nectin2* in the outer layer, among others, expanding our understanding of ectodermal lineage-specific gene expression patterns.

By examining the expression patterns of Foxi2 and Sox3 direct target genes in our UMAP of the early gastrula embryo (Figure 2.10), we discovered that these TFs coordinate the expression of pan-ectodermal genes. For example, genes such as *dlx3 and tfap2a* are co-regulated by both factors, while *klf5* expression is mainly regulated by Foxi2, and *igf3, lhx5* and *tp53inp2* are regulated by Sox3. Since all these genes are expressed across the five ectodermal cell clusters (Figure 2.10B,C), we propose that Foxi2 and Sox3 exhibit both overlapping functions and distinct, non-overlapping roles in ectoderm development. Among Foxi2 and Sox3 targets, genes like *dlx5*, *hes5.10, krt7*, and *krt70* are exclusively expressed in the outer ectoderm, while *neurog3, prdm14, szl, unc45b*, and *zic4*, and are specific to the inner ectoderm. This differential expression suggests that additional factors uniquely active or expressed in each layer may play a role. This highlights that other regulatory mechanisms are superimposed on Foxi2/Sox3 regulated targets that underlie this layer-specific regionalization of ectodermal cells occurring early in gastrulation.

Two notable candidates involved in this process are the kinases Prkci (also known as aPKC) and Mark3. Prkci is localized in apical cell membranes by the 4-cell stage (Chalmers et al., 2003) and contributes to the segregation of outer (superficial) ectodermal cells at later stages (Ossipova et al., 2007). On the other hand, Mark3 is localized basally and influences the inner layer of cells (Ossipova et al., 2007). This interplay may be essential for initiating outer and inner ectodermal differences that intersect with Foxi2/Sox3 regulated gene expression in the early *Xenopu*s embryo.

Additional factors potentially involved in outer and inner ectoderm development include the Grainyhead-like (Grhl) TFs. Our motif analysis in regions bound by Ep300 revealed a significant enrichment of the Grhl motif in early gastrula ectoderm, but not in endoderm (Figure 2.2D). The *Grhl* gene family comprises three highly conserved members in vertebrates (*Grhl1-3*) (Kudryavtseva et al., 2003; Ting et al., 2003b; Wilanowski et al., 2002). Among these, *grhl1* is the only maternally expressed family member in *Xenopus*, which is also animally enriched

(Paraiso et al., 2019) and continues to be expressed zygotically in both the outer and inner layer of the ectoderm based on our snRNA-seq data. Disruption of *grhl1* activity in *Xenopus* results in severe defects in epidermal differentiation, directly affecting keratin gene expression through binding of Grhl1 to the promoter region of *krt12.4* (Tao et al., 2005; our unpublished data). Similarly, *Grhl1* knockout models in both mouse and zebrafish exhibit disrupted epidermal cell differentiation (Wilanowski et al., 2008; Janicke et al., 2010). Both *grhl2* and *3* are zygotically expressed in *Xenopus,* starting during gastrulation and continuing into later stages (Chalmers et al., 2006; Owens et al., 2016). *grhl2* is expressed in the inner layer while *grhl3* is expressed in the outer layer of gastrula ectoderm, and later in the superficial layer of epidermis (Chalmers et al., 2006). Our snRNA-seq data confirms these *grhl* expression domains. In mice, loss of *Grhl2* causes non-neural ectoderm disruption, leading to disorganized cell junctions, aberrant mesenchymal protein vimentin, and decreased epithelial integrity (Ray and Niswander, 2016). *Grhl3*-deficient mouse embryos die shortly after birth due to impaired skin barrier function (Ting et al., 2005). We observed that a Grhl motif is not enriched in Foxi2- and Sox3-bound regions (Figure 2.2D), suggesting that *grhl1* likely regulates a distinct set of ectodermal target genes compared to those of Foxi2 and Sox3. We propose that Grhl1 functions as a maternal ectodermal TF that functions in parallel with Foxi2 and Sox3 to initiate the global ectodermal specification programming, potentially through a separate pathway. Additionally, *grhl2* and *grhl3* may take over zygotic functions of *grhl1*, operating within the two ectodermal layers during later stages of development. Our future goals focus on dissecting the regulatory pathways of the ectoderm by combining loss-of-function analysis of maternal TFs with single-nucleus transcriptomics. This approach aims to determine the timing of lineage segregation and uncover the contributions of the maternal TFs to the specification of various ectodermal cell lineages and epigenetic changes.

Experimental Procedures

Chromatin Immunoprecipitation (ChIP) Assays

Antibodies for Foxi2 (Cha et al., 2012) and Sox3 (Zhang et al., 2004) were validated previously, while the Ep300 antibody was from Santa Cruz sc-585, the H3K27me3 antibody from Upstate/Millipore 07-449, and the H3K27ac antibody from Abcam ab4279. ChIP-qPCR was performed as described in Chiu et al. (2014), using whole embryos or dissected tissue fragments with specific primer sets. ChIP-seq libraries were generated using NEB E7645S DNA sequencing kit or the Bioo Scientific NEXTflex ChIP-seq kit, verified using an Agilent Bioanalyzer 2100, and sequenced at UC Irvine's Genomics Research and Technology Hub using the Illumina Novaseq platform.

Western Blot

Embryos were homogenized in 1xRIPA buffer (50mM Tris-HCl pH7.6, 1% NP40, 0.25% Na-deoxycholate, 150mM NaCl, 1mM EDTA, 0.1% SDS, 0.5mM DTT) supplemented with Roche's cOmplete protease inhibitor. The homogenate was centrifuged at 14,000 rpm, and the supernatant was collected and centrifuged again. Western blotting was performed on the final supernatant using anti-Foxi2, anti-Sox3, alpha-tubulin (Sigma, T6168), or beta-actin antibodies (Sigma, A5316).

RNA Assays

Total RNA was extracted from embryos using TRIzol reagent (ThermoFisher). Polyadenylated mRNA transcripts were isolated using NEBNext PolyA mRNA Magnetic Isolation Module (NEB E7490S). RNA libraries were prepared using NEBNext Ultra II Library Preparation Kit (NEB E7770S), validated using an Agilent Bioanalyzer 2100, and sequenced on the Illumina Novaseq platform. RT-qPCR analyses were performed using primers listed in the primer table Reverse

transcription was performed using the MMLV reverse transcriptase (ThermoFisher Superscript II). qPCR was carried out on a Roche Lightcycler 480 II using Roche SYBR green I master mix.

Morpholino Knockdown, Rescue and Vegetal RNA Injections

foxi2 translation blocking morpholino was created by GeneTools, Inc. 5'-TTATGAAGTCTGGTGGGACATTCAC-'3. Morpholino rescue was performed using mRNA prepared from a pCS2+ FLAG-*foxi2* construct. *sox3* translation blocking morpholino is 5'-GTCTGTGTCCAACATGCTATACATC-3'. *sox3* morpholino rescue was performed using a pCS2+ FLAG-*sox3* construct. The *X. tropicalis foxi2* coding sequence was acquired from the *X. tropicalis* Unigene library (TGas144f13) in the pCS107 vector and the *X. tropicalis sox3* coding sequence was cloned into the pCS2+ vector. The *foxi2* plasmid was linearized with HpaI, and the *sox3* plasmid with XbaI, for generating capped mRNA using the SP6 mMessage Machine kit. Morpholino knockdowns were performed by injecting directly into opposing sides of the animal cap at the 1-cell stage or into each animal blastomere at the 2-cell stage. Animal caps were dissected one hour prior to harvesting for RNA preparation. Vegetal RNA injections were performed using indicated amounts of mRNA per embryo into opposing sides of the vegetal mass at the 1-cell stage, or in each vegetal blastomere at the 2-cell stage. Vegetal masses were dissected at blastula stage ~1 hour before harvesting with Trizol.

Nuclei Preparation and snRNA Sequencing

Nuclei were isolated from stage 10.5 embryos using previously published discontinuous sucrose gradient protocols followed by a separate centrifugation through 80% glycerol (Wormington and Brown, 1983; Wolffe, 1989; Nakayama et al., 2022). Briefly, 200 embryos were homogenized in a 250mM sucrose solution containing glycerol and snap frozen in liquid nitrogen (Nakayama et al., 2022). Homogenates were later thawed on ice, brought to ~2.2M sucrose and centrifuged through a 2.4M sucrose layer at 130,000g for 2 hours at 4oC using a Beckman SW55Ti rotor,

followed by a 3400xg centrifugation for 10 min at 4oC through an 80% glycerol cushion. RNAse (NEB) and protease inhibitors (Roche 7x cOmplete, Mini, EDTA-free) at 0.2 U/ml and 5 mg/ml respectively were used throughout the previous steps. Nuclei were finally resuspended in “nuclear PBS” (0.7x PBS, 2mM MgCl2) containing 0.5% BSA and 0.2 U/ml RNase inhibitor. DAPI-stained nuclei were counted using a hemocytometer, and then were subject to fixation using the Parse Bioscience Evercode Fixation Kit (SB1003). Nuclei in DMSO were slow-frozen in a -80oC overnight according to the kit manual. A bar-coded snRNA-seq library was prepared using the Parse WT Mini Kit (ECW01010) and sequenced at the University of California, Irvine Genomics Research and Technology Hub.

Chromatin Immunoprecipitation Analysis

ChIP-qPCR: Percent input was calculated according to (Lin et al., 2012), where Input % = 100/2^([Cp[ChIP] – (Cp[Input] – Log2(Dilution Factor)). **ChIP-seq peak calling and IDR**: Reads were aligned to the *X. tropicalis* genome V10.0 using Bowtie 2 v2.4.1 (Langmead and Salzberg, 2012) using default options. The .sam alignment was converted to .bam, duplicates were removed and files were converted to .bed format using samtools (Li et al., 2009). Peaks were called against stage specific (this paper & Charney et al., 2017) and tissue dissected input DNA using MACS2 v2.2.7.1 (Zhang et al., 2008) with the “-p .001” argument as the only non-default option. For narrowPeaks, Irreproducibility discovery rate (IDR) was followed according to (Li et al., 2011), where optimal peaks were selected using 0.05 p-value threshold. **Heatmap generation**: Bigwig files were created using “bamCoverage” where “—scale-factor” was used to evenly scale reads between ChIP-seq experiments using the same antibody, and RPKM normalized using DeepTools (Ramirez et al., 2014). “computeMatrix” was used to generate a matrix by mapping .bigwig coverage files to .bed peak regions, then “plotHeatmap” was used to visualize the matrix. Average signal intensity profiles (Fig2E, Supp1B, Fig5A) were made from matrices using “plotProfile”. **Motif analysis:** HOMER (V4.11) (Heinz et al., 2010) was used to

predict de novo motifs using the “findMotifsGenome.pl” command within 100bp of the peak summit. To analyze motif occurrences within Foxi2 peaks, the following command was used: “annotatePeaks.pl $PEAKS $GENOME -size 2000 -hist 20 -ghist -m $MOTIF -mbed $MOTIF_BED > $OUTPUT”. The resulting matrix was visualized in Python using numpy (v1.26.2 (Harris et al. 2020)) and matplotlib (v3.8.2 (Hunter 2007)). **Peak location annotation**: To categorize whether a peak fell within a particular genomic region “annotatePeaks.pl $PEAKS $GENOME_FASTA -gtf $GFF3 > $OUTPUT” was used. **Genome browser visualization**: After alignment, .bam files were converted to .bed files used samtools command ‘bamtobed’. HOMER’s “makeTagDirectory” was then used to generate a tag directory as an input for “makeUCSCfile” which outputs a bedgraph. The Integrative Genome Viewer (IGV) was then used to convert the bedgraph into a .tdf file using igvtools “toTDF”. **Enhancer ranking**: The rank ordered super enhancer (ROSE) from the Young lab (Whyte et al., 2013) was used to categorically assign epigenetic peaks as regular enhancers (REs) or super enhancers (SEs) based on an enhancers over-all length and signal density. SEs were generated by stitching adjacent enhancer loci when loci passed a signal threshold. **Published ChIP-seq datasets:** Ep300 Stage 9, 10.5 (Hontelez et al., 2015), H3K4me1 Stage 8 (Gentsch et al., 2019), Stage 9, 10.5 (Hontelez et al., 2015), H3K27ac Stage 8, 9, 10.5 (Gupta et al., 2014). Animal and vegetal H3K4me1 at stage 10.25 (Paraiso et al., 2025).

Quantification and Statistical Analysis

RT-qPCR*:* The ΔΔCp method (Livak and Schmittgen ,2001) was utilized for calculating the fold-change in gene expression between treatment and control where the error among biological replicates was calculated using standard deviation and significance using a 2-tailed t-test. Bulk RNA-seq: Reads were aligned using RSEM V1.3.3 (Li and Dewey, 2011) with STAR V2.7.3 (Dobin et al., 2013) to the *Xenopus tropicalis* V10.0 genome to generate normalized expected read counts. Differential gene expression analysis was performed in R V4.1.1 using DEseq2

V1.34.0 (Love et al., 2014). **Localized gene expression analysis:** Early gastrula tissue dissection RNA-seq data from (Blitz et al., 2017) was used to determine ectoderm and endoderm localized genes. When comparing vegetal mass and animal cap dissections, genes with a 2-fold enrichment in either germ layer were categorized as local, then the top 250 zygotic genes ranked by false discovery rate (FDR) were extracted. **Zygotic gene expression timecourse*:*** Temporal RNAseq data from (Owens et al. 2016) was used to generate expression timecourses for zygotic gene sets. The 0HPF timepoint was used for detecting maternal transcript expression (at least 1TPM) to segregate zygotically expressed genes for analysis of downstream timepoints. 0HPF timepoint TPMs were compared with downstream timepoint TPMs to calculate zygotic gene expression log fold-changes.

snRNA-seq Analysis

Alignment: Parse Biosciences' in-house alignment software (dnanexus.com) command "Parse Batch Analysis v1.1.4" was used with the default commands against the UCB_Xtro_10.0 (GCA_000004195.4) reference. **Formatting:** The unfiltered Parse alignment output containing "all_genes.csv", "cell_metadata.csv" and "DGE.mtx" were first amalgamated into a .h5Seurat object using the R v4.3.1(http://www.r-project.org) software Seurat v4.3.0, Matrix v1.6.5, SeuratDisk v0.0.0.9015 (https://github.com/mojaveazure/seurat-disk), Reticulate v1.37.0 and the command "CreateSeuratObject". Finally, the .h5Seurat object was converted into an .h5ad file using the "Convert" command with the option "dest = "h5ad"". **Pre-processing:** Using scanpy v1.9.6 (Wolf et al. 2018) , pandas v2.1.4 (McKinney et al. 2010), the nuclear data was log transformed and normalized and highly variable genes were annotated. Doublets were predicted using Scrublet (Wolock et al. 2019), then manually inspected, confirmed and removed based on illogical ectopic co-expression of germ-layer specific markers and outlier read counts. **Cell lineage annotation:** Leiden (Traag et al. 2019) was used to predict de novo cluster formation, visualized via Uniform Manifold Approximation Projection (UMAP) (McInnes et al.

2018). Scanpy was used to calculate differential gene expression analysis of known marker genes between de novo clusters which were assigned to their germ-layer identity. Accordingly, clusters were merged based on co-expression of known marker genes. In this way, cluster boundaries are initially formed in an unbiased way through de novo clustering, based on differential gene expression. *In-situ* hybridization studies of marker genes were subsequently used for appropriate cluster annotation and merger. **Gene expression analysis*:*** Pandas was used for both super enhancer genes', and Foxi2/Sox3 associated genes' z-score localization calculations by examining gene expression within the cells from each cell-type annotation, or merged annotations. Coefficient of Variation (COV) and average expression were calculated using numpy v1.26.2 (Harris et al. 2020).

Acknowledgements:

This work was made possible, in part, through access to the University of California, Irvine Genomics Research and Technology Hub (GRT Hub) parts of which are supported by NIH grants to the Comprehensive Cancer Center (P30CA-062203) and the UCI Skin Biology Resource Based Center (P30AR075047), as well as to the GRT Hub for instrumentation (1S10OD010794 and 1S10OD021718). We thank Xenbase (http://www.xenbase.org/, RRID: SCR_003280) and the National *Xenopus* Resource (RRID:SCR_013731), for genomic and community resources, and the University of California, Irvine High Performance Computing Cluster (https://hpc.oit.uci.edu/) for their valuable resources and helpful staff. This research was funded by the following grants awarded to K.W.Y.C. National Institute of Health R21 HD109696, and R35 GM139617, and National Science Foundation 1755214. CLH is a recipient of a US Department of Education GAANN fellowship (P200A220015). GEO accession number of data: GSE288636, GSE288637, and GSE288638.

Author contributions

C.L.H., I.L.B. and K.W.Y.C. designed the study, wrote the manuscript and performed experiments. A.H., J.C., and K.P. performed Ep300, H3K27ac, H3K27me3 and H3K4me1 ChIP-seq; M.W.K. generated the Sox3 antibody and M.J.K. generated the Foxi2 antibody. C.L.H performed bioinformatics analyses.

Chapter 3: High resolution ectoderm lineage specification and the role of maternal Foxi2 during gastrulation

---

Abstract:

During gastrulation the primordial germ layers establish heterogeneity and express unique spatiotemporal gene programs for sub-lineage specification, often controlled by maternal TFs. Temporal single nucleus sequencing offers the highest resolution for detecting zygotic gene co-expression and early cell state transitions. In this work, snRNA-seq is used to characterize all cell types during *Xenopus* gastrulation. Temporal ectoderm specification trajectories reveal the hierarchical inheritance of both inner and outer non-neuroectoderm, as well as neural plate and neural plate border lineages. Neural crest cells and pre-placodal region progenitors temporally express unique TF cohorts and undergo antero-posterior specification during gastrulation. Open chromatin signatures from bulk data were mined for TF motif presence and used to predict the ionocyte TF network arising during gastrulation. Knockdown of the maternal ectoderm TF Foxi2 reveals its role in ectoderm progenitor formation as well as pre-placodal and neural specification. Surprisingly, Foxi2 was shown to inhibit ectopic ciliogenesis transcription factor and signaling pathway activation. These analyses represent the most resolved temporal maps characterizing gastrula neural and non-neuroectoderm cell state transitions, and the first investigation of maternal TF control over ectoderm specification at single cell resolution, during *Xenopus* gastrulation.

Introduction:

Pivotal advances in genomic sequencing techniques allowed for the high throughput detection and analysis of thousands of genes within a biological sample (Mortazavi et al., 2008). This

landmark paper gave the first glimpse into organ specific transcript expression and revealed heterogeneic transcription profiles in mouse tissues, like the brain, liver and muscle. However, these sequencing results lack the resolution to characterize sub-cell type heterogeneity and instead reveal the average gene expression combined across the complex cell types of the organ. Therefore, bulk organ/tissue RNA-seq lacks the spatial information required to resolve cell type complexity. Soon thereafter, the first single cell was sequenced (Tang et al., 2009), and the first high throughput single cell RNA-seq experiments were performed in tens (Ramskold et al., 2012) and thousands (Zheng et al., 2015) of cells. scRNA-seq surveys reveal transcriptional complexity on a cell-by-cell basis and allow for more comprehensive investigations into the transcriptional requirements for cell fate specification.

Although all cell types begin from a totipotent progenitor cell, the hierarchical progression of cell state specification is far from being completely understood. Major questions remain about the formation of primordial ectoderm and the timing of its segregation into neural and non-neural derivatives. The first single cell papers comparing *Xenopus* and zebrafish germ layer specification in early development demonstrated highly heterogeneous and conserved cell states (Briggs et al., 2018, Weinreb et al., 2018, Farrell et al., 2018). Early blastula until larval stages were mapped, recapitulating many known ectodermal lineages and the transcription factors characterizing their transition states. Another study temporally profiled the mucociliary epithelium using ectoderm dissections from the blastula until the larval stage, defining lineage marking epidermal TFs (Lee et al., 2023). Other single cell experiments have focused on adult tissues (Liao et al., 2022), tail (Aztekin et al., 2019) and limb regeneration (Yanagi et al., 2022) and corneal epithelial (Sonam et al., 2023) complexity, but have not focused explicitly on the developing ectoderm. Notably, the only single cell experiment to involve a genetic perturbation comparison was FGF treated versus untreated limbs (Yanagi et al., 2022).

Maternal pioneer factors are required to initially bind and activate target genes which facilitate germ layer formation cell type specification. Previous investigation of the ectodermally

localized maternal TF, Foxi2, demonstrated its role in CRM binding and activation of foxi1, the ectoderm defining ionocyte master regulator (Cha et al., 2012, Suri et al., 2005). Work in our lab further characterized its binding motif and requirement, alongside Sox3, for Ep300 recruitment and the subsequent activation of inner and outer layer ectodermal progenitor genes during early gastrulation (Hendrickson et al., 2025). Across vertebrates Foxi2 plays a conserved role in craniofacial and pharyngeal arch development (Soloman et al., 2003, Ohyama et al., 2006, Freter et al., 2008, Urness et al., 2010, Hendrickson et al., 2025). To date, no functional analysis of maternal factors involved in ectodermal specification has been investigated at sc/nRNAseq resolution. As evidence suggests Foxi2 as a maternal master regulator of the early ectoderm in *Xenopus*, we sought to characterize its role in ectodermal specification.

Histological *in situ* hybridization studies demonstrate some early ectoderm marker expression becomes spatially restricted between the inner and outer ectoderm, earlier than previously reported in high throughput sequencing experiments (Chalmers et al., 2006). While inner and outer ectodermal differences are likely established by the early gastrula (Chalmers et al., 2002, 2003, 2006) their divergent transcriptomes have not been confirmed in high resolution. New commercially available single nucleus sequencing techniques offer the most robust detection of emergent zygotic transcripts. As the timing of antero-posterior fate acquisition of the pre-placodal and neuroectoderm are not well understood, robust transcript detection could help elucidate the earliest TF defined fate decisions. Additionally, software and accompanying motif databases have been developed to mine bulk epigenetic data for predicting TF-target interactions in sc/nRNA-seq data (Aibar et al., 2017, Pliner et al., 2018, Kamimoto et al., 2023). Our preliminary data suggest that early inner and outer ectoderm transcriptomes are distinct by early gastrulation and by mapping temporal transcriptional changes in segregating cell states we can reveal lineage defining TF interaction networks. We hypothesize that maternal Foxi2 controls ectodermal progenitor formation and pre-placodal ectoderm specification in the middle gastrula.

Results:

Temporal single nucleus sequencing during *Xenopus* gastrulation

In *Xenopus* (Briggs et al., 2018) and zebrafish (Wagner et al., 2018, Farrell et al., 2018) single cell experiments, the very first temporal lineage maps of vertebrate gastrulation revealed orthologous cell state formation conserved between each species' early development. While many known cell states were recapitulated, the timing of their induction, as well as their early regional heterogeneities may not be fully resolved. Cell type specification is initially determined by marker gene expression, therefore it is crucial to detect the first zygotic expression of lineage defining transcripts. As previous experiments sequenced both the nuclear and cytoplasmic transcriptomes, they are inherently more prone to miss the detection of nuclear low abundance lineage defining zygotic transcripts. For this reason, we sought to remove cytoplasmic transcripts.

To sequence gastrulating embryos at the highest resolution for detecting newly generated zygotic transcripts, we utilized a nuclear extraction approach combined with split pool barcode sequencing (Figure 3.1A). As maternal transcripts are stored in the cytoplasm, collecting nuclei can avoid their detection and the subsequent loss of sequencing depth. To survey the entirety of gastrulation, five timepoints were chosen, stage 10.5 (early gastrula), 11.25 (mid gastrula), 12.0 (mid-late gastrula), 12.5 (late gastrula) and 13 (end of gastrulation) (Figure 3.1A). Although stage 10.5 recovered 13,711 cells, the most cells of any stage to pass the minimum quality 1000 gene per cell threshold, it also had the most cells with less than 2000 genes (Figure3.1B,C). One explanation for this is that in subsequent experiments nuclei were cleaned more robustly than in the stage 10.5 experiment. In the stage 11.25, 12.0, 12.5 and 13.0 the median genes per cell is above 2000, indicating there are many high quality cells, even hundreds with more than 3000 transcribed genes (Figure 3.1B,C). In terms of total cells

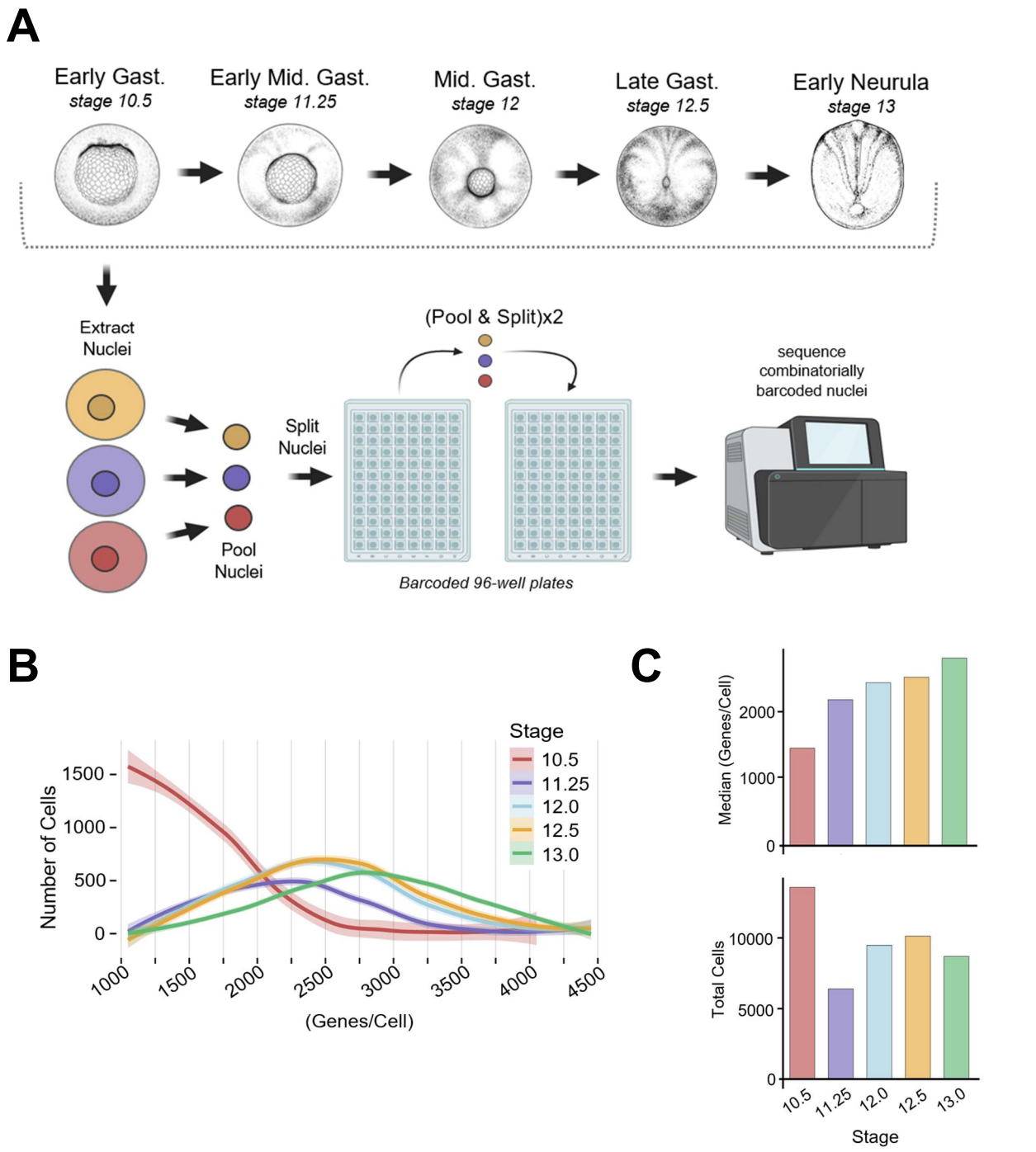

Figure 3.1: ***Temporal single-nucleus sequencing during Xenopus gastrulation.***
(A) Schematic illustrating stage 10.5, 11.25, 12, 12.5 and 13 nuclear extraction and combinatorial barcode sequencing. **(B)** Total distribution of the numbers of cells containing a minimum of 1000 genes. **(C)** Median numbers of genes per cell per stage (top) and total cells per stage with at least 1000 genes per cell (bottom).

meeting the minimum 1000 gene quality requirement, stage 11.25, 12.0, 12.5 and 13 yielded 6,447, 9,564, 10,218 and 8,773 cells respectively (Figure 3.1C).

Probing and testing relationships between thousands of cells which individually express thousands of genes can be obscure. The inherent scale and complexity of single cell/nucleus sequencing experiments requires analysis of high dimensional non-linear data structures. Non-linear dimension reduction techniques, like t-stochastic neighborhood embedding (tSNE) or uniform manifold approximation and projection (UMAP), can be used to create best fitted 2-dimensional visualizations of high dimensional non-linear objects (van der Maaten et al., 2008, McInnes et al., 2018). In these visualizations, cells are placed closer together into the 2-dimensional embedding based on their transcriptome similarity, with UMAP arguably outperforming tSNE (Becht et al., 2018, Kobak & Linderman 2021).

UMAP analysis clusters cells together with distinct expression profiles from the endoderm, mesoderm, neuroectoderm and non-neural ectoderm (Figure 3.2). Highly variable genes were selected without supervision to calculate each UMAP plot and form unbiased clusters. Marker gene expression was then examined within the UMAP plot to annotate cell states. Surprisingly, there is a transient novel cluster which does not match any known early literature annotation. It expresses unique markers, namely *dscaml1*, *ttc30a* and *tp73*, among others, leading us to believe it has a role in ciliogenesis. However, it clusters distinctly from ciliated progenitors in the mid-gastrula, and cannot be detected in subsequent stages (Figure 3.2). Importantly, both non-neural and neuroectoderm derivatives were also found to segregate into two distinct lobed clusters, therefore we sought to further characterize their differences (Figure 3.2).

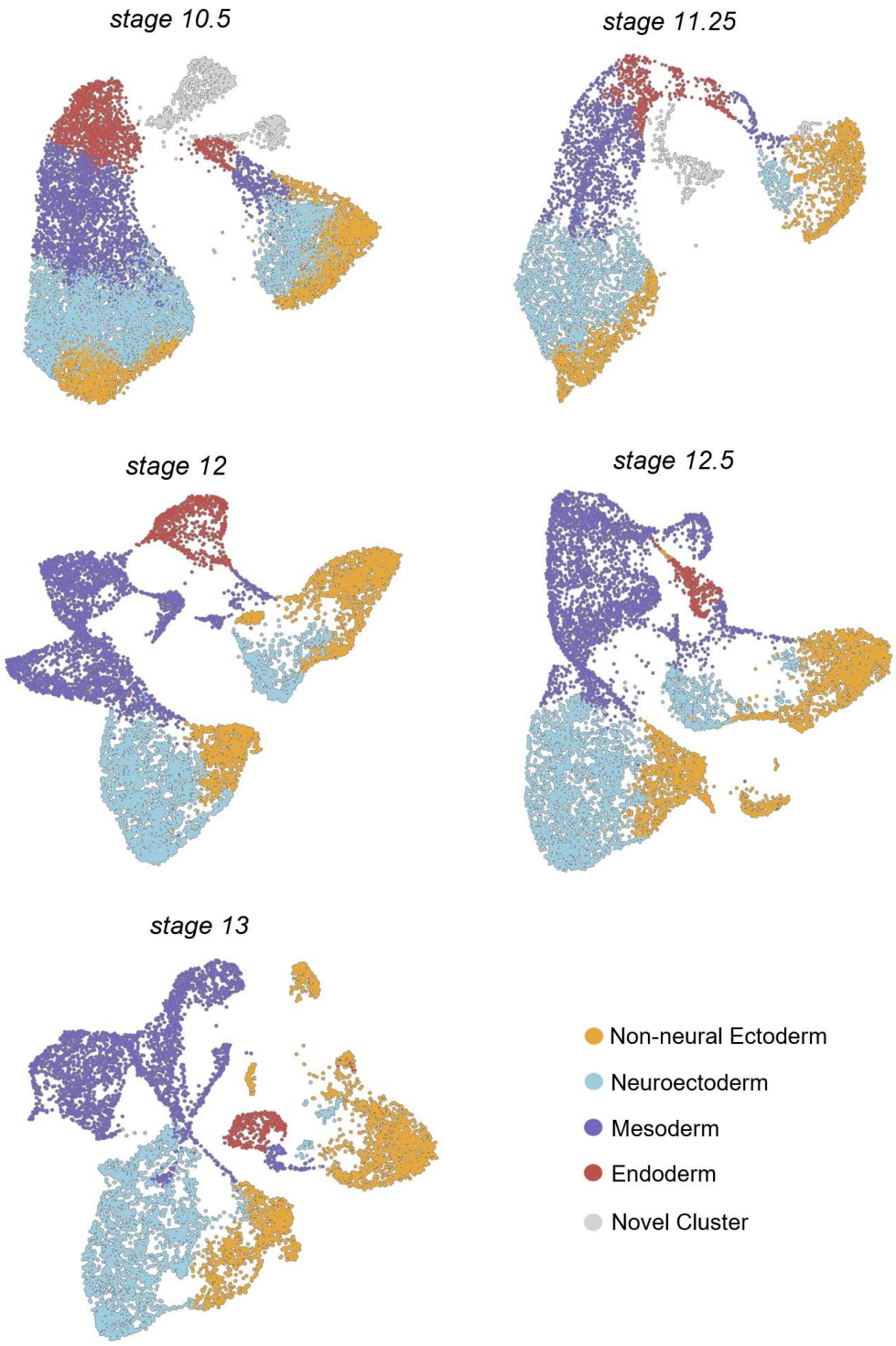

Figure 3.2: ***Major germ layer identification during gastrulation.*** Uniform manifold approximation and projection plots (UMAP) displaying major germ layers of stage 10.5 (early gastrula), 11.25 (early-mid-gastrula), 12.0 (mid-gastrula), 12.5 (late gastrula), and 13.0 (early neurula) nuclei.

Inner and outer ectoderm is established and maintained during gastrulation

The histology of hemisected early gastrula embryos reveals morphological distinctions between the inner and outer layer ectoderm. Protein marker staining shows differential localization between these layers (Chalmers 2003). However, previously published single cell experiments of the early gastrula do not resolve this known heterogeneity. Therefore, we wondered if we could resolve inner and outer layer transcriptomes. Examining the differentially expressed genes from the two early gastrula ectodermal lobe clusters (Figure 3.3A) reveals an inner ectodermal state expressing neural TFs (*neurog3*, *zic5*, *zeb2*) including a notch signaling modulator (*hes7.2*), as well as an outer ectodermal state expressing epidermal TFs (*grhl1*/*3*, *id2*) including an oxygen inducible factor (*epas1*) (Figure 3.3B). In addition to these TFs, 1,825 and 1,675 genes were found to be at least 2-fold differentially expressed between the inner and outer layer ectoderm respectively (Figure 3.3A). These data demonstrate that by the early gastrula inner and outer layer ectoderm progenitors have segregated into transcriptionally distinct cell types.

To better understand whether these ectodermal domains preserve their inner and outer layer identity throughout gastrulation (Figure 3.4A), we examined the temporal expression of differentially expressed inner and outer layer localized genes. Both *krt7*, a keratinocyte marker (Chalmers et al., 2006), and epas1, were found to be significantly enriched within the outer layer throughout gastrulation. Interestingly, both factors' expression increases in cell types of the inner ectoderm when they presumably migrate to the epidermal surface, such as ciliated epidermal progenitors and ionocytes (Figure 3.4B). Conversely, known basal membrane markers, t*p63* and *col18a1*, remain localized and highly expressed in the inner ectoderm compared with the outer. While *col18a1* remains expressed both in neuro- and non-neuroectoderm, *tp63* becomes regionally restricted to the inner non-neuroectoderm cells (Figure 3.4C).

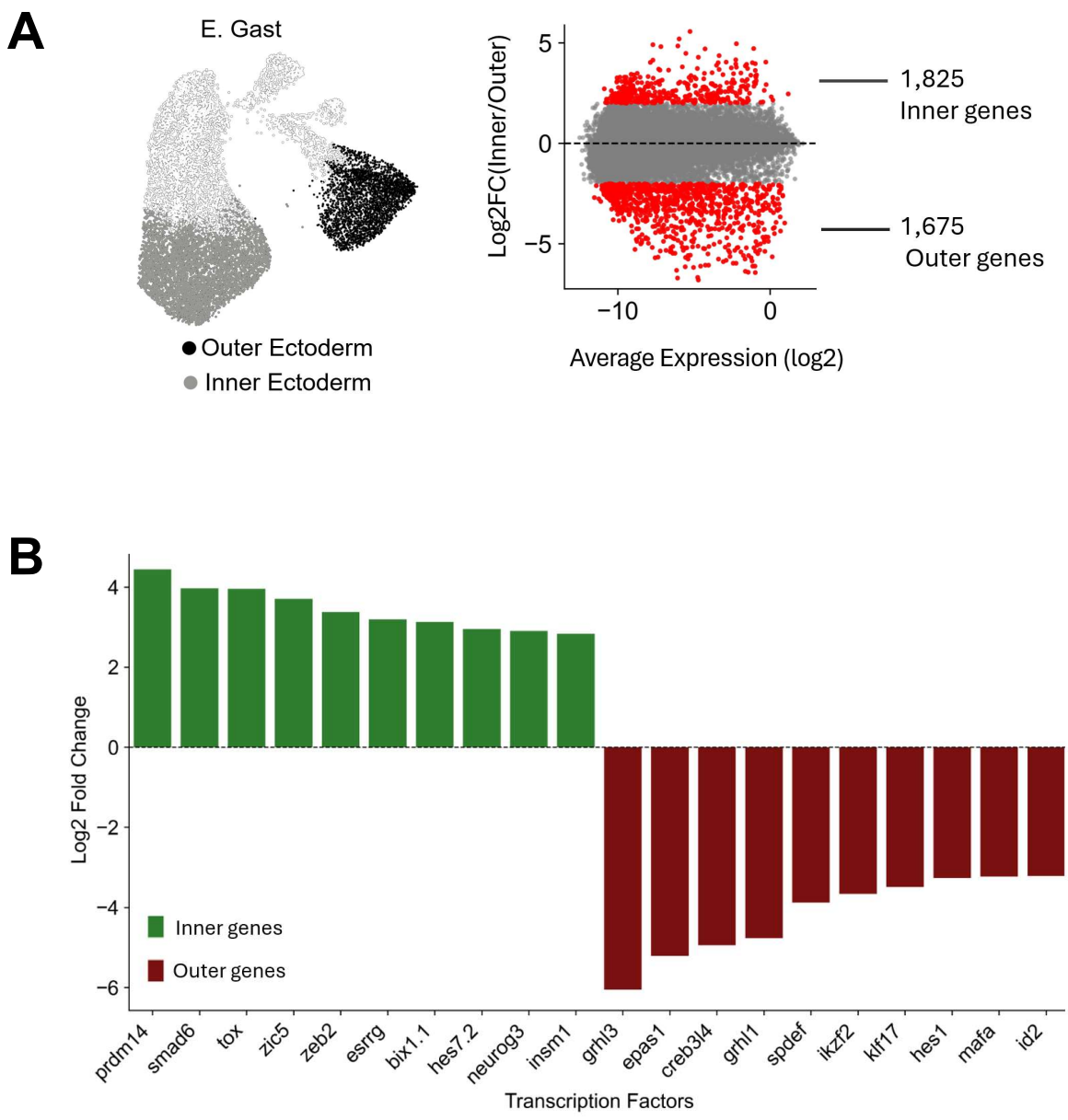

Figure 3.3: ***Inner and outer layer ectoderm is established by early gastrulation.***
(A) UMAP highlighting inner and outer ectoderm nuclei clusters (left) and the total genes differentially expressed between (right). **(B)** Top 10 transcription factors differentially expressed between inner and outer ectoderm in the early gastrula.

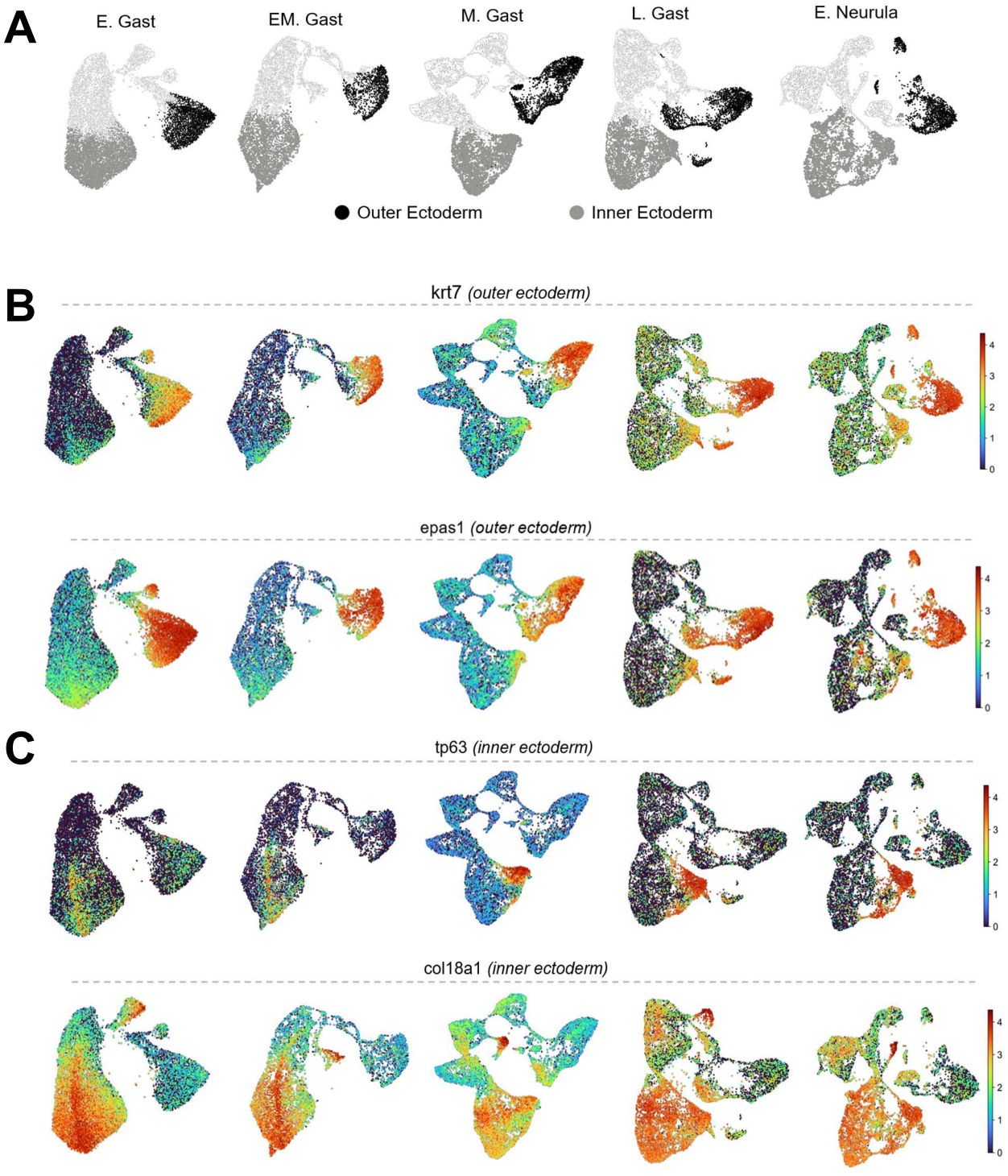

Figure 3.4: ***Inner and outer layer ectoderm maintains segregation during gastrulation.*** **(A)** Stage 10.5, 11.25, 12, 12.5, and 13 UMAPs showing inner and outer layered ectoderm. **(B)** Outer ectoderm marker krt7 (top) and epas1 (bottom) gastrulation expression. **(C)** Inner ectoderm markers tp63 (top) and col18a1 (bottom) gastrulation expression.

Taken together, inner progenitors arising from the *pax3/sox2* expression domain allow for the investigation of and outer ectoderm progenitor cells are heterogeneic, established within the early gastrula, and maintain identity throughout gastrulation.

Cell type complexity of the *Xenopus* gastrula

The progenitors formed from maintained local expression of early inner TFs, like *tp63*, can be interrogated for emergent non-neuroectoderm specification. Likewise, emergent neural lineages can be followed within the neuroectoderm. Within the continued expression domains of these progenitor markers, newly emergent cell type marker genes can be detected, further subdividing and specializing the lineage. By the end of gastrulation the inner ectoderm specifies numerous cell types of both the neural and non-neural ectoderm lineages earlier than previously appreciated (Figure 3.5A). The early neuron progenitors expressing *neurog1* and *elavl4* (Figure 3.5B), the anterior neural plate expressing *rax* and *six6* (Figure 3.5C), the posterior pre-placodal region expressing *pax8* and *tbx1* (Figure 3.5D), the anterior pre-placodal region expressing *pitx1* and *pitx2* (Figure 3.5E) , the posterior neural crest expressing *mafb* and *fgf9* (Figure 3.5F), and the anterior neural crest expressing rpe65, ltk, twist1 (Figure 3.5G). The antero-posterior specification of neural crest and pre-placodal ectoderm, as well as early neural or basal cell progenitors within the ectoderm have not previously been appreciated to occur during gastrulation.

In addition to the inner ectoderm, many cell types emerge in each germ layer during *Xenopus* gastrulation. At stage 10.5, 4 endoderm, 4 mesoderm and 5 ectoderm cell states are annotated, besides the novel cluster (Figure 3.6A). At stage 11.25, there are 4 endoderm, 5 mesoderm, and 7 ectoderm cell states (Figure 3.6B). At stage 12.0 there are 4 endoderm, 10 mesoderm, and 16 ectoderm cell states (Figure 3.6C). At stage 12.5 there are 4 endoderm, 12 mesoderm and 20 ectoderm cell states (Figure 3.6D). At stage 13 there are 7 endoderm, 12

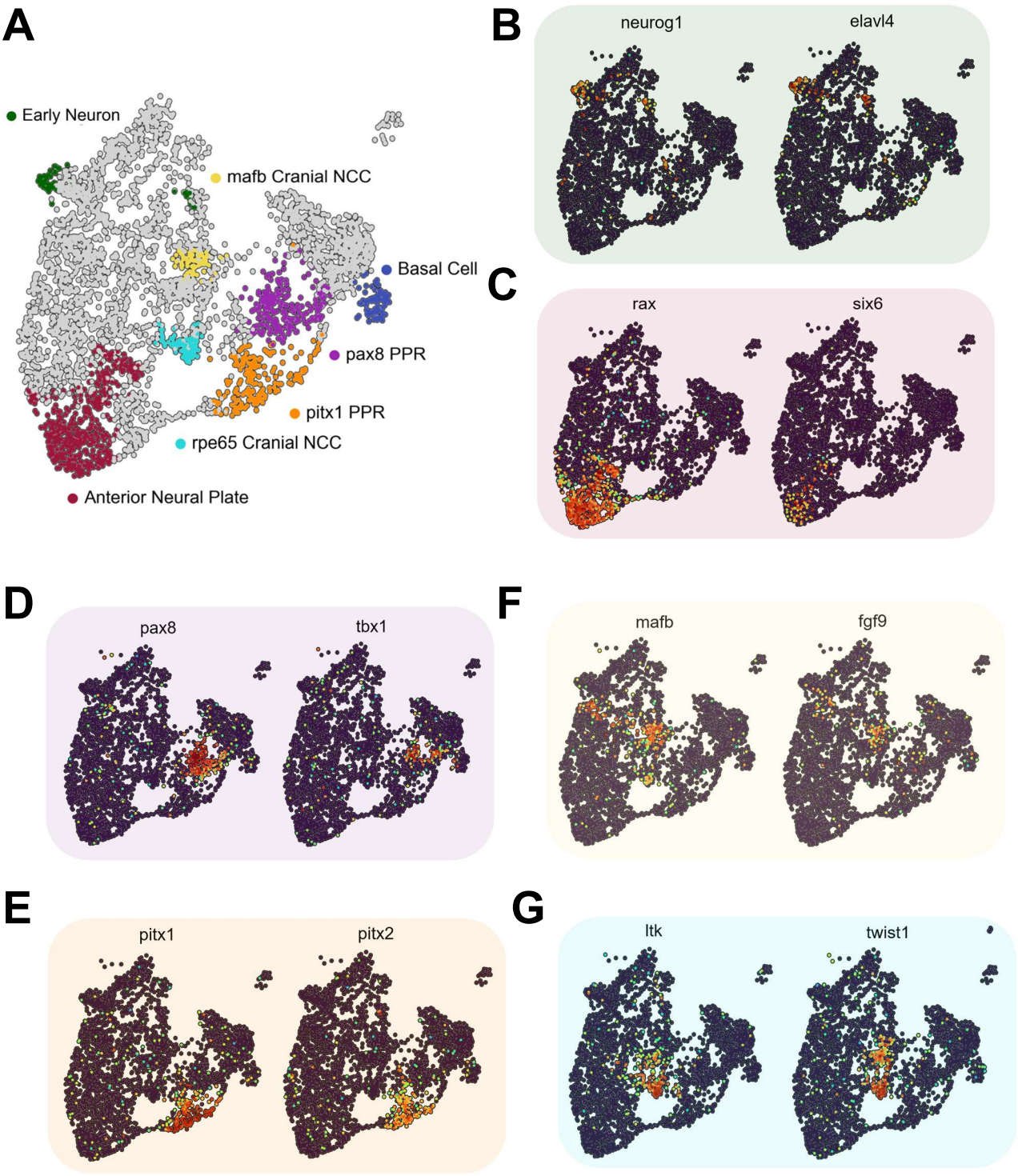

Figure 3.5: ***Emergent inner ectoderm cell-types and associated marker expression*****.** **(A)** Stage 13 (end of gastrulation) inner ectoderm subsetted UMAP. Marker gene expression for **(B)** early neuron, **(C)** anterior neural plate, **(D)** posterior (*pax8*) pre-placodal region, **(E)** anterior (*pitx1*) pre-placodal region, **(F)** posterior (*mafb*) cranial neural crest cell, and **(G)** anterior (*rpe65*) cranial neural crest cell.

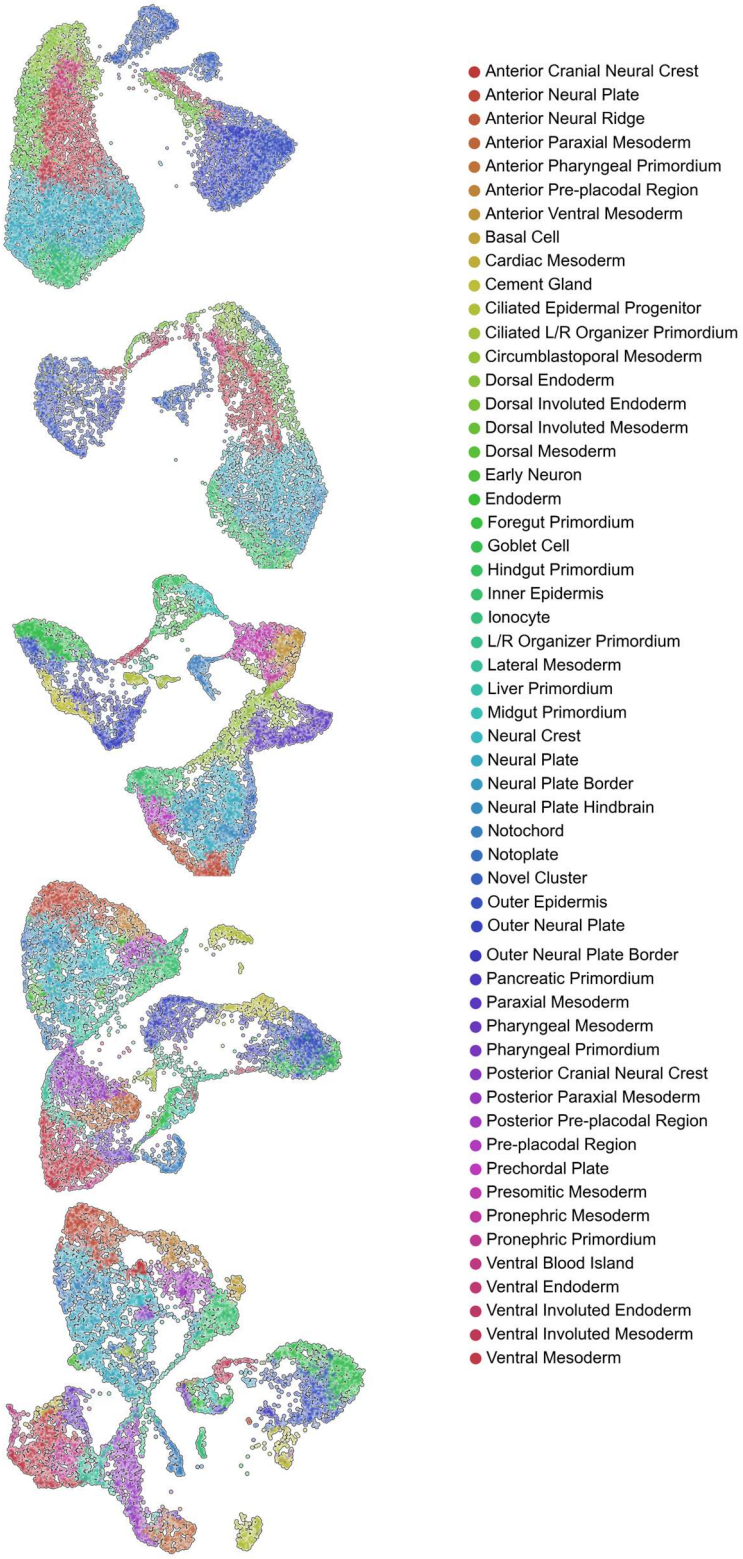

Figure 3.6: ***Cell type complexity of Xenopus gastrulation.*** Total germ layer annotations from stages 10.5 (top), 11.25, 12(middle), 12.5 and 13 (bottom).

mesoderm and 21 ectoderm cell states (Figure 3.6E). Of all germ layers, the ectoderm establishes the highest degree of heterogeneity during gastrulation. To better understand the required timing of gene expression associated with ectodermal cell state specification, we sought to characterize the temporal trajectories of all ectodermal sub-lineages.

Temporal trajectory of neuroectoderm specification

The neuroectoderm is initially established by the expression of *sox3*, and partially subdivided into *sox2* and *pax3* expression domains. While the initial *sox2* and *pax3* domains overlap extensively, they become further restricted during the progression of gastrulation to specify the neural plate (NP) and neural plate border (NPB), respectively. During gastrulation the neural plate is specified into 6 distinct cell types (Figure 3.7A, B). While *sox3* expression remains high during the early and mid-gastrula, it decreases at stage 12, coinciding with the induction of several neural plate cell types (Figure 3.7C). The anterior neural ridge expresses *emx1l*, the anterior neural plate expresses *arx*, the posterior neural plate expresses *pax2*, while early neurons express *ebf2* and the notoplate expresses *shh* (Figure 3.7C). These results demonstrate that the neural plate rapidly sub-divides into numerous progenitor states during the mid- to late-gastrula, before neurulation occurs.

The neural plate border arises from cells which establish *pax3* expression during the early to mid-gastrula, and gain antero-posterior specification states by the late gastrula (Figure 3.8A, B). As *sox2* expression becomes neural plate restricted, neural crest cells emerge with the expression of *snai2* (Figure 3.8C) and *sox9*. By stage 12.5, anterior neural crest cells expressing *twist1*, *ltk*, *rpe65* (Figure 3.8C, 3.5G) are specified, while posterior neural crest cells expressing *mafb* and *fgf9* become specified at gastrulation denouement, stage 13 (Figure 3.8C). *Pax3* expression remains high in all neural plate border sub-lineages while neuroectoderm

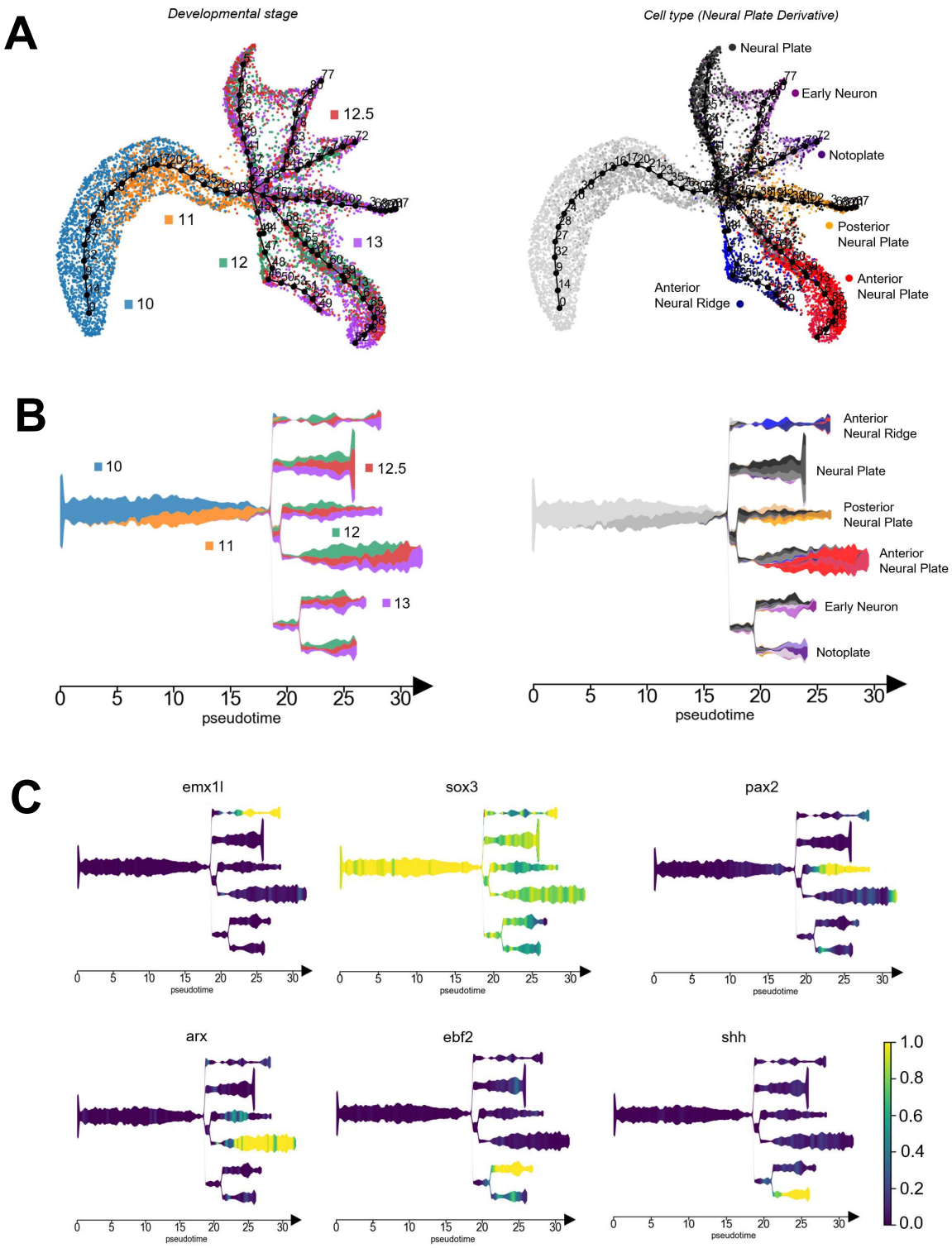

Figure 3.7: ***Neural plate cell type specification during gastrulation.***
(A) UMAP temporal trajectory of neural plate by developmental stage (left) and cell type (right). **(B)** STREAM subway temporal trajectory of neural plate by developmental stage (left) and cell type (right). **(C)** Neural plate temporal subway plots displayed neural plate lineage marker expression.

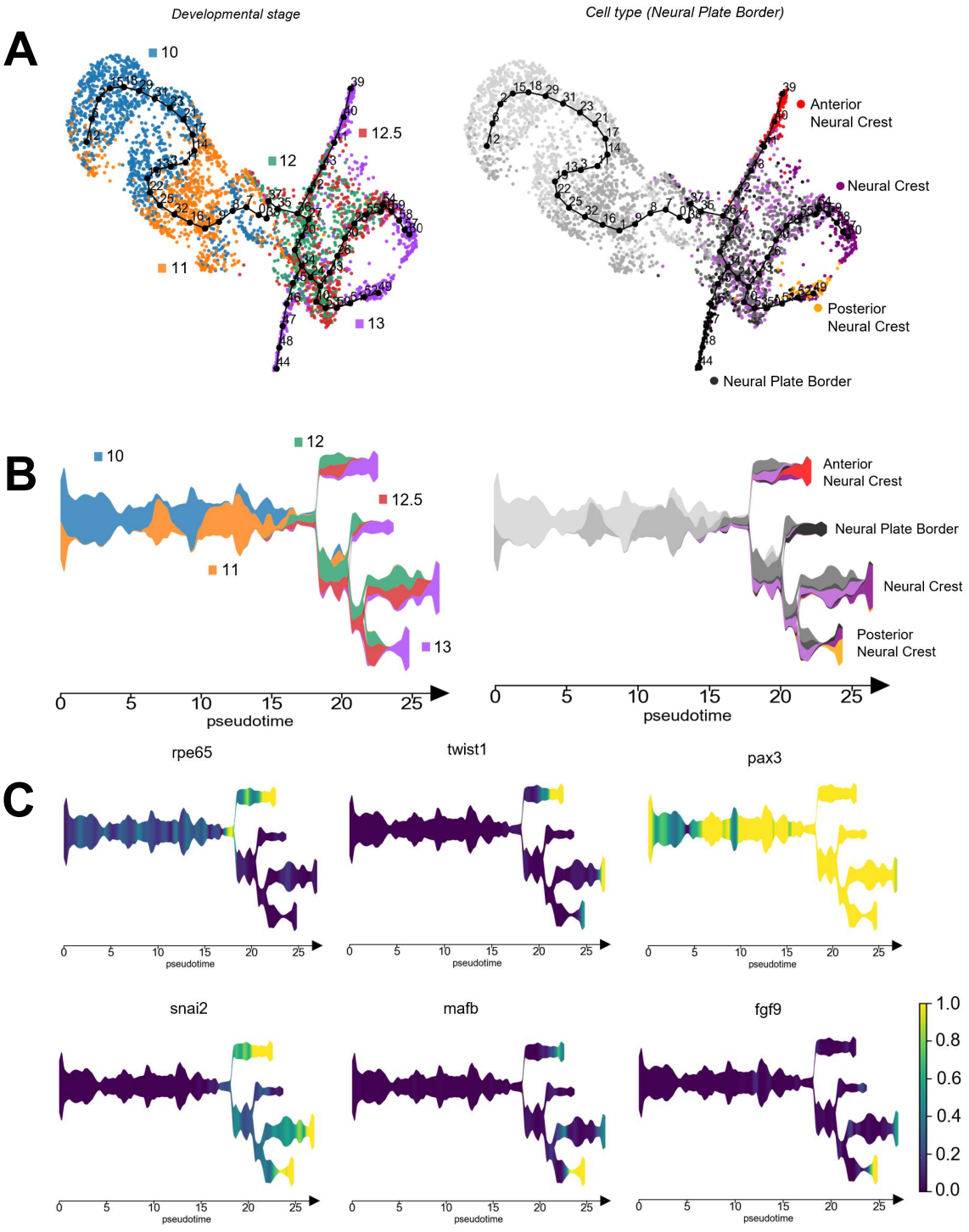

Figure 3.8: ***Neural plate border (NPB) cell type specification during gastrulation.*** **(A)** UMAP temporal trajectory of NPB by developmental stage (left) and cell type (right). **(B)** STREAM subway temporal trajectory of NPB by developmental stage (left) and cell type (right). **(C)** NPB temporal subway plots displayed NPB lineage marker expression.

(*sox2)* and non-neuroectoderm (*tp63)* are excluded. Due to these features of neural plate border development, it appears that at least by early gastrulation, the neural plate border represents its own distinct lineage from the interior neural plate and surrounding non-neuroectoderm. Finally, anterior neural crest cells appear to become specified before posterior neural crest cells. Taken together, the neuroectoderm can be divided into neural plate and neural plate border domains which begin to exit pluripotency in the late gastrula to rapidly sub-divide into 10 cell types exhibiting restricted lineage marker expression.

Temporal trajectory of non-neuroectoderm specification

Two major cell type derivatives from the outer layer non-neural ectoderm, also known as the epidermis, become temporally specified during gastrulation (Figure 3.9A, B). While the cement gland marker, *ag1*, is already expressed by stage 11.25, other markers like *agr2* and *pitx1* are not detected appreciably until stage 12 (Figure 3.9C). Additionally while goblet cells are known to express *itln1* and *itln2*, we find that they prematurely express *muc4* (Figure 3.9C). These outer cells also remain high in the expression of *grhl1/3* as well as *krt7/70* throughout gastrulation. In addition, other specialized non-neuroectoderm cell types like ionocytes and ciliated epidermal progenitors are first formed within the inner layer and likely migrate to the outer layer by the end of gastrulation. This is because both *krt7* and *epas1,* two key outer layer markers, become upregulated in these specialized cell states as gastrulation progresses (Figure 3.4B).

The inner layer ectoderm is initially marked by the expression of basal markers *tp63* and *col18a1* (Figure 3.4C). Notably, these cells express low levels of keratins and grainyheads, but not pax3, or sox2/3. This demonstrates that the inner non-neuroectoderm progenitors are transcriptionally distinct at least by the early gastrula. Throughout gastrulation, the inner non-neuroectoderm becomes specified into 6 cell states, ciliated epidermal progenitors,

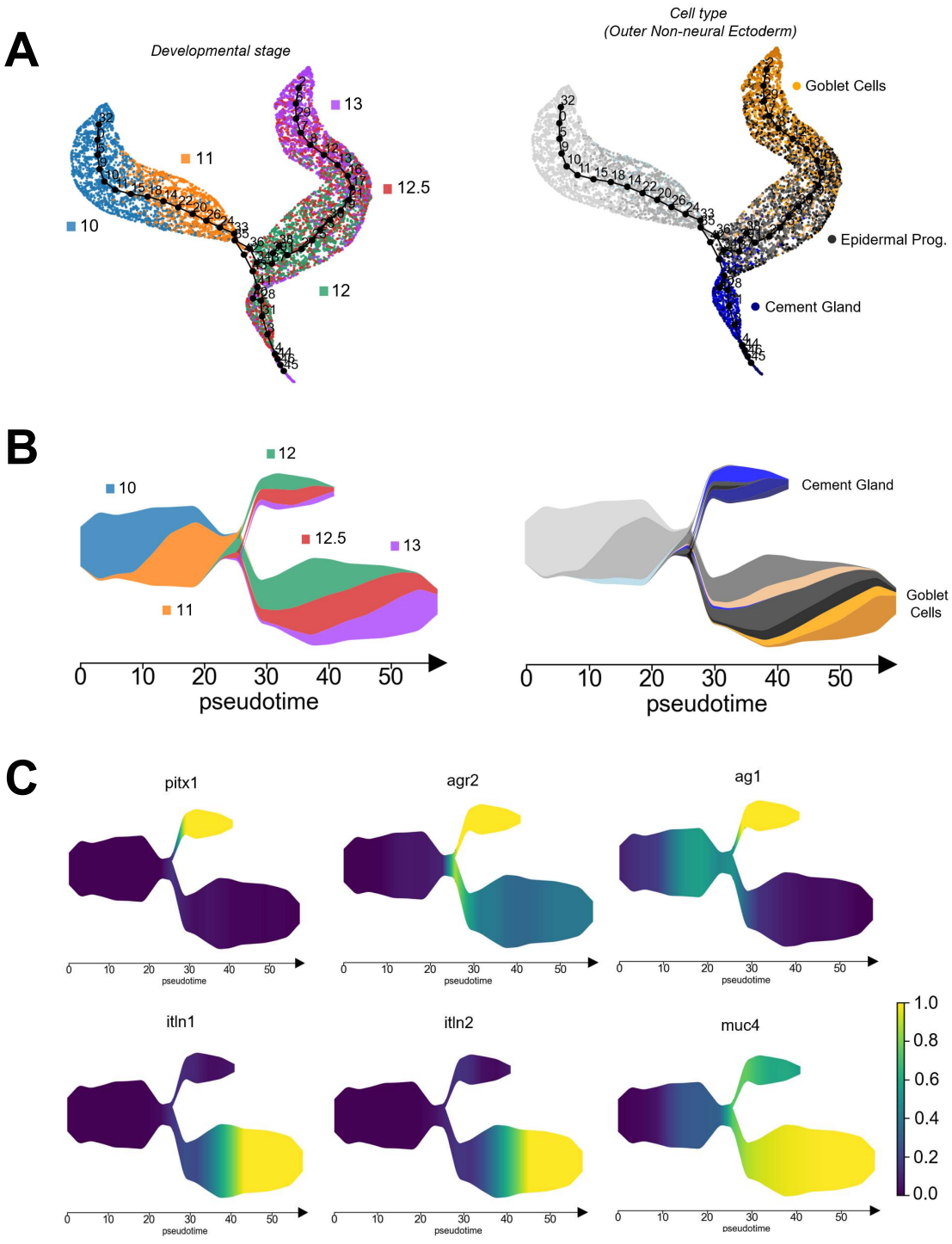

Figure 3.9: ***Outer non-neural ectoderm (NNE) cell type specification during gastrulation.*** **(A)** UMAP temporal trajectory of outer NNE by developmental stage (left) and cell type (right). **(B)** STREAM subway temporal trajectory of outer NNE by developmental stage (left) and cell type (right). **(C)** Outer NNE temporal subway plots displayed outer NNE lineage marker expression.

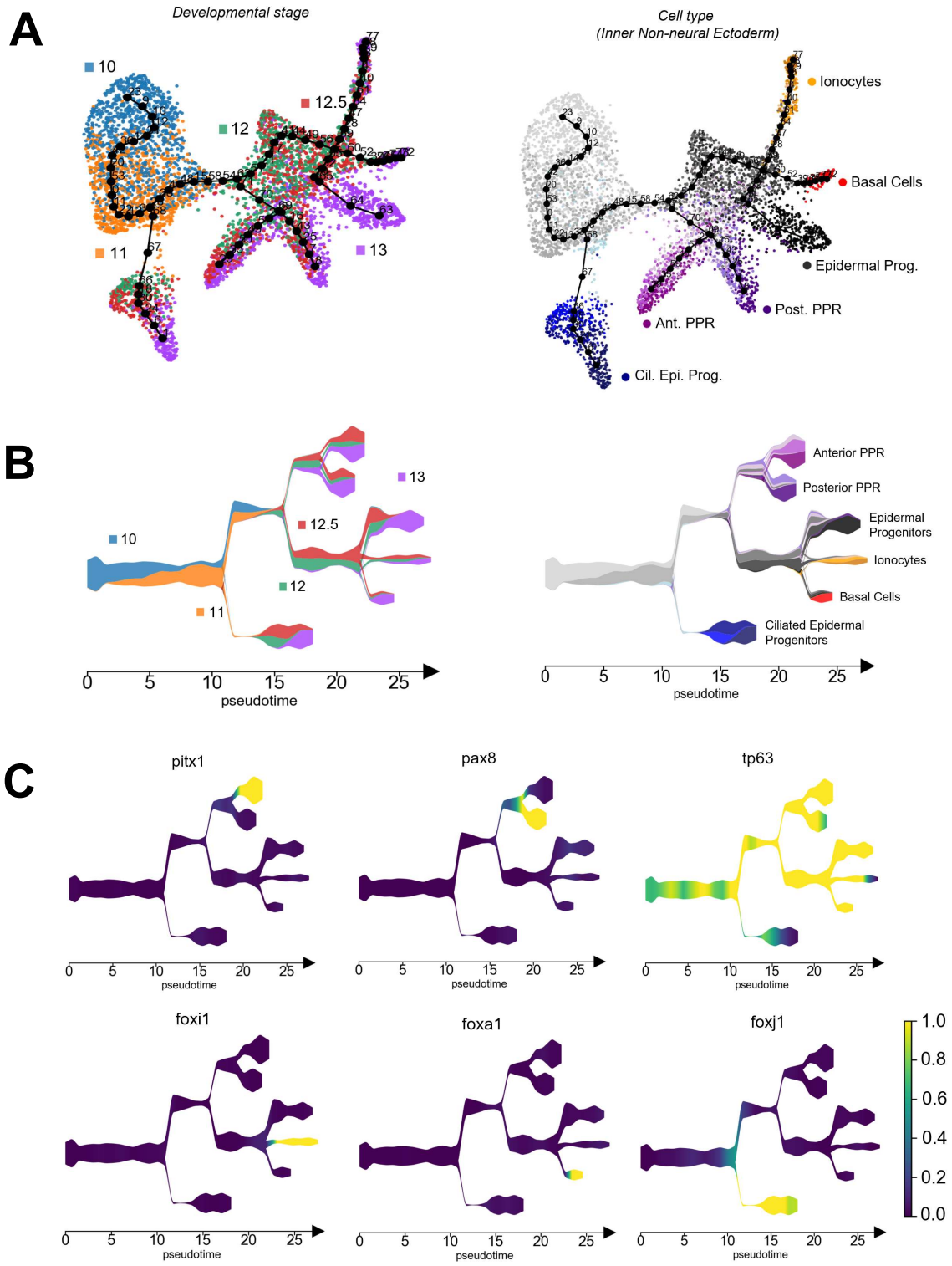

Figure 3.10: ***Inner non-neural ectoderm (NNE) cell type specification during gastrulation.*** **(A)** UMAP temporal trajectory of inner NNE by developmental stage (left) and cell type (right). **(B)** STREAM subway temporal trajectory of inner NNE by developmental stage (left) and cell type (right). **(C)** Inner NNE temporal subway plots displayed inner NNE lineage marker expression.

ionocytes, antero-posterior pre-placodal region, inner non-neuroectodermal progenitors and basal cells (Figure 3.10A, B). By stage 11.25, ciliated progenitors first transcriptionally bifurcate due to the expression of factors like *foxj1* and *mcidas* (Figure 3.10C). Later by the mid gastrula, ionocytes, expressing *foxi1* and *atp6v1b1* (Figure 3.10C). At stage 12.5 the pre-placodal region acquires antero-posterior identity by the expression of *pitx1* and *pax2* (Figure 3.10C). At gastrulation denouement, stage 13, basal cells bifurcate from the expression of *foxa1* (Figure 3.10C).

Transcription factor networks govern gastrula cell state specification

Ectodermal lineage segregation within the temporal cell state trajectories can be defined by emergent transcription factor expression (Figure 3.11). To further understand the temporal role transcription factors play in the emergence and subsequent segregation of progenitor cell states, the pre-placodal region was investigated. The pre-placodal progenitor state is established by stage 12 with the expression of *eya1* and *six1* (Figure 3.12A). Later at stage 12.5 and 13, the expression of *isl1* and *foxo1* begins only in the anterior of the pre-placodal region (Figure 3.12A). Alternatively, the expression of *prdm12* and *sox9* are restricted in the posterior pre-placodal region (Figure 3.12A). Exploring TF expression leading to this antero-posterior pre-placodal region segregation reveals the activation of early gastrula NNE progenitor markers, *tfap2a, klf5, tp63*, followed by the activation of core PPR markers *eya1* and *six1*, starting at stage 12 (Figure 3.12B). The antero-posterior pre-placodal marker regional localization becomes clear by stage 12.5 and 13, when gastrulation is concluding (Figure 3.12B). These results demonstrate sequential TF activation defines pre-placodal lineage specification during gastrulation.

Transcription factors utilize DNA binding domains to recognize specific motifs and interact with the chromatin to activate gene expression. Although the single nucleus data itself

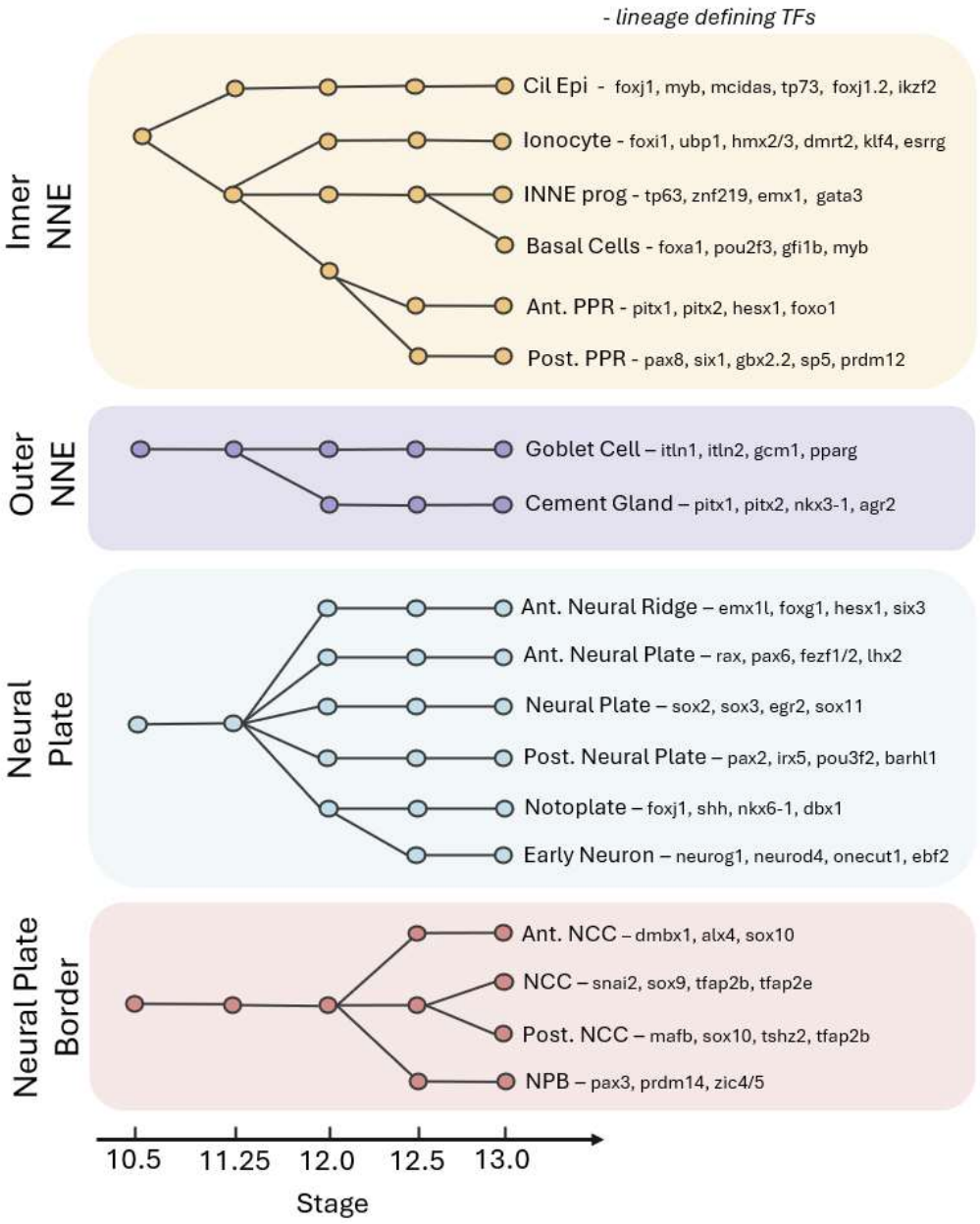

Figure 3.11: ***Summary of ectoderm specification throughout Xenopus gastrulation.*** Summation of the temporal lineage trajectories of neural plate, neural plate border, as well as inner and outer NNE.

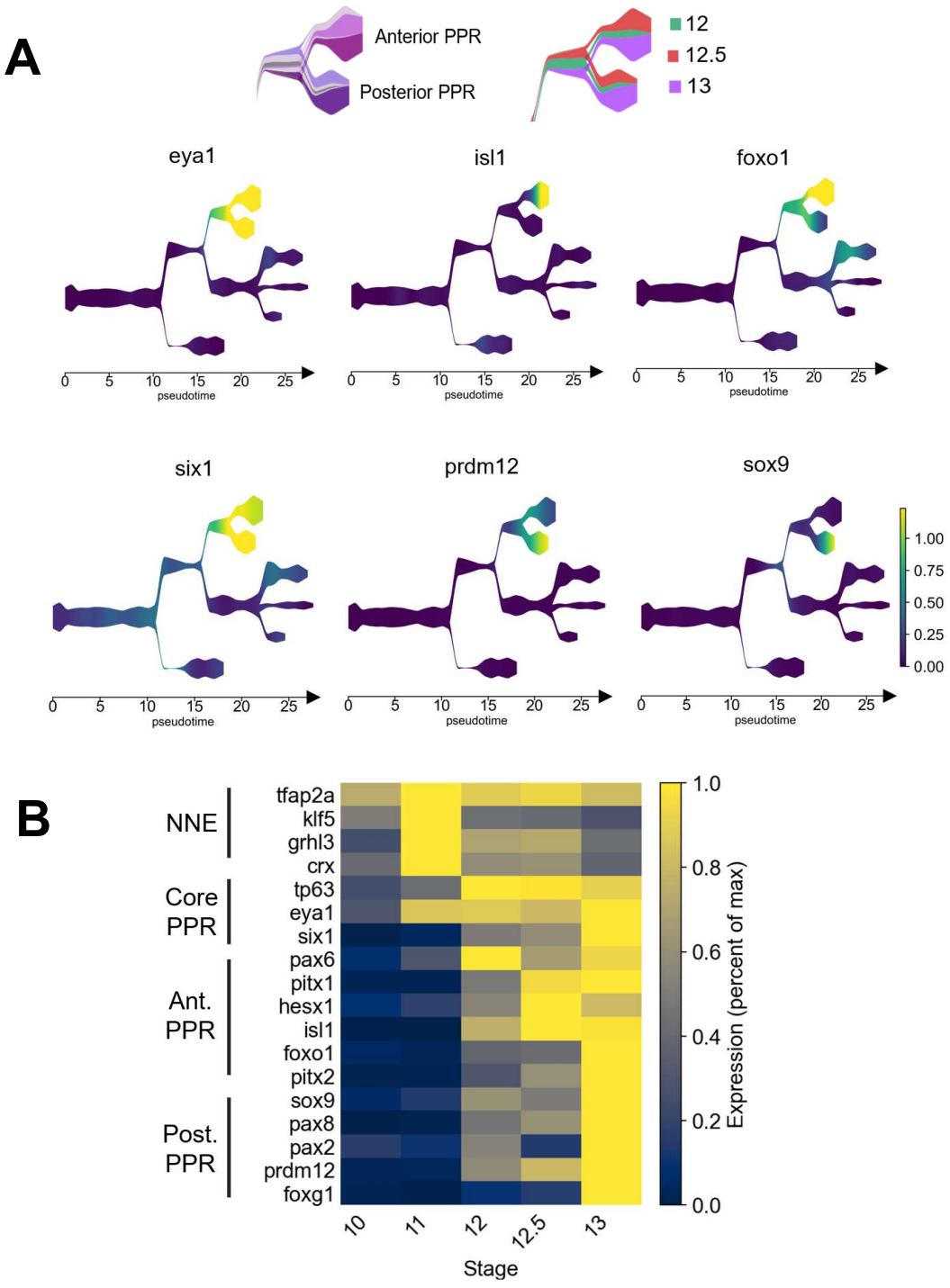

Figure 3.12: ***Temporal transcription factor expression of the pre-placodal region (PPR).*** **(A)** Subsetted subway plot of anterior and posterior pre-placodal region specification by cell type (left) and developmental stage (right). **(B)** Heatmap of temporally expressed pre-placodal region marker TFs, normalized by scoring each factor as a percentage of the stage with its maximum expression.

does not provide epigenetic information, we sought to leverage existing gastrula-staged whole embryo ATAC-seq datasets with motif databases to bolster TF-target predictions. The SCENIC software pipeline (Figure 3.13A, Aibar et al., 2017) utilizes the nuclei expression matrix to score TF co-expression with potential target genes. Next, bulk ATAC-seq data from the mid-Gastrula was processed where the upstream and downstream regions of open chromatin were mined for TF motif presence using the SCENIC associated motif database. Finally, for co-expressed TF-target modules containing a TF motif in open chromatin, the area under the curve (AUC) score calculates the strength of TF-target interactions occurring in each individual cell. At stage 12 *rax* begins expression at the presumptive anterior neural plate, and its predicted TF-target interactions also score highest within this expression domain (Figure 3.13B). *Rax* is predicted to activate factors like *pax6*, *fezf2*, *hesx1* within the anterior neural plate domain (Figure 3.13C). The total distribution of AUC scores shows that only the anterior neural plate cells are flagged for the *rax* regulatory network to be “on”, or considered active (Figure 3.13D).

In addition to *rax* stage specific regulon formation in the stage 12 anterior neural plate, we sought to characterize the regulons forming within a particular lineage over time. SCENIC analysis was also extended to characterize how TF-target interactions shape the ionocyte lineage. As the ionocyte lineage bifurcates from inner non-neuroectodermal progenitors by stage 12, it begins to form *foxi1*, *foxo3*, *esrrg* and *ubp1* lineage specific regulons (Figure 3.14A). As developmental time of the ionocyte trajectory inference increases, the regulons for all four factors concordantly increase AUC scores (Figure 3.14A). This suggests these TFs increase target gene activation over time to permit ionocyte differentiation. Examining all combined ionocyte specific regulons, including *foxp1*, reveals a coordinated activation of 15 genes, including ionocyte associated TFs *hmx2* and *ubp1* (Figure 3.14B). These overlapping gene regulatory network predictions suggest TF redundancy in the ionocyte network activation (Figure 3.14B). Taken together, SCENIC can leverage single nuclei expression data with bulk epigenetic motif analysis to score TF-target network formation in cell types emerging at a

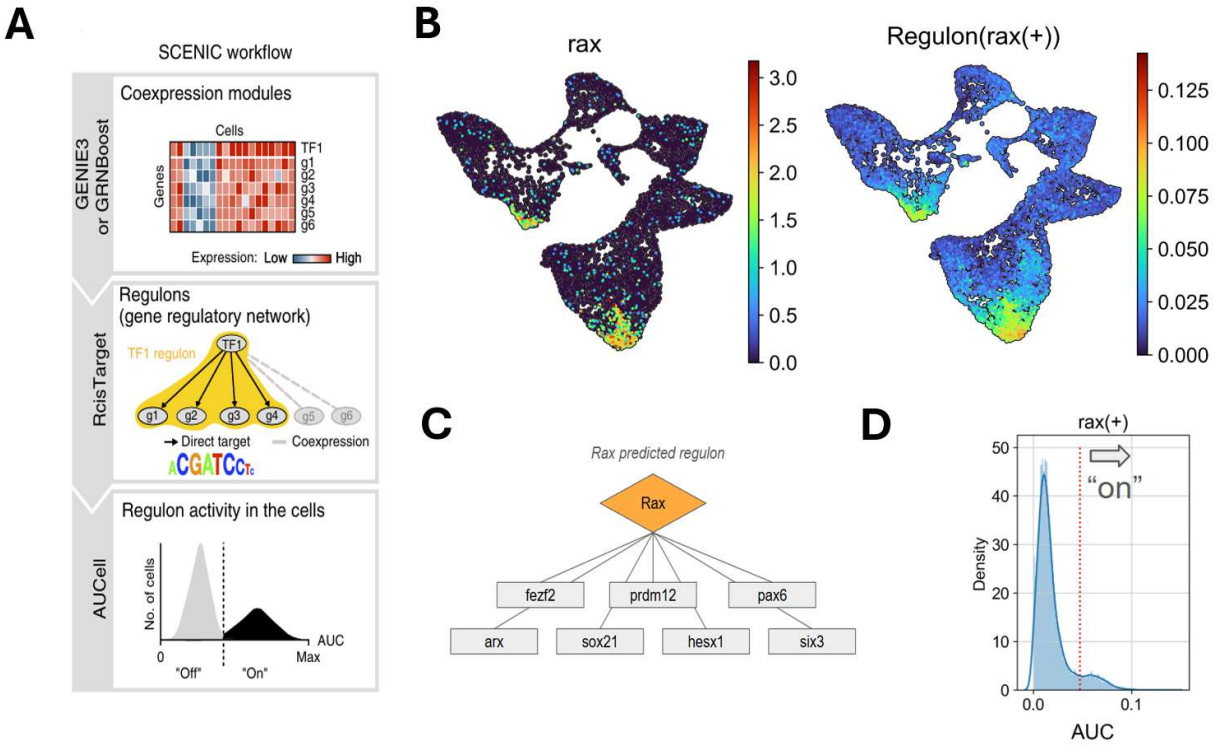

Figure 3.13: ***SCENIC regulon predictions in emergent cell types.***
(A) SCENIC workflow schematic from Aibar et al., 2017; (top) GRNBoost characterizes co-expressed TFs and genes, (middle) RcisTarget characterizes motifs within genomic sequencing, (bottom) AUCell calculates the probability that a motif associated TF-target activation is occurring within a given cell, i.e. “Regulon activity”. **(B)** Anterior neural plate marker *rax* expression (left) and AUC regulon activity score (right). **(C)** *rax* predicted regulon based on TF-target co-expression and motif association. **(D)** *rax* AUC scores where the red line denotes the threshold for cells with an active regulon.

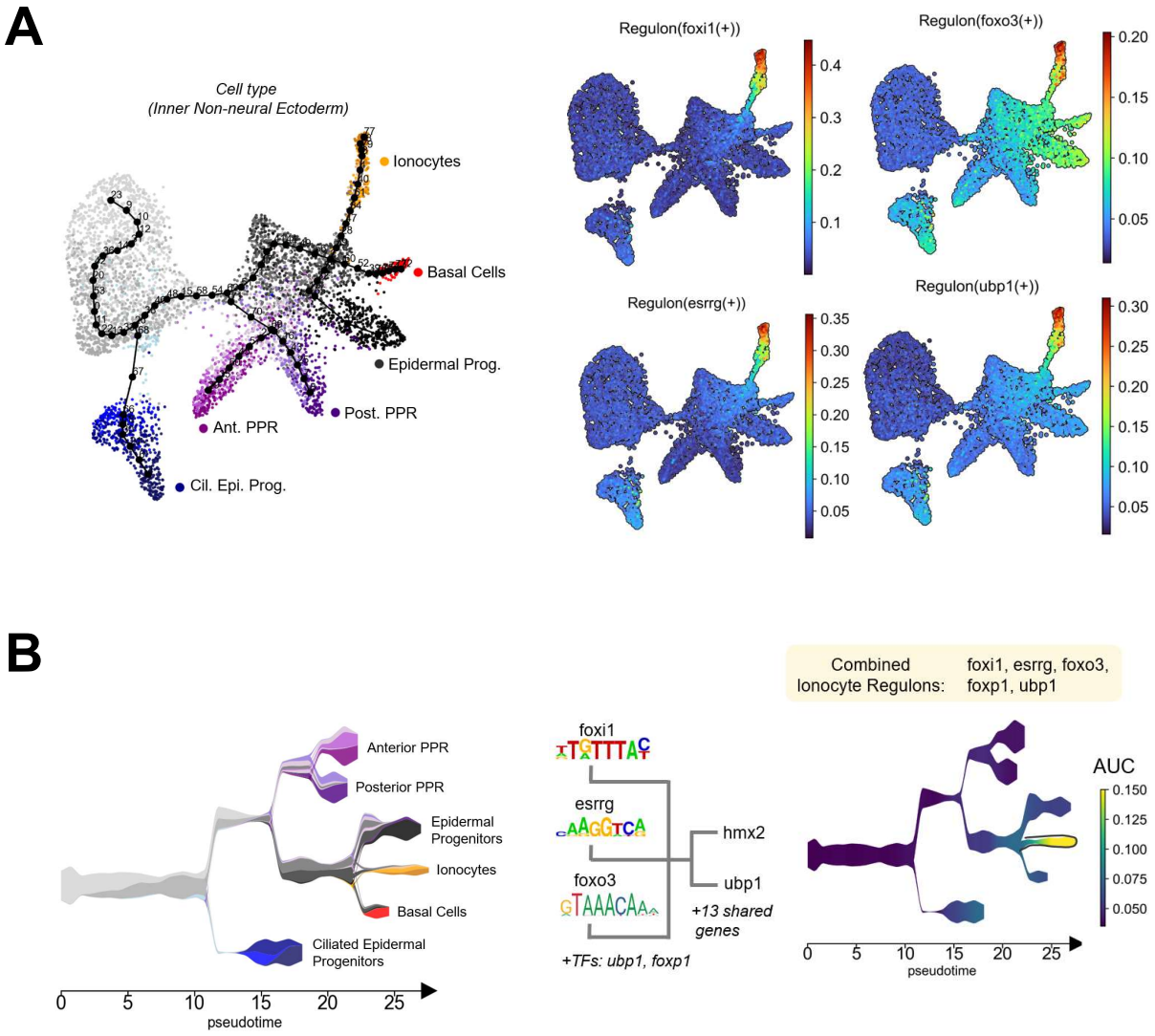

Figure 3.14: ***SCENIC regulon predictions in temporally defined specification states.***
(A) Regulons (right) localized within the ionocyte cluster of the UMAP temporal trajectory (left).
(B) Proposed ionocyte specification regulon network (right) and subway temporal trajectory (left).

particular stage (Figure 3.13) or during lineage formation over-time (Figure 3.14).

Maternal Foxi2 knockdown attenuates NNE progenitor formation and ectopically activates *rfx3* at stage 11.25

Maternal TFs play pivotal roles in binding chromatin, establishing the epigenetic state, and activating gene targets to form germ layers and the first specialized cell types. Work in *Xenopus* demonstrates maternal Foxi2 as an animally localized ectodermal activator (Cha et al., 2012). Foxi2 is an early Sox3 binding partner in pre-ZGA chromatin, recruiting Ep300 within ectoderm specific CRMs. These CRMs form enriched enhancer regions which coordinate robust ectoderm marker activation with reduced variation in expression (See Chapter 2, Hendrickson et al., 2025). As the work concerning Foxi2 regulation over ectoderm specification has not extended past the beginning of gastrulation, we sought to utilize high resolution single nucleus sequencing to understand its role in ectoderm specification in the mid-gastrula.

Single nucleus sequencing of stage 11.25 wild-type (6,447) and Foxi2 knockdown (6,132) cells reveals that the ectoderm is the most transcriptionally affected germ layer (Figure 3.15A). Further examination shows that both the inner and outer layer non-neuroectoderm cells cluster the most divergently in response to Foxi2 knockdown (Figure 3.15A). Within the outer non-neuroectoderm the activation of several factors, including *dlx3/5*, *gata2, klf5,* as well as structural genes, *krt7/70,* were greatly reduced by Foxi2 knockdown (Figure 3.15B). Conversely, both notch and hedgehog signaling factors show an increase in outer ectoderm expression, including *rfx3*, a conserved ancient ciliogenesis factor (Figure 3.15B). Within the inner non-neuroectoderm, Foxi2 knockdown inhibits the activation of inner non-neural ectodermal progenitor markers, *tp63, hgf, dlx3, klf5* (Figure 3.15C). However, while Foxi2 knockdown does not alter expression of the core neural plate marker *sox2*, it does misactivate neural plate border marker *pax3* (Figure 3.15C). Throughout the inner ectoderm notch and

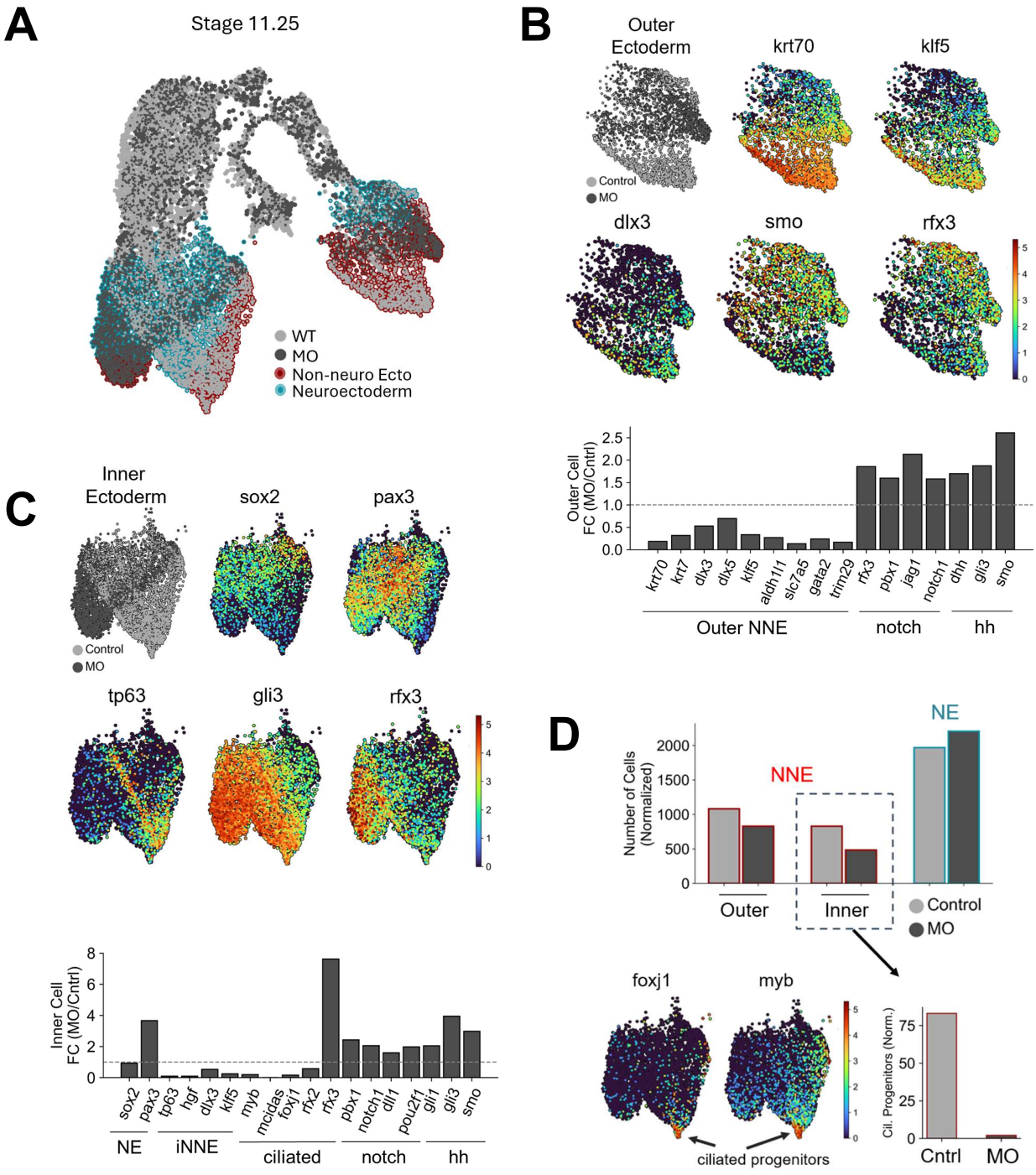

Figure 3.15: ***Maternal Foxi2 knockdown attenuates NNE programming and activates ectopic rfx3 expression at stage 11.25.***

(A) Stage 11.25 nuclei of WT (light gray) or Foxi2 MO injected (dark gray) embryos, with highlighted neuroectoderm (blue) and non-neuroectoderm (red) clusters. **(B)** Outer non-neuroectoderm subset with affected marker expression. **(C)** Inner non-neuroectoderm subset with affected marker expression. **(D)** Comparison of specialized ciliated progenitor non-neuroectoderm formation.

hedgehog factor expression is elevated, with the most drastic increase of *rfx3,* like the outer ectoderm (Figure 3.15C). Additionally, *foxj1* and *myb* expression is abolished, and ciliated progenitor formation is greatly reduced by stage 11.25 (Figure 3.15D).

SCENIC analysis of the WT ciliated progenitor cells at stage 11.25, shows that *myb* is highly expressed and lies upstream of the ciliated markers *foxj1* and *mcidas* in its regulon formation (Figure 3.16A). Maternal Foxi2 ChIPseq (Chapter 2) reveal its direct binding to the putative *myb* CRM, and the loss of both *myb* expression and myb regulon formation in the Foxi2 knockdown demonstrate its role in proper ciliated progenitor formation (Figure 3.16A,B). Similarly, the decrease of tp63, dlx3, dlx5 regulon formation demonstrates Foxi2 control over the transcriptional state of inner non-neuroectoderm progenitor formation, and confirms bulk RNA-seq results from Chapter 2 (Figure 3.16B,C). However, throughout the Foxi2 knockdown inner and outer ectoderm, there are increases in pbx1 and pou2f1 regulon formation, and extensive ectopic rfx3 regulon formation, not observed in WT cells (Figure 3.16B,C). Foxi2 forms very strong and sharp peaks near *myb, foxj1, mcidas, tp63,* and *dlx3/5*, however its *pbx1*, *pou2f1,* and *rfx3* associated peaks form more weakly. Considering that Foxi2 is a known activator and Ep300 co-factor, the mechanism by which Foxi2 typically represses these factors, whether direct or indirect, is not yet well understood. Taken together these data suggest maternal Foxi2 activates both non-neuroectoderm and ciliated progenitor expression states, while inhibiting ectopic *rfx3* signaling, especially within the inner ectoderm at stage 11.25 (Figure 3.17).

Maternal Foxi2 knockdown misregulates ciliogenesis and restricts PPR specification at stage 12

To further characterize the role of Foxi2 in downstream gastrulation we sequenced additional stage 12 knockdown and WT datasets yielding WT (9,564) and (9,282) MO cells (Figure 3.18A).

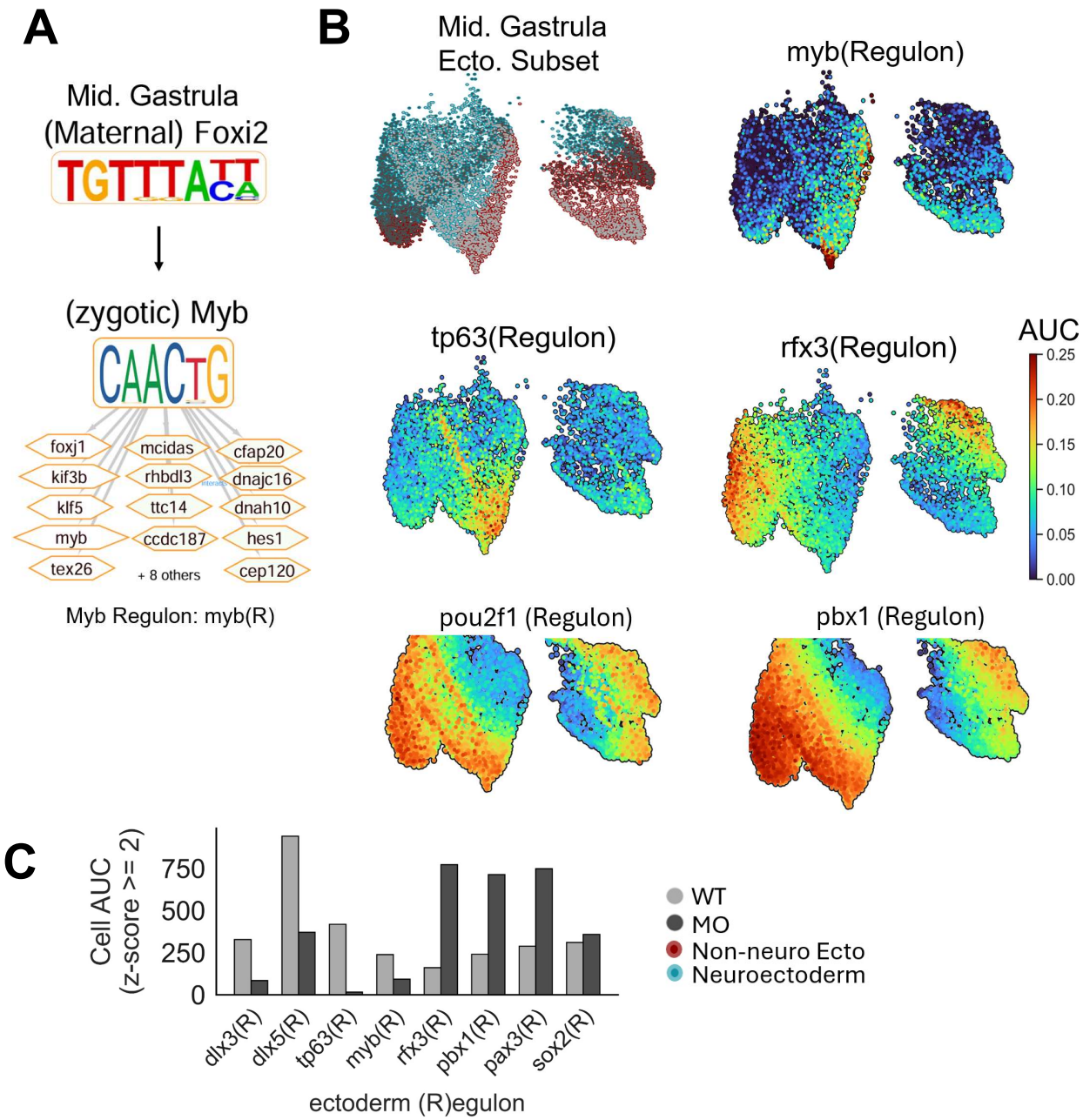

Figure 3.16: ***Maternal Foxi2 knockdown affects mid-gastrula regulon formation.***
(A) Foxi2 activation of SCENIC derived myb regulon. **(B)** Mid-gastrula ectoderm subsets highlighting regulon AUC activity scores within WT (light gray) and Foxi2 MO (dark gray) nuclei. **(C)** Comparison of WT (light gray) and Foxi2 MO (dark gray) total cells with AUC activity where z-score > 2.

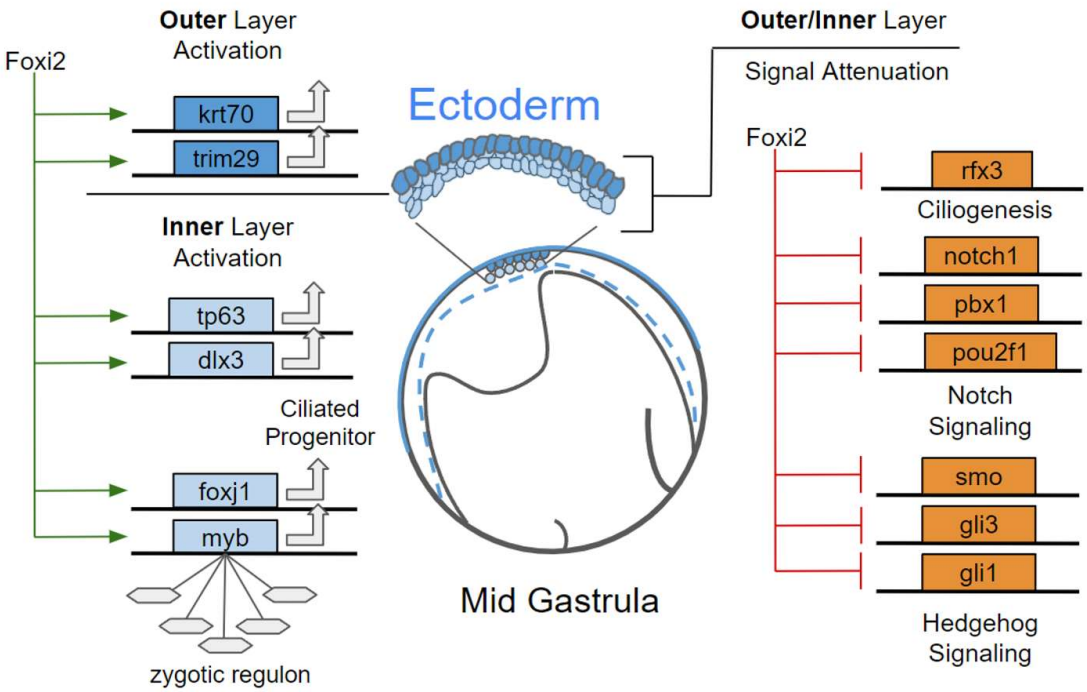

Figure 3.17: ***Summary of maternal Foxi2 control over mid-gastrula ectoderm formation.*** Foxi2 inner and outer layer ectoderm activation (left) and repression (right) at stage 11.25.

Like stage 11.25, major clustering differences can be observed in ectodermal cells. Focusing on the inner non-neuroectoderm compared to stage 11.25 slight decreases in the progenitor markers *hgf*, *dlx3*, *tp63*, although there is compensation in Foxi2 control over their expression (Figure 3.18B). This is likely due to the drastic reduction in Foxi2 expression after the onset of gastrulation (Cha 2012 (protein), xenbase.org (mRNA)). In the knockdown, these same inner ectoderm cells continue ectopic *rfx3* activation from stage 11.25 and subsequently upregulate the ciliated progenitor markers *foxj1* and *mcidas* at stage 12 (Figure 3.18B). These data suggest that during WT embryo gastrulation progression, Foxi2 helps establish proper ciliogenesis, while attenuating ectopic *rfx3* driven ciliogenesis.

As Foxi factors are known to be associated with pre-placodal development, we investigated the effects of pre-placodal progenitors expressing specification markers. Within the pre-placodal region the progenitor markers *eya1* and *six1* expression is not significantly affected by Foxi2 knockdown (Figure 3.18C). However, the activation of the anterior specification markers *pitx1* and *isl1*, as well as the posterior specification marker *pax8* expression are significantly inhibited (Figure 3.18C). Therefore, while the number of total progenitors (*eya1*/*six1*) remains roughly equal, the number of PPR cells undergoing further specification (*isl1*/*pax8*/*pitx1*) decreases significantly in stage 12 Foxi2 knockdown non-neuroectoderm (Figure 3.18C). Examining the total amounts of neural and non-neural ectodermal tissues, we see a drastic expansion of ciliated progenitors in Foxi2 knockdown embryos (Figure 3.18D). This expansion accounts for the Foxi2 knockdown total increase of non-neuroectoderm cells compared to the wild type, and likely contributes to the decreased proportion of neuroectodermal cells (Figure 3.18D).

Interestingly, stage 11.25 neuroectoderm cells, presumably exposed to ectopic *rfx3* and elevated *pax3* in the Foxi2 knockdown, express increased levels of non-neuroectoderm signaling markers compared to WT at stage 12. Although by stage 12, *rfx3* and *pax3* expression in the Foxi2 knockdown mostly resembles that of the WT, there are an increase in expression in

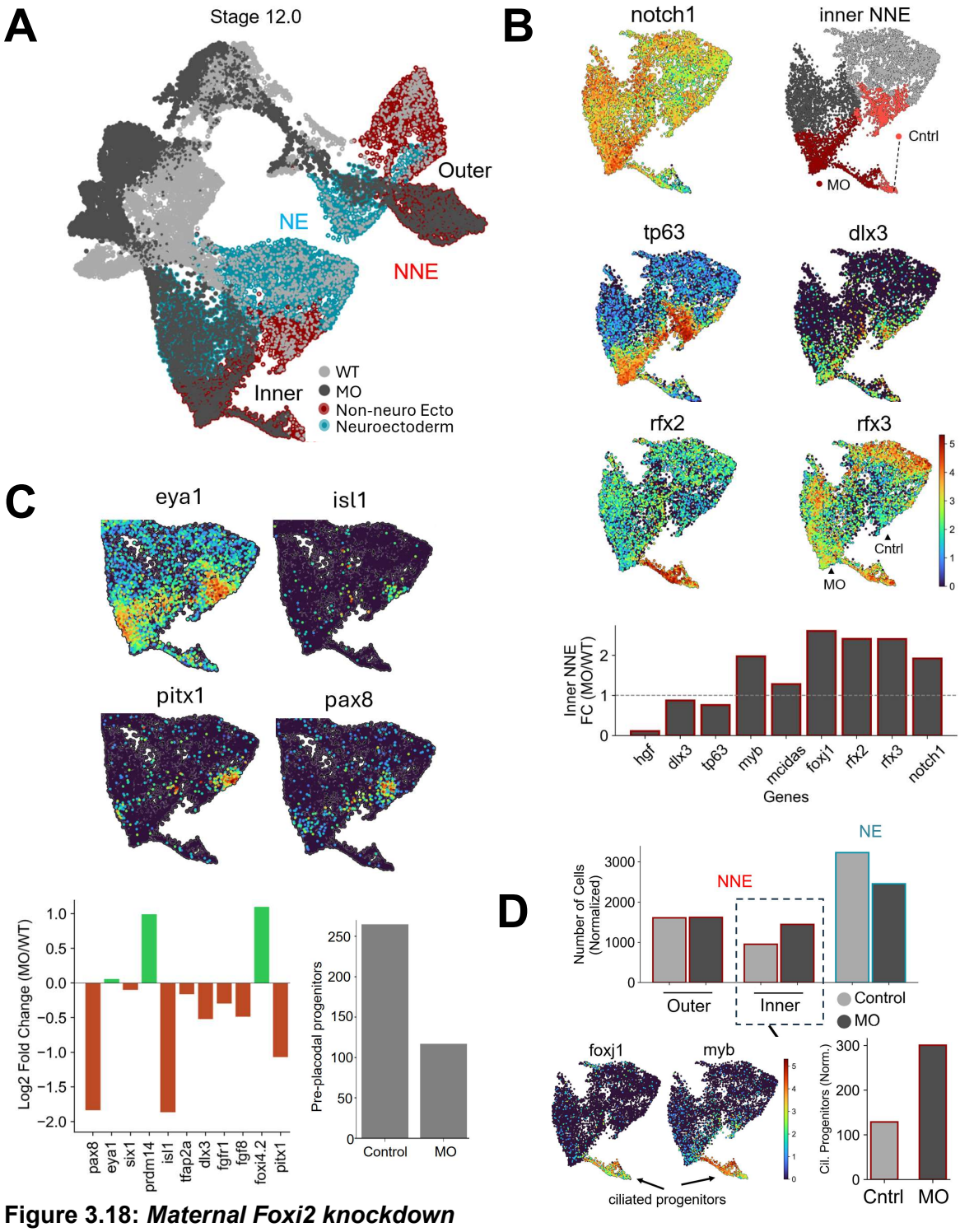

Figure 3.18: ***Maternal Foxi2 knockdown restricts pre-placodal specification and misregulates ciliogenesis in late gastrula.***
(A) Stage 12 nuclei of WT (light gray) or Foxi2 MO injected (dark gray) embryos, with highlighted neuroectoderm (blue) and non-neuroectoderm (red) clusters. **(B)** Inner ectoderm comparison of affected marker expression. **(C)** Pre-placodal marker expression comparison and specialized PPR cell formation. **(D)** Comparison of cell type formation (top) and ciliated progenitor formation (bottom).

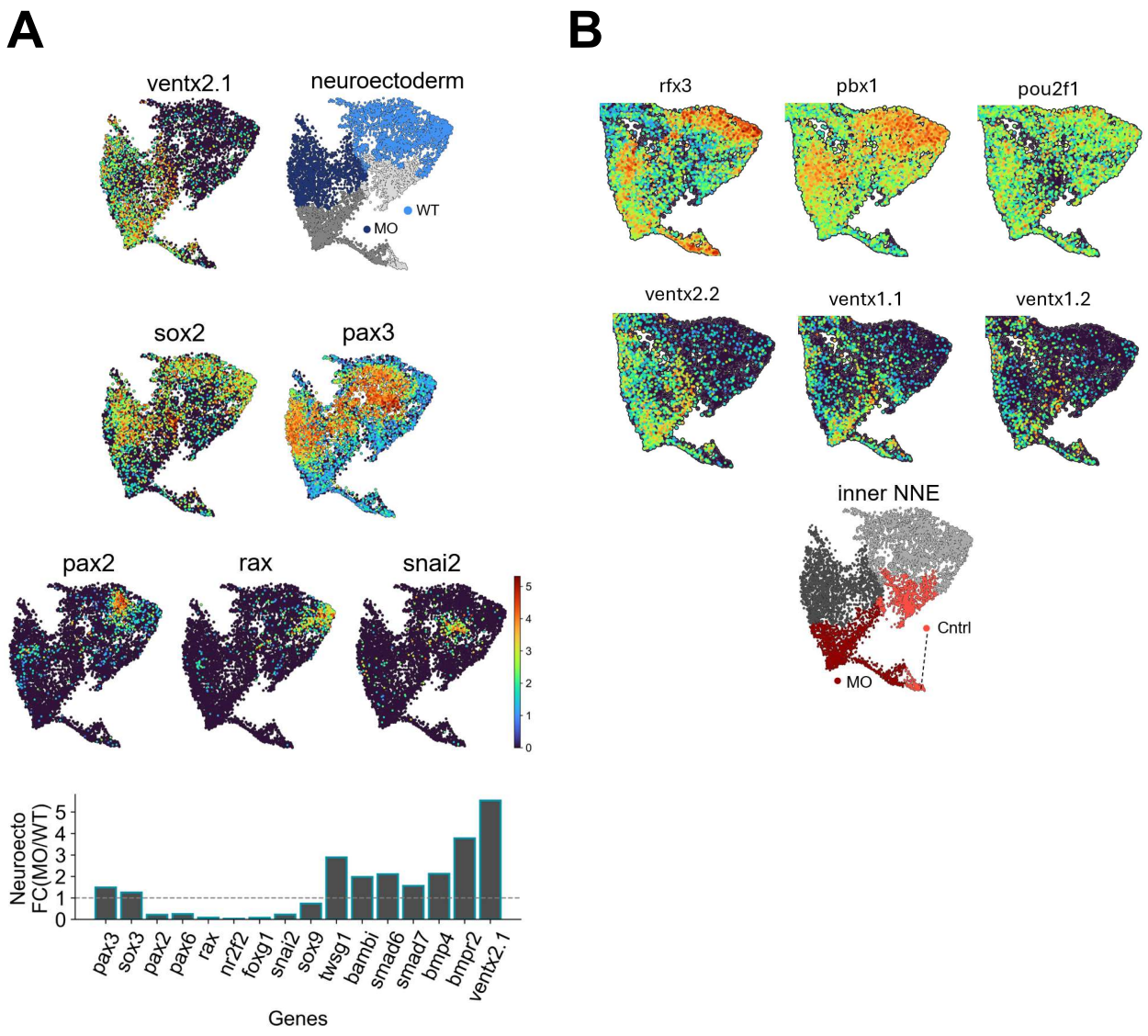

Figure 3.19: ***Maternal Foxi2 knockdown alters signaling throughout the late gastrula ectoderm.***

(A) Late gastrula expression comparison of neuroectoderm specification markers and the BMP syn-expression group. **(B)** Late gastrula expression comparison of ectoderm factors misregulated in the mid-Gastrula (top) and late gastrula (bottom).

the BMP syn-expression group containing *twsg1*, *bambi, smad6/7, bmp4, bmpr2 and ventx2.1.* Coinciding with this increase of BMP signaling associated factors, there is also a decrease in different specification markers of the neuroectoderm, like *snai2, rax* and *pax2.* Furthermore, there is an increased expression of all *ventx* homologues throughout the Foxi2 knockdown inner ectoderm. Taken together, these data suggest a model where Foxi2 is required to activate genes which specify proper ectoderm and repress genes which canalize ciliogenesis from a non-neuroectodermal progenitor state.

Discussion:

In this study, gastrulating *Xenopus* embryos at multiple stages were subjected to snRNA-seq (Figure 3.1) to impute a high resolution lineage annotation of all major germ layers based on gene expression (Figure 3.2, 3.6) Focusing on the ectoderm, the inner and outer layer progenitors were revealed to be transcriptionally distinct and segregate by the beginning of gastrulation (Figure 3.3, 3.4). Temporal trajectories of four main ectoderm cell types, the inner non-neuroectoderm, outer non-neuroectoderm, the neural plate and neural plate border capture the temporal transcriptional requirements for the earliest cell fate specification decisions (Figure 3.7, 3.8, 3.9, 3.10, 3.11). Temporal transcription factor activation during gastrulation defines antero-posterior specification of the neural plate border and pre-placodal regions (Figure 3.5, 3.12). Motif calculations within open epigenetic signatures predict emergent TF regulatory networks forming during cell fate specification (Figure 3.13, 3.14). Finally, Foxi2 knockdown during the mid-late gastrula stages demonstrates maternal TF control for proper non-neuroectoderm progenitor formation, cell state specification, and the inhibition of ectopic ciliogenesis associated signaling (Figure 3.15, 3.16, 3.17, 3.18, 3.19).

Hierarchical inheritance of the neural plate border and pre-placodal ectoderm

In chick, the core neural plate border marker *pax7* becomes activated during the onset of neurulation where it is excluded from the pre-placodal ectoderm (Khudyakov & Bronner-Fraser 2009). In *Xenopus pax3* is activated in the neural plate border region during gastrulation and restricted to the neural crest cell forming region during neurulation (Hong & Saint-Jeannet 2007). Although a substantial amount of work has characterized the gene regulatory networks governing neural plate border and pre-placodal region specification (Betancur et al., 2010, Groves & Labonne 2014, Schlosser 2014, Pla and Monsoro-Burq, 2018, Thawani et al., 2020, Stundl et al., 2021, Williams et al., 2022, Trevers et al., 2023), there is debate about the hierarchical establishment of these early ectoderm lineages. Both the binary and dual (multipotent) competence models of the neural border region specification have supporting evidence. Evolutionary considerations and grafting experiments (Ahrens and Schlosser et al., 2005, Schlosser 2008, Pieper et al., 2012, Maharana and Schlosser, 2018) support the binary competence model where neuroectoderm can only be induced to form neural crest, and non-neural ectoderm can only form the pre-placodal region. However, the dual competence model suggests that the neural plate border region forms multipotent progenitors co-expressing neural and non-neural markers, including *pax3/7*, which temporally segregate into neural crest or pre-placodal lineages (Roellig et al., 2017, Pla and Monsoro-Burq, 2018, Thiery et al., 2020, 2023, Williams et al., 2022, Kotov et al., 2024). Considering opposing support for both models, we compared both neural (*sox2/3, pax3*) and non-neural markers (*tp63, grhl1, eya1, six1*) temporal expression during gastrulation in the snRNAseq datasets.

While *sox2/3* are broadly expressed throughout the neuroectoderm, *pax3* is only expressed in a subset of neuroectoderm, closest to the inner non-neural ectoderm cluster. *Pax3* expressing cells from this subset of developing neuroectoderm demonstrate continuous *pax3*

expression from the early gastrula, stage 10.5, through mid-late gastrula, stage 12 temporal trajectory. Notably, by stage 12, some *pax3* positive cells acquire *snai2* and *sox9* expression to specify neural crest, while *sox2* expression is restricted from the majority of *pax3* expressing cells. These cells do not express *six1* or *eya1*. Later at stage 12.5, anterior neural crest is specified by *rpe65* expression, and at stage 13, posterior neural crest are specified by *mafb* expression. Taken together, neuroectoderm cells continually expressing *pax3* in the early gastrula do not appreciably express core pre-placodal markers *six1* or *eya1*, and gradually restrict *sox2* expression while acquiring specialized neural crest cell marker expression. These data suggest that from early gastrulation the neural plate border is a transcriptionally distinct cell type that forms neural crest but not placodes.

Tp63, klf5 and grhl1 are expressed within inner non-neuroectoderm cells from the early gastrula, stage 10.5, demarcating the neural and non-neural boundary. By stage 11.25, *eya1* expression begins mainly in the region co-expressing non-neuroectodermal factors, and barely overlaps with cells expressing *pax3*. At stage 12, pre-placodal progenitors are specified by the combined expression of *eya1* and *six1* in a region of ectoderm that still does not express *pax3* or *sox2*, and also restricts *tp63, klf5* and *grhl1* expression. By stage 12.5 the anterior and posterior pre-placodal progenitors maintain *six1* and *eya1* expression and become specified by regional expression of *pitx1* and *pax8*. Taken together, these data suggest that pre-placodal progenitor expression begins within the domain of inner non-neuroectoderm, but not within *pax3* or *sox2* positive cells of the neural plate border or neural plate. Therefore, it appears that the pre-placodal region is a derivative of non-neuroectoderm, but not neural plate border.

Notably, recent results describing models of neural plate border and pre-placodal region formation at single cell level come from experiments in chick (Williams et al., 2022, Thiery et al., 2023). Thiery and Williams both demonstrate that a *pax7* defined neural plate border region is formed during early neurulation and co-expresses both neural and non-neural markers. Therefore, their data support a multi-potent progenitor model. Importantly, *Xenopus* expresses

pax3 in the neural plate border region during gastrulation but does not express *pax7* until much later. This indicates an inherent species differential compared to the recent chick data, in terms of the choice and timing of the first *pax* factor expressed in the neural plate border region. While some of our marker detection UMAP data analysis results closely resemble theirs, there are also significant differences. In particular, we detect earlier localized expression of *pax3* by the early gastrula stage, but not *pax7*.

Taken together, our snRNAseq data appear to agree most with the binary competence model where neural derivatives form neural plate border and neural crest, and non-neural ectoderm derivative cells form the pre-placodal region. However, as we did not perform deep co-expression analyses (Thiery et al., 2023, Kotov et al., 2024) we cannot say whether there are some small number of cells which co-express *pax3* and *tp63* or *eya1/six1*. Therefore, future analyses should endeavor these previous analyses to better address whether multipotent progenitors can be detected in our snRNAseq data.

Epigenetic analysis caveats of single cell/nucleus sequencing

As gene regulation is a function of epigenetic interactions, the accessibility and occupancy of a genomic region determine its expression. While the single nucleus experiments reported in this study, as well as all other single cell experiments in *Xenopus* (Briggs et al., 2018, Aztekin et al., 2019, Liao et al., 2022, Yanagi et al., 2022, Lee et al., 2023), are able to capture transcript expression at the highest resolution, they are completely devoid of epigenetic information. Transcription factors govern gene expression through physical DNA binding domain mediated motif interactions and recruitment of epigenetic modifiers. Therefore, single cell/nucleus expression data itself lacks the required epigenetic information to build a true gene regulatory network. Because of this, software like SCENIC has been created in an attempt to leverage

epigenetic information derived from bulk sequencing in conjunction with single cell expression information.

To ameliorate this gap of epigenetic information, whole embryo stage 12 ATAC-seq datasets (Bright et al., 2021) were analyzed to find regions of open chromatin. The comprehensive Aertz lab motif database (https://resources.aertslab.org/cistarget/databases/) was then used to locate motifs within regions up to 50kb upstream or downstream of each gene. The original SCENIC paper simply used upstream regions without knowledge of their accessibility; therefore it seemed practical to throttle the genomic window for motif searching by only investigating open chromatin regions, albeit from bulk sequencing data. However, there are caveats to the analysis. Namely, the set of epigenetic regions used to consider TF binding potential is the exact same for all cells. This is a significant issue because other tissue dissected epigenetic experiments, as well as multiomic studies in other species, reveal cell type specific chromatin accessibility signatures. Therefore, without experimental validation, we cannot realize which network predictions may be false positives or negatives. Although no multiomic experiments have been published in Xenopus, we have completed a preliminary multiomic experiment at stage 11.25 and can find different epigenetic signatures between inner and outer ectodermal clusters (unpublished data). Taken together, future network validation and multiomic experiments using updated SCENIC+ software (Gonzales-Blas et al., 2023) are required for interrogating cell type specific epigenetic states and forming the most accurate gene regulatory network prediction.

The role of maternal Foxi2 in ectodermal programming

The Foxi family of transcription factors evolved alongside the appearance of ionocytes and specialized placodal structures, like the inner ear and pharyngeal arch epithelium (Pohl and Knochel 2005, Edlund et al., 2015). There are three members of the Foxi family, Foxi1, Foxi2

and Foxi3. Foxi2 is known to affect sensory placodes, the pharyngeal arches and craniofacial development in chick and mouse, but it is restricted from the otic placode (Ohyama et al., 2006, Jayasena et al., 2008, Freter et al., 2008, Urness et al. 2010). Although highly conserved, the maternal role of Foxi2 appears to be specific to *Xenopus*, and in some ways antithetical to VegT, another *Xenopus* master regulator specifying mesendoderm. In *Xenopus* maternal foxi2 activates Foxi1 (Cha 2012), a factor that demarcates the ecto-mesendoderm boundary (Suri et al., 2005, Mir et al., 2007, 2008). Recently, we showed that maternal Foxi2 complexes with maternal Sox3 to directly activate gene targets within the neural and non-neural, inner and outer layer ectoderm lineages. Foxi2/Sox3 are required for initiating Ep300 recruitment to developmentally relevant ectodermal CRMs, which facilitate the formation of super enhancers during early gastrulation, stage 10.5 (Hendrickson et al., 2025).

In this study we further examine the role of maternal Foxi2 in ectoderm development during the mid-late blastula, stage 11.25-12. Expectedly, we find that Foxi2 does control pre-placodal ectoderm specification, as well as the expression of anterior neural plate markers. Previously generated Foxi2 ChIPseq and bulk RNAseq support a mechanism of gene activation where Foxi2 directly binds these neural and non-neural ectodermal progenitor gene CRMs. In addition, Foxi2 is required to inhibit the ectopic expression of *rfx3* and *pbx1* throughout the ectoderm. While Foxi2 does form a weak peak at *rfx3* and *pbx1* CRMs, and binds about half of the genes it represses in the early gastrula (Chapter 2), we lack evidence of its repression mechanism and cannot say whether it occurs directly or indirectly. To address whether Foxi2 participates in direct gene repression, future experiments should measure its association with ezh2 or jarid, the DNA interacting subunits of the polycomb-repressive complex.

Presumably, *rfx3*, *pbx1* and both notch and hedgehog signaling members were upregulated in stage 11.25 Foxi2 depleted ectoderm which subsequently increased the expression of ciliated progenitor markers in stage 12 ectoderm. *Rfx3* is the most anciently conserved ciliogenic factor working with *foxj1* (Didon et al., 2013, Coyle et al., 2023). It is

implicated in the activation of hedgehog signaling (Benadiba et al., 2012, Chen et al., 2018, Xie et al., 2025) and the co-activation of *pbx1* (Longobardi et al., 2013, Li et al., 2020). In chick neuroprogenitors, and mouse NIH 3T3 cells, *rfx3* overexpression is sufficient to induce long monocilia through hedgehog signaling activation (Cruz et al., 2010). *Pbx1* regulates hedgehog signaling in distal limb patterning (Capellini et al., 2006, Mok et al., 2024), is a target of notch signaling (Park et al., 2008, Shen et al., 2021) and also may activate *rfx3* (Hau et al., 2021).

Studies demonstrate hedgehog and notch signaling factor cross-talk where notch signaling regulates Gli TFs and the localization of hedgehog pathway members within primary cilia (Stasiulewicz et al., 2015, Jacobs and Huang 2019). These findings are quite interesting, as the only other Foxi family member to have been implicated in hedgehog signaling is Foxi3 in mice, where it also represses hedgehog signaling during tooth development (Mogollon et al., 2022). While other Foxi members have been implicated in fgf signaling, it is not particularly enriched at the level of RNA expression within the pre-placodal ectoderm snRNAseq datasets. Taken together, these mid-late gastrula Foxi2 knockdown experiments confirm its role in establishing ectoderm progenitors and pre-placodal specification states, but also reveal a surprising role in inhibiting the activation of ectopic ciliogenesis programming. Future experiments should validate *rfx3, pbx1,* notch or hedgehog signaling differentials in Foxi2 knockdown embryos using in situ hybridization techniques. To help decipher its regulation mechanism Foxi2 occupancy of these genes should be surveyed at stage 11.25 and 12.

Experimental Procedures:

Nuclei Preparation and snRNA Sequencing

Nuclei were isolated from stage 10.5 embryos using previously published discontinuous sucrose gradient protocols followed by a separate centrifugation through 80% glycerol (Wormington and Brown, 1983; Wolffe, 1989; Nakayama et al., 2022). Briefly, 200 embryos were homogenized in

a 250mM sucrose solution containing glycerol and snap frozen in liquid nitrogen (Nakayama et al., 2022). Homogenates were later thawed on ice, brought to ~2.2M sucrose and centrifuged through a 2.4M sucrose layer at 130,000g for 2 hours at 4oC using a Beckman SW55Ti rotor, followed by a 3400xg centrifugation for 10 min at 4oC through an 80% glycerol cushion. RNAse (NEB) and protease inhibitors (Roche 7x cOmplete, Mini, EDTA-free) at 0.2 U/ml and 5 mg/ml respectively were used throughout the previous steps. Nuclei were finally resuspended in "nuclear PBS" (0.7x PBS, 2mM MgCl2) containing 0.5% BSA and 0.2 U/ml RNase inhibitor. DAPI-stained nuclei were counted using a hemocytometer, and then were subject to fixation using the Parse Bioscience Evercode Fixation Kit (SB1003). Nuclei in DMSO were slow-frozen in a -80oC overnight according to the kit manual. A bar-coded snRNA-seq library was prepared using the Parse WT Mini Kit (ECW01010) and sequenced at the University of California, Irvine Genomics Research and Technology Hub.

Morpholino Knockdown, Rescue and Vegetal RNA Injections

foxi2 translation blocking morpholino was created by GeneTools, Inc. 5'-TTATGAAGTCTGGTGGGACATTCAC-'3. Morpholino rescue was validated in (Hendrickson et al., 2025, Chapter 2) where the *X. tropicalis foxi2* coding sequence was acquired from the *X. tropicalis* Unigene library (TGas144f13) in the pCS107 vector. Morpholino knockdowns were performed by injecting directly into opposing sides of the animal cap at the 1-cell stage or into each animal blastomere at the 2-cell stage.

snRNA-seq Analysis

Alignment: Parse Biosciences' in-house alignment software (dnanexus.com) command "Parse Batch Analysis v1.1.4" was used with the default commands against the UCB_Xtro_10.0 (GCA_000004195.4) reference. **Formatting:** The unfiltered Parse alignment output containing

"all_genes.csv", "cell_metadata.csv" and "DGE.mtx" were first amalgamated into a .h5Seurat object using the R v4.3.1(http://www.r-project.org) software Seurat v4.3.0, Matrix v1.6.5, SeuratDisk v0.0.0.9015 (https://github.com/mojaveazure/seurat-disk), Reticulate v1.37.0 and the command "CreateSeuratObject". Finally, the .h5Seurat object was converted into an .h5ad file using the "Convert" command with the option "dest = "h5ad"". **Pre-processing:** Using scanpy v1.9.6 (Wolf et al. 2018) , pandas v2.1.4 (McKinney et al. 2010), the nuclear data was log transformed and normalized and highly variable genes were annotated. Doublets were predicted using Scrublet (Wolock et al. 2019), then manually inspected, confirmed and removed based on illogical ectopic co-expression of germ-layer specific markers and outlier read counts. **Cell lineage annotation:** Leiden (Traag et al. 2019) was used to predict de novo cluster formation, visualized via Uniform Manifold Approximation Projection (UMAP) (McInnes et al. 2018). Scanpy was used to calculate differential gene expression analysis of known marker genes between de novo clusters which were assigned to their germ-layer identity. Accordingly, clusters were merged based on co-expression of known marker genes. In this way, cluster boundaries are initially formed in an unbiased way through de novo clustering, based on differential gene expression. *In-situ* hybridization studies of marker genes as well as Briggs et al., 2018 marker gene list were subsequently used for appropriate cluster annotation and merger.

SCENIC analysis

Motif database configuration: Aerts lab motif collection (https://resources.aertslab.org/cistarget/motif_collections/) PWMs were collected and human gene names were best matched to their *Xenopus* counterparts using Briggs et al., 2018 (Supplemental Table 7). **Epigenetic region motif scoring:** Mid-gastrula ATACseq datasets from (Bright et al., 2020 - GSE145619) were called against stage specific input DNA using MACS2 v2.2.7.1 (Zhang et al., 2008) broadpeak with the “-p .001” argument as the only non-

default option. ATAC regions were then correlated to their nearest gene using bedtools v2.31.0 closestbed with option -d to report the peak to gene distance. Next, distances more than 50k upstream or downstream were discarded, and fasta sequences were printed for the remaining peak coordinate regions. Finally, fasta sequences were appended on a per gene basis, and each gene's associated ATACseq peak sequences were mined using the converted Aerts lab motif database. **SCENIC analysis:** GRNboost was performed using all *Xenopus* TFs (Blitz et al., 2017) and adjacencies above .005 were used according to Aibar et al., 2017. Only the top three categories of Target-gene predictions were considered for each transcription factor. SCENIC "ctx" and "aucell" commands were run using default settings and the results were visualized in Python.

STREAM analysis

Temporal trajectory mapping: Seed graph calculations utilized Cell type specific annotations with "paths_favored" command using "label_strength=25". "Learn_graph" was run with default settings besides "n_nodes" which was typically set above 50 to resolve path granularity. Disfavored paths were trimmed using "st2.tl.del_path" and adjacent paths were connected using "st2.tl.add_path(n_nodes=0)". Subway and stream plots were made using default settings, where the "source=(earliest stage cluster within the dataset)" and "dist_scale=1".

Acknowledgements

This work was made possible, in part, through access to the University of California, Irvine Genomics Research and Technology Hub (GRT Hub) parts of which are supported by NIH grants to the Comprehensive Cancer Center (P30CA-062203) and the UCI Skin Biology Resource Based Center (P30AR075047), as well as to the GRT Hub for instrumentation (1S10OD010794 and 1S10OD021718). We thank Xenbase (http://www.xenbase.org/, RRID:

SCR_003280) and the National *Xenopus* Resource (RRID:SCR_013731), for genomic and community resources, and the University of California, Irvine High Performance Computing Cluster (https://hpc.oit.uci.edu/) for their valuable resources and helpful staff. This research was funded by the following grants awarded to K.W.Y.C. National Institute of Health R21 HD109696, and R35 GM139617, and National Science Foundation 1755214. CLH is a recipient of a US Department of Education GAANN fellowship (P200A220015).

Author Contributions

C.L.H., I.L.B. and K.W.Y.C. designed the study. I.L.B performed experiments. C.L.H. and I.L.B. performed Foxi2 MO knockdowns. C.L.H. wrote the manuscript. C.L.H performed bioinformatic analyses.

Chapter 4: Conclusions and outlook

My dissertation focused on the early functions of the maternal TFs Foxi2 and Sox3, as well as ectodermal lineage specification as a whole. Through the investigation of Foxi2 and Sox3's regulated genes (knockdown RNA-seq) and in vivo genomic occupancy (ChIP-seq) over the time course of early development and ectoderm specification, I propose critical master regulatory roles for these TFs in the initiation and regulation of the ectoderm GRN. This novel study not only highlights the temporal dynamics of Foxi2 and Sox3-mediated regulation, but also demonstrates a mechanism for the establishment of the ectodermal epigenetic landscape, including the formation of super enhancers. Additionally, high resolution sequencing (snRNA-seq) establishes inner and outer ectoderm cell states, while temporal lineage maps of ectoderm specification demonstrate early neural and non-neuroectodermal progenitor formation. Finally, the first investigation of maternal TF knockdown at single cell resolution suggests Foxi2 role in non-neuroectoderm progenitor formation and pre-placodal specification.

The timing of epigenetic establishment

64-cell stage ChIP-seq of Foxi2 and Sox3 demonstrates that these maternal TFs pre-mark developmentally relevant CRMs by at least stage ~6, long before the initiation of zygotic genome activation. However, Ep300 binding cannot be detected within these same regions, showing that it is not yet recruited to the chromatin by stage 6. Previous work from our lab (unpublished), and others (Hontelez et al., 2017), also does not report detectable Ep300 binding until the blastula at stage ~8-9, coinciding with ZGA. Given that Foxi2, Sox3 and Ep300 are all maternally endowed factors, what is the mechanism governing the early exclusion of Ep300 from the chromatin assembly? While Foxi2, Sox3 and Ep300 maternal mRNA (Owens et al., 2016) is present, only Foxi2 (Cha et al., 2012) and Sox3 (Zhang et al., 2003) proteins have

been detected at fertilization. Because of this, the delayed Ep300 recruitment could be explained by a lack of protein translation and physical availability. In fact, other factors in *Xenopus*, like Vg1 and VegT, are maternally endowed and vegetally localized, where their translation is repressed until stage 6, albeit through unique mechanisms (Willhelm et al., 2000, Otero et al., 2001). Therefore, it's possible that an uncharacterized translation repression mechanism exists for Ep300 mRNA in presumptive ectoderm cells.

In addition, the sub-cellular localization of Ep300 could also dictate its timing for genomic accessibility. As translation occurs within the cytoplasm, factors require active transport by Importin transporters to cross the nuclear pore and gain nuclear entry (Cordes et al., 1997). Interestingly, the differential affinity of factors with Importin determined their rate of nuclear entry during embryogenesis (Nguyen et al., 2022). With this in mind, a simple model where Foxi2 and Sox3 have higher Importin affinity could explain Ep300 delayed nuclear entry and genomic accessibility. However, the paper does not report Ep300 explicitly, and it is not included in their supplemental data, potentially because it uses a different nuclear transporter outside of their screen. While I conclude that Foxi2 and Sox3 pre-mark ectoderm CRMs to recruit Ep300, future experiments could better resolve the timing of Ep300 genomic accessibility. CUT&RUN (Phelps et al., 2023) could be used to survey the timing of Ep300 occupancy at higher resolution than current ChIP-seq. Immunofluorescence (Jeschonek et al., 2018) could be used to visualize the timing of Ep300 nuclear entry. These experiments will help elucidate why Ep300 may be present, but lacks genomic recruitment until the blastula stages.

Maternal factor complex formation and repressive interactions

The Foxi2 and Sox3 genomic occupancy and transcriptomic analyses demonstrate their high degree of motif localization, co-binding and epigenetic accrual during early gastrulation. Correlating single nucleus sequencing, these factors directly coordinate ectoderm gene activation in the neural and non-neuroectoderm progenitor cells of the inner and outer layers.

Given that even in the Foxi2 and Sox3 double knockdown embryos, there is a limited degree of ectoderm formation, it highlights the redundant capabilities of embryogenesis, and implies that there are other master regulatory factors at play.

Sox3 is a maternal Pou5f3 co-factor (Gentsch et al., 2019). Even in choanoflagellates, segregated by hundreds of millions of years of species divergence, Sox and Pou factors are believed to interact (Gao et al., 2024). In *Xenopus* Sox3 and Pou5f3 work together to bind the chromatin early and facilitate CRM accessibility to approximately half of the CRMs utilized during ZGA (Gentsch et al., 2019). Both factors can bind a Oct4-Sox2 heterodimer motif, suggesting that they can form a complex similar to mammalian Oct4-Sox2 (Dailey and Basilico 2001, Boyer, et al., 2005, Phelps et al., 2023). My analysis within Foxi2 peaks shows that the Fox motif co-occurs with the Sox and Pou motifs ~70% and ~40% of the time, where they are enriched within the peak center. This suggests that, for at least some subset of peaks, Foxi2, Sox3 and Pou5f3 likely form a complex together. However, Pou5f3 binding data is not available for *Xenopus tropicalis*. In *Xenopus* Foxh1, VegT and Otx1 were found to co-bind and physically recruit one another pre-ZGA to initiate mesendoderm specification (Paraiso et al., 2019) and in zebrafish Nanog, Pou5f3 and Sox19 (Sox3 homologue), their cobinding mildly or strongly controls the enhancer accessibility landscape (Miao et al., 2022). Future experiments should include Pou5f3 perturbations in tandem with Foxi2 and Sox3 knockdown to test redundancy, and Pou5f3 genomic occupancy should be surveyed to better understand their potential complex formation.

In addition to their role as direct activators promoting chromatin accessibility, both Foxi2 and Sox3 bind and repress a number of genes independently in the early gastrula. In the mid-gastrula, Foxi2 represses the ectopic activation of ciliogenesis related genes within ectodermal cells. Notably, Foxi2 and Sox3 function as co-activators, but not as co-repressors. Previously, Sox3 has been shown to directly bind the *snai2* promoter and facilitate repression, delineating

ingressing vs non-ingressing cells in the chick epiblast (Acloque et al., 2011). In *Xenopus* Sox3 indirectly represses *ventx2* (Rogers et al., 2009) and directly represses *nodal5*, presumably through promoter interactions (Zhang et al., 2003). In zebrafish Sox3 can repress *cyc* (Zhang et al., 2004) and directly repress genes expressed in the organizer, like *nog* (Shih et al., 2010). While no Foxi factor has been implicated as a direct repressor, other Fox factors, like FoxP and FoxO have. Foxp2 directly represses *lmo4* in neurons (Vernes et al., 2011) and Foxp1 represses *bik* to prevent Foxo3 mediated cell death (van Boxtel et al., 2013). Foxa1, the first discovered pioneer Fox factor, is known to directly repress basal genes in breast cancer (Mehta et al., 2011).

Taken together, there is ample evidence of Sox3 and implied evidence of Foxi2 as a direct repressor. However, their mechanism of repression, besides genomic occupancy, is unknown. It is possible that Foxi2 and/or Sox3 recruit histone de-acetylases like the NURD (Millard et al., 2016) or REST-corepressor complex (Hwang et al., 2018), which would be quite interesting as they serve directly antithetical roles to Ep300, a histone acetyltransferase. Additionally, they may recruit Ezh2 (Caretti et al., 2004), or Jarid (Sanulli et al., 2015), members of the polycomb repressive-complex which facilitates the deposition of H3K27me3, a repressive histone mark. Future experiments measuring tissue dissected Ezh2 and Jarid occupancy would help in understanding the Foxi2 and Sox3 repression mechanism.

A path toward solving early cell type heterogeneity

In the study we generated the most resolved maps of temporal ectodermal cell type segregation and highlighted lineage defining marker TFs. Through examining the temporal expression of the pre-placodal region, we identify a temporal transition from inner- (*tp63*, *klf5*) and pan ectodermal (*tfap2a)* markers, to core PPR (*eya1*, *six1*) and finally antero- (*pitx1*) posterior (*pax8)* PPR markers during gastrulation progression. In the neural plate border, we see a similar trajectory where *pax3* expressing cells eventually acquire neural crest identity through *snai2* and *sox9*,

before segregating into antero- (*rpe65)* and posterior (*mafb*) territories. These results tentatively support the binary competence model of neural plate border specification (Schlosser and Maharana 2018). Importantly, Thiery et al., 2023 and Kotov et al., 2024 have produced additional and deeper co-expression analysis of neural plate border region cells than I have completed in my analysis. Because of this, (1) I cannot discount their evidence towards a dual competence or multipotent progenitor model of neural plate border development, and (2) I cannot conclude that my data does not fit their model considering that I have not performed their analysis. Therefore, future steps to better understanding neural plate border specification is to implore their co-expression analysis to determine whether we detect the multipotent progenitor state within our snRNA-seq dataset. Additionally, there are differences in the timing of the early neural plate border marker expression of *pax3* and *pax7* between *Xenopus* and chick. These differences may lead to inconsistencies in our ability to define induction of the neural plate border cluster across species. A final explanation for these discrepancies are the potential to miss low abundance transcripts in sequencing experiments. This leads to an incomplete transcriptional picture that could mislead model justifications, despite best data analysis attempts.

The capability to discern cell type specification and TF regulatory network formation is directly correlated to both transcript and epigenetic state detection in single cells/nuclei. snRNA-seq is beneficial in the sense that it only sequences new zygotic transcripts, and does not "waste" sequencing reads on cytoplasmic transcripts. However, even by maximizing zygotic transcript detection, we are still missing epigenetic information about the cell. Multiomic sequencing can capture both transcript and epigenetic information from a single cell (Lake et al., 2017). Brain tissue from mouse, human, and monkey have been subjected to multiomic sequencing, revealing unique species specific distal regulatory elements (Loupe et al., 2024, Liu et al., 2025). New results in gastrulating mice reveal left-right axis symmetry breaking and complex GRN formation (Yang et al., 2024). In zebrafish a slight multiomic variation called

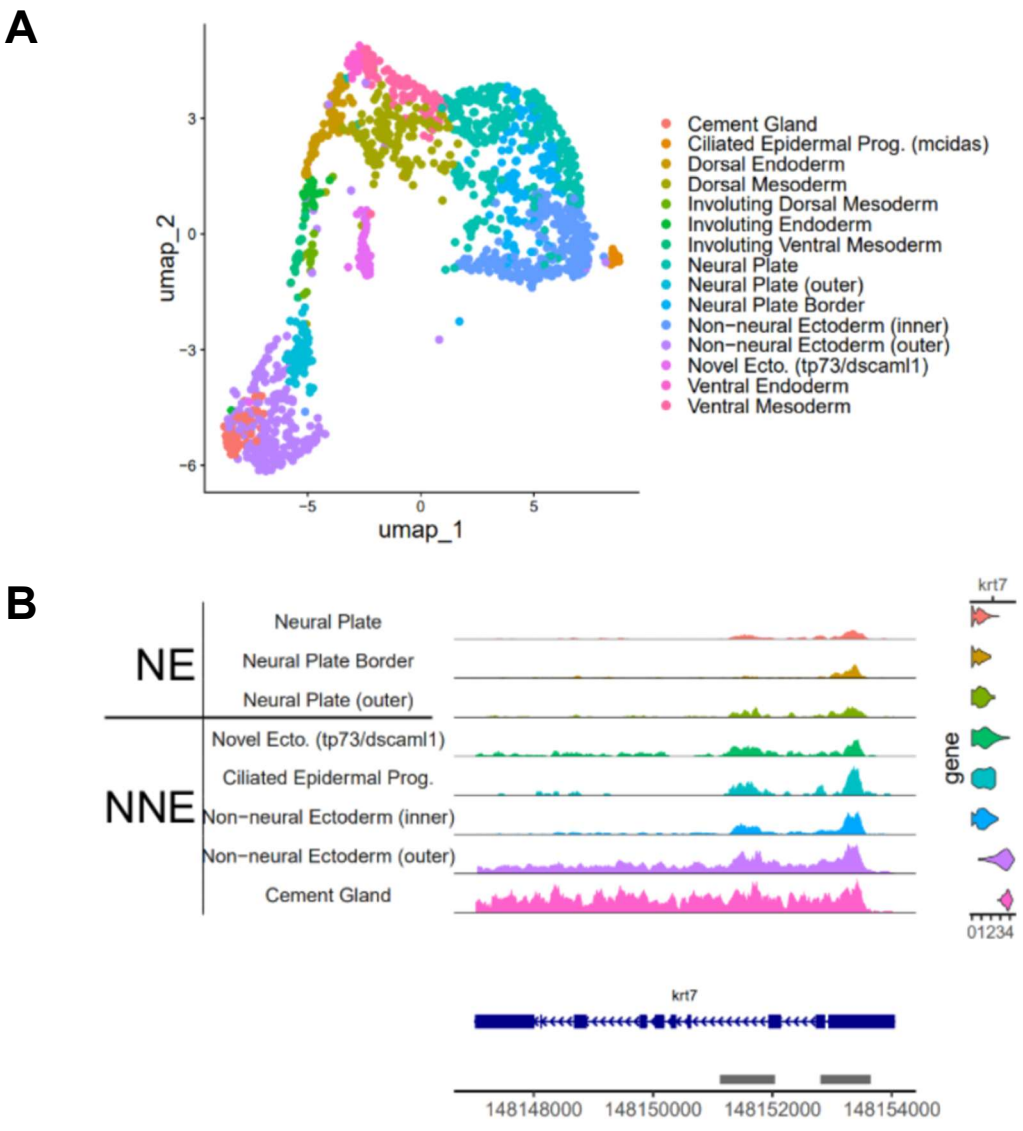

Figure 4.1: Multiomic sequencing at stage 11.25.

(A) UMAP clustering of both the transcriptome and accessible epigenome of stage 11.25 early-mid-Gastrula embryos, via 10xGenomics. **(B)** Genome browser visualization of epigentic differences across ectoderm clusters at the krt7 locus.

T-ChIC was used to confirm a model of repressive histone modification spreading (Bhardwaj et al., 2024). These results demonstrate the increasing use of multiomics to discern early cell type heterogeneity and to validate models of development, however multiomic techniques have not yet been adopted in *Xenopus*.

We recognize this need, and have accordingly generated a stage 11.25 multiomic dataset, the first described in *Xenopus* (Figure 4.1). Preliminary analysis demonstrates that for the outer ectoderm localized gene *krt7*, there is a shared, open profile across the genomic window for the NNE outer and cement gland cell types (Figure 4.1B). However, for the other inner ectodermal clusters, as well as neuroectoderm clusters, the window of open chromatin is greatly reduced to two peaks occurring in the promoter and second intron (Figure 4.1B). These results demonstrate that epigenetic signatures are not only different between the major ectodermal lineages, but also within sub-lineage specifications. Admittedly, the sequencing results yielded many fewer high-quality cells (1,624) compared to the previous snRNA-seq data (6,000(+) cells in each) showcased in this study. After gaining more experience with the 10xGenomics unfixed protocol, we believe that we can increase the high-quality cell yield. If so, we will leverage the sub-cell type specific epigenetic signatures to make robust GRN predictions and potentially resolve discrepancies in models of neural plate border and pre-placodal ectoderm specification.

Reference list

Adameyko, I., Lallemend, F., Furlan, A., Zinin, N., Aranda, S., Kitambi, S.S., Blanchart, A., Favaro, R., Nicolis, S., Lübke, M., Müller, T., Birchmeier, C., Suter, U., Zaitoun, I., Takahashi, Y. and Ernfors, P. (2012). Sox2 and Mitf cross-regulatory interactions consolidate progenitor and melanocyte lineages in the cranial neural crest. *Development (Cambridge, England)*, [online] 139(2), pp.397–410. doi:https://doi.org/10.1242/dev.065581.

Ahrens, K. and Schlosser, G. (2005). Tissues and signals involved in the induction of placodal Six1 expression in Xenopus laevis. *Developmental Biology*, [online] 288(1), pp.40–59. doi:https://doi.org/10.1016/j.ydbio.2005.07.022.

Aibar, S., González-Blas, C.B., Moerman, T., Huynh-Thu, V.A., Imrichova, H., Hulselmans, G., Rambow, F., Marine, J.-C., Geurts, P., Aerts, J., van den Oord, J., Atak, Z.K., Wouters, J. and Aerts, S. (2017). SCENIC: single-cell regulatory network inference and clustering. *Nature Methods*, 14(11), pp.1083–1086. doi:https://doi.org/10.1038/nmeth.4463.

Akkers, R.C., van Heeringen, S.J., Jacobi, U.G., Janssen-Megens, E.M., Françoijs, K.-J., Stunnenberg, H.G. and Veenstra, G.J.C. (2009). A Hierarchy of H3K4me3 and H3K27me3 Acquisition in Spatial Gene Regulation in Xenopus Embryos. *Developmental Cell*, 17(3), pp.425–434. doi:https://doi.org/10.1016/j.devcel.2009.08.005.

Anishchenko, E., Arnone, M.I. and D'Aniello, S. (2018). SoxB2 in sea urchin development: implications in neurogenesis, ciliogenesis and skeletal patterning. *EvoDevo*, 9(1). doi:https://doi.org/10.1186/s13227-018-0094-1.

Argenton, F., Giudici, S., Gianluca Deflorian, Cimbro, S., Franco Cotelli and Beltrame, M. (2004). Ectopic expression and knockdown of a zebrafish sox21 reveal its role as a transcriptional repressor in early development. *Mechanisms of Development*, 121(2), pp.131–142. doi:https://doi.org/10.1016/j.mod.2004.01.001.

Arrigoni, R., Alam, S.L., Wamstad, J.A., Bardwell, V.J., Sundquist, W.I. and Schreiber-Agus, N. (2006). The Polycomb-associated protein Rybp is a ubiquitin binding protein. *FEBS Letters*, 580(26), pp.6233–6241. doi:https://doi.org/10.1016/j.febslet.2006.10.027.

Asashima, M., Nakano, H., Uchiyama, H., Davids, M., Plessow, S., Loppnow-Blinde, B., Hoppe, P., Dau, H. and Tiedemann, H. (1990). The vegetalizing factor belongs to a family of mesoderm-inducing proteins related to erythroid differentiation factor. *Die Naturwissenschaften*, [online] 77(8), pp.389–91. doi:https://doi.org/10.1007/BF01135742.

Aztekin, C., Hiscock, T.W., Marioni, J.C., Gurdon, J.B., Simons, B.D. and Jullien, J. (2019). Identification of a regeneration-organizing cell in the Xenopus tail. *Science*, 364(6441), pp.653–658. doi:https://doi.org/10.1126/science.aav9996.

Bae, S. and Lesch, B.J. (2020). H3K4me1 Distribution Predicts Transcription State and Poising at Promoters. *Frontiers in Cell and Developmental Biology*, 8. doi:https://doi.org/10.3389/fcell.2020.00289.

Baker, C., Stark, M.R., Marcelle, C. and Bronner-Fraser, M. (1999). Competence, specification and induction of Pax-3 in the trigeminal placode. *Development*, [online] 126(1), pp.147–156. doi:https://doi.org/10.1242/dev.126.1.147.

Becht, E., McInnes, L., Healy, J., Dutertre, C.-A., Kwok, I.W.H., Ng, L.G., Ginhoux, F. and Newell, E.W. (2018). Dimensionality reduction for visualizing single-cell data using UMAP. *Nature Biotechnology*, [online] 37(1), pp.38–44. doi:https://doi.org/10.1038/nbt.4314.

Benadiba, C., Magnani, D., Niquille, M., Morlé, L., Valloton, D., Nawabi, H., Ait-Lounis, A., Otsmane, B., Reith, W., Theil, T., Hornung, J.-P., Lebrand, C. and Durand, B. (2012). The Ciliogenic Transcription Factor RFX3 Regulates Early Midline Distribution of Guidepost Neurons Required for Corpus Callosum Development. *PLoS Genetics*, 8(3), p.e1002606. doi:https://doi.org/10.1371/journal.pgen.1002606.

Bentley, M.L., Corn, J.E., Dong, K.C., Phung, Q., Cheung, T.K. and Cochran, A.G. (2011). Recognition of UbcH5c and the nucleosome by the Bmi1/Ring1b ubiquitin ligase complex. *The EMBO Journal*, 30(16), pp.3285–3297. doi:https://doi.org/10.1038/emboj.2011.243.

Benveniste, D., Sonntag, H.-J., Sanguinetti, G. and Sproul, D. (2014). Transcription factor binding predicts histone modifications in human cell lines. *Proceedings of the National Academy of Sciences*, 111(37), pp.13367–13372. doi:https://doi.org/10.1073/pnas.1412081111.

Betancur, P., Bronner-Fraser, M. and Sauka-Spengler, T. (2010). Assembling Neural Crest Regulatory Circuits into a Gene Regulatory Network. *Annual Review of Cell and Developmental Biology*, 26(1), pp.581–603. doi:https://doi.org/10.1146/annurev.cellbio.042308.113245.

Bhardwaj, V., Griffa, A., Gaza, H.V., Zeller, P. and van Oudenaarden, A. (2024). Single-cell multi-omic analysis reveals principles of transcription-chromatin interaction during embryogenesis. doi:https://doi.org/10.1101/2024.09.23.614335.

Bhat, N., Kwon, H.-J. and Riley, B.B. (2013). A gene network that coordinates preplacodal competence and neural crest specification in zebrafish. *Developmental Biology*, 373(1), pp.107–117. doi:https://doi.org/10.1016/j.ydbio.2012.10.012.

Blackledge, N.P., Farcas, A., Kondo, T., King, H.R., McGouran, J.F., Lars, Ito, S., Cooper, S., Kondo, K., Haruhiko Koseki, Tomoyuki Ishikura, Long, H.K., Sheahan, T.C., Brockdorff, N., Kessler, B.M. and Klose, R.J. (2014). Variant PRC1 Complex-Dependent H2A Ubiquitylation Drives PRC2 Recruitment and Polycomb Domain Formation. *Cell*, 157(6), pp.1445–1459. doi:https://doi.org/10.1016/j.cell.2014.05.004.

Blackledge, N.P., Fursova, N.A., Kelley, J.R., Huseyin, M.K., Feldmann, A. and Klose, R.J. (2020). PRC1 Catalytic Activity Is Central to Polycomb System Function. *Molecular Cell*, 77(4), pp.857-874.e9. doi:https://doi.org/10.1016/j.molcel.2019.12.001.

Blitz, I.L. and Cho, K.W.Y. (2021). Control of zygotic genome activation in Xenopus. *Current topics in developmental biology/Current Topics in Developmental Biology*, pp.167–204. doi:https://doi.org/10.1016/bs.ctdb.2021.03.003.

Blitz, I.L., Paraiso, K.D., Ilya Patrushev, Chiu, W., Ken W.Y. Cho and Gilchrist, M.J. (2017). A catalog of Xenopus tropicalis transcription factors and their regional expression in the early gastrula stage embryo. *Developmental Biology*, 426(2), pp.409–417. doi:https://doi.org/10.1016/j.ydbio.2016.07.002.

Bowden, S., Brislinger-Engelhardt, M.M., Hansen, M., Temporal-Plo, A., Weber, D., Hägele, S., Lorenz, F., Litwin, T., Kreutz, C. and Walentek, P. (2024). Foxi1 regulates multiple steps of mucociliary development and ionocyte specification through transcriptional and epigenetic mechanisms. *bioRxiv : the preprint server for biology*, [online] p.2024.10.27.620464. doi:https://doi.org/10.1101/2024.10.27.620464.

Bowles, J., Schepers, G. and Koopman, P. (2000). Phylogeny of the SOX Family of Developmental Transcription Factors Based on Sequence and Structural Indicators. *Developmental Biology*, [online] 227(2), pp.239–255. doi:https://doi.org/10.1006/dbio.2000.9883.

Boyer, L.A., Lee, T.I., Cole, M.F., Johnstone, S.E., Levine, S.S., Zucker, J.P., Guenther, M.G., Kumar, R.M., Murray, H.L., Jenner, R.G., Gifford, D.K., Melton, D.A., Jaenisch, R. and Young, R.A. (2005). Core Transcriptional Regulatory Circuitry in Human Embryonic Stem Cells. *Cell*, 122(6), pp.947–956. doi:https://doi.org/10.1016/j.cell.2005.08.020.

Bragança, J., Eloranta, J.J., Bamforth, S.D., Ibbitt, J.C., Hurst, H.C. and Bhattacharya, S. (2003). Physical and Functional Interactions among AP-2 Transcription Factors, p300/CREB-binding Protein, and CITED2. *Journal of Biological Chemistry*, 278(18), pp.16021–16029. doi:https://doi.org/10.1074/jbc.m208144200.

BragançaJ., Swingler, T., Marques, F.I.R., Jones, T., Eloranta, J.J., Hurst, H.C., Shioda, T. and Bhattacharya, S. (2002). Human CREB-binding Protein/p300-interacting Transactivator with ED-rich Tail (CITED) 4, a New Member of the CITED Family, Functions as a Co-activator for Transcription Factor AP-2 *. *Journal of Biological Chemistry*, [online] 277(10), pp.8559–8565. doi:https://doi.org/10.1074/jbc.M110850200.

Bravo González-Blas, C., De Winter, S., Hulselmans, G., Hecker, N., Matetovici, I., Christiaens, V., Poovathingal, S., Wouters, J., Aibar, S. and Aerts, S. (2023). SCENIC+: single-cell multiomic inference of enhancers and gene regulatory networks. *Nature Methods*, [online] 20(9), pp.1355–1367. doi:https://doi.org/10.1038/s41592-023-01938-4.

Briggs, J.A., Weinreb, C., Wagner, D.E., Megason, S., Peshkin, L., Kirschner, M.W. and Klein, A.M. (2018). The dynamics of gene expression in vertebrate embryogenesis at single-cell resolution. *Science*, 360(6392). doi:https://doi.org/10.1126/science.aar5780.

Bright, A.R., Siebe van Genesen, Li, Q., Grasso, A., Siebren Frölich, van, Simon and Veenstra, J.C. (2021). Combinatorial transcription factor activities on open chromatin induce embryonic heterogeneity in vertebrates. *The EMBO Journal*, 40(9). doi:https://doi.org/10.15252/embj.2020104913.

Buitrago-Delgado, E., Schock, E.N., Nordin, K. and LaBonne, C. (2018). A transition from SoxB1 to SoxE transcription factors is essential for progression from pluripotent blastula cells to neural crest cells. *Developmental Biology*, 444(2), pp.50–61. doi:https://doi.org/10.1016/j.ydbio.2018.08.008.

Cao, C., Lemaire, L.A., Wang, W., Yoon, P.H., Choi, Y.A., Parsons, L.R., Matese, J.C., Wang, W., Levine, M. and Chen, K. (2019). Comprehensive single-cell transcriptome lineages of a proto-vertebrate. *Nature*, [online] 571(7765), pp.349–354. doi:https://doi.org/10.1038/s41586-019-1385-y.

Capellini, T.D. (2006). Pbx1/Pbx2 requirement for distal limb patterning is mediated by the hierarchical control of Hox gene spatial distribution and Shh expression. *Development*, 133(11), pp.2263–2273. doi:https://doi.org/10.1242/dev.02395.

Caravaca, J.M., Donahue, G., Becker, J.S., He, X., Vinson, C. and Zaret, K.S. (2013). Bookmarking by specific and nonspecific binding of FoxA1 pioneer factor to mitotic chromosomes. *Genes & Development*, 27(3), pp.251–260. doi:https://doi.org/10.1101/gad.206458.112.

Caretti, G. (2004). The Polycomb Ezh2 methyltransferase regulates muscle gene expression and skeletal muscle differentiation. *Genes & Development*, 18(21), pp.2627–2638. doi:https://doi.org/10.1101/gad.1241904.

Cattell, M.V., Garnett, A.T., Klymkowsky, M.W. and Medeiros, D.M. (2012). A maternally establishedSoxB1/SoxFaxis is a conserved feature of chordate germ layer patterning. *Evolution & Development*, 14(1), pp.104–115. doi:https://doi.org/10.1111/j.1525-142x.2011.00525.x.

Cha, S.-W., McAdams, M., Kormish, J., Wylie, C. and Kofron, M. (2012). Foxi2 Is an Animally Localized Maternal mRNA in Xenopus, and an Activator of the Zygotic Ectoderm Activator Foxi1e. *PLoS ONE*, 7(7), p.e41782. doi:https://doi.org/10.1371/journal.pone.0041782.

Chalmers, A.D. (2003). Oriented cell divisions asymmetrically segregate aPKC and generate cell fate diversity in the early Xenopus embryo. *Development*, 130(12), pp.2657–2668. doi:https://doi.org/10.1242/dev.00490.

Chalmers, A.D., Lachani, K., Shin, Y., Sherwood, V., Cho, K.W.Y. and Papalopulu, N. (2006). Grainyhead-like 3, a transcription factor identified in a microarray screen, promotes the

specification of the superficial layer of the embryonic epidermis. *Mechanisms of development*, [online] 123(9), pp.702–18. doi:https://doi.org/10.1016/j.mod.2006.04.006.

Chalmers, A.D., Welchman, D. and Papalopulu, N. (2002). Intrinsic Differences between the Superficial and Deep Layers of the Xenopus Ectoderm Control Primary Neuronal Differentiation. *Developmental Cell*, 2(2), pp.171–182. doi:https://doi.org/10.1016/s1534-5807(02)00113-2.

Chan, S.H., Tang, Y., Miao, L., Darwich-Codore, H., Vejnar, C.E., Beaudoin, J.-D., Musaev, D., Fernandez, J.P., Benitez, M.D.J., Bazzini, A.A., Moreno-Mateos, M.A. and Giraldez, A.J. (2019). Brd4 and P300 Confer Transcriptional Competency during Zygotic Genome Activation. *Developmental Cell*, 49(6), pp.867-881.e8. doi:https://doi.org/10.1016/j.devcel.2019.05.037.

Charney, R.M., Forouzmand, E., Jin Whan Cho, Cheung, J.Y., Paraiso, K.D., Yuuri Yasuoka, Takahashi, S., Taira, M., Blitz, I.L., Xie, X. and Cho, K. (2017). Foxh1 Occupies cis-Regulatory Modules Prior to Dynamic Transcription Factor Interactions Controlling the Mesendoderm Gene Program. 40(6), pp.595-607.e4. doi:https://doi.org/10.1016/j.devcel.2017.02.017.

Chen, B., Niu, J., Kreuzer, J., Zheng, B., Jarugumilli, G.K., Haas, W. and Wu, X. (2018). Auto-fatty acylation of transcription factor RFX3 regulates ciliogenesis. *Proceedings of the National Academy of Sciences*, 115(36). doi:https://doi.org/10.1073/pnas.1800949115.

Chiu, W., Charney, R.M., Blitz, I.L., Fish, M., Li, Y., Biesinger, J., Xie, X. and Cho, K. (2014). Genome-wide view of TGFβ/Foxh1 regulation of the early mesendoderm program. *Development*, 141(23), pp.4537–4547. doi:https://doi.org/10.1242/dev.107227.

Choi, Y., Luo, Y., Lee, S., Jin, H., Yoon, H.-J., Hahn, Y., Bae, J. and Lee, H.H. (2022). FOXL2 and FOXA1 cooperatively assemble on the *TP53* promoter in alternative dimer configurations. *Nucleic Acids Research*, [online] 50(15), pp.8929–8946. doi:https://doi.org/10.1093/nar/gkac673.

CHOMZYNSKI, P. and Sacchi, N. (1987). Single-Step Method of RNA Isolation by Acid Guanidinium Thiocyanate–Phenol–Chloroform Extraction. *Analytical Biochemistry*, 162(1), pp.156–159. doi:https://doi.org/10.1006/abio.1987.9999.

Cimadamore, F., Fishwick, K., Giusto, E., Gnedeva, K., Cattarossi, G., Miller, A., Pluchino, S., Brill, Laurence M., Bronner-Fraser, M. and Terskikh, Alexey V. (2011). Human ESC-Derived Neural Crest Model Reveals a Key Role for SOX2 in Sensory Neurogenesis. *Cell Stem Cell*, 8(5), pp.538–551. doi:https://doi.org/10.1016/j.stem.2011.03.011.

Cordes, V.C., Rackwitz, H.R. and Reidenbach, S. (1997). Mediators of nuclear protein import target karyophilic proteins to pore complexes of cytoplasmic annulate lamellae. *Experimental cell research*, [online] 237(2), pp.419–33. doi:https://doi.org/10.1006/excr.1997.3806.

Coyle, M.C., Tajima, A.M., Leon, F., Choksi, S.P., Yang, A., Espinoza, S., Hughes, T.R., Reiter, J.F., Booth, D.S. and King, N. (2023). An RFX transcription factor regulates ciliogenesis in the

closest living relatives of animals. *Current Biology*, 33(17), pp.3747-3758.e9. doi:https://doi.org/10.1016/j.cub.2023.07.022.

Cruz, C.C., Ribes, V., Kutejova, E., Jordi Cayuso, Lawson, V., Norris, D.P., Stevens, J.R., Davey, M., Blight, K., Bangs, F., Mynett, A., Elizabeth, Chung, R., Nikolaos Balaskas, Brody, S.L., Martí, E. and Briscoe, J. (2010). Foxj1 regulates floor plate cilia architecture and modifies the response of cells to sonic hedgehog signalling. 137(24), pp.4271–4282. doi:https://doi.org/10.1242/dev.051714.

Dailey, L. and Basilico, C. (2001). Coevolution of HMG domains and homeodomains and the generation of transcriptional regulation by Sox/POU complexes. *Journal of cellular physiology*, [online] 186(3), pp.315–28. doi:https://doi.org/10.1002/1097-4652(2001)9999:9999%3C000::AID-JCP1046%3E3.0.CO;2-Y.

Davis, R.L., Weintraub, H. and Lassar, A.B. (1987). Expression of a single transfected cDNA converts fibroblasts to myoblasts. *Cell*, 51(6), pp.987–1000. doi:https://doi.org/10.1016/0092-8674(87)90585-x.

Deshmukh, S. and Prashanth, S. (2012). Ectodermal Dysplasia: A Genetic Review. *International Journal of Clinical Pediatric Dentistry*, [online] 5(3), pp.197–202. doi:https://doi.org/10.5005/jp-journals-10005-1165.

Didon, L., Zwick, R.K., Chao, I.W., Walters, M.S., Wang, R., Hackett, N.R. and Crystal, R.G. (2013). RFX3 Modulation of FOXJ1 regulation of cilia genes in the human airway epithelium. *Respiratory Research*, 14(1). doi:https://doi.org/10.1186/1465-9921-14-70.

Dobin, A., Davis, C.A., Schlesinger, F., Drenkow, J., Zaleski, C., Jha, S., Batut, P., Chaisson, M. and Gingeras, T.R. (2012). STAR: ultrafast universal RNA-seq aligner. *Bioinformatics*, 29(1), pp.15–21. doi:https://doi.org/10.1093/bioinformatics/bts635.

DrögemüllerC., Karlsson, E.K., HytönenM.K., Perloski, M., Dolf, G., Sainio, K., Lohi, H., Lindblad-Toh, K. and Leeb, T. (2008). A Mutation in Hairless Dogs Implicates *FOXI3* in Ectodermal Development. *Science*, 321(5895), pp.1462–1462. doi:https://doi.org/10.1126/science.1162525.

Dude, C.M., Kuan, C.-Y. . K., Bradshaw, J.R., Greene, N.D.E., Relaix, F., Stark, M.R. and Baker, C.V.H. (2009). Activation of Pax3 target genes is necessary but not sufficient for neurogenesis in the ophthalmic trigeminal placode. *Developmental Biology*, 326(2), pp.314–326. doi:https://doi.org/10.1016/j.ydbio.2008.11.032.

Edlund, R.K., Ohyama, T., Kantarci, H., Riley, B.B. and Groves, A.K. (2014). Foxi transcription factors promote pharyngeal arch development by regulating formation of FGF signaling centers. *Developmental Biology*, 390(1), pp.1–13. doi:https://doi.org/10.1016/j.ydbio.2014.03.004.

Edlund, R.K., Onur Birol and Groves, A.K. (2015). The Role of Foxi Family Transcription Factors in the Development of the Ear and Jaw. *Current topics in developmental biology/Current Topics in Developmental Biology*, [online] pp.461–495. doi:https://doi.org/10.1016/bs.ctdb.2014.11.014.

Farrell, J.A., Wang, Y., Riesenfeld, S.J., Shekhar, K., Regev, A. and Schier, A.F. (2018). Single-cell reconstruction of developmental trajectories during zebrafish embryogenesis. *Science*, [online] 360(6392). doi:https://doi.org/10.1126/science.aar3131.

Ferrie, J.J., Karr, J.P., Thomas G.W. Graham, Dailey, G.M., Zhang, G., Tjian, R. and Darzacq, X. (2024). p300 is an obligate integrator of combinatorial transcription factor inputs. *Molecular cell*, 84(2), pp.234-243.e4. doi:https://doi.org/10.1016/j.molcel.2023.12.004.

Fisher, R.C. and Scott, E.W. (1998). Role of PU.1 in Hematopoiesis. *Stem Cells*, 16(1), pp.25–37. doi:https://doi.org/10.1002/stem.160025.

Fortunato, S., Adamski, M., Bergum, B., Guder, C., Jordal, S., Leininger, S., Zwafink, C., Rapp, H.T. and Adamska, M. (2012). Genome-wide analysis of the sox family in the calcareous sponge Sycon ciliatum: multiple genes with unique expression patterns. *EvoDevo*, 3(1). doi:https://doi.org/10.1186/2041-9139-3-14.

Fortunato, S.A.V., Adamski, M. and Adamska, M. (2015). Comparative analyses of developmental transcription factor repertoires in sponges reveal unexpected complexity of the earliest animals. *Marine Genomics*, 24, pp.121–129. doi:https://doi.org/10.1016/j.margen.2015.07.008.

Francois-Campion, V., Berger, F., Mami Oikawa, Maissa Goumeidane, Nolwenn Mouniée, Chenouard, V., Petrova, K., Abreu, J.G., Fourgeux, C., Jeremie Poschmann, Leonid Peshkin, Romain Gibeaux and Jérôme Jullien (2025). Sperm derived H2AK119ub1 is required for embryonic development in Xenopus laevis. *Nature Communications*, [online] 16(1). doi:https://doi.org/10.1038/s41467-025-58615-7.

Freter, S., Muta, Y., Mak, S.-S. ., Rinkwitz, S. and Ladher, R.K. (2008). Progressive restriction of otic fate: the role of FGF and Wnt in resolving inner ear potential. *Development*, 135(20), pp.3415–3424. doi:https://doi.org/10.1242/dev.026674.

Fritzenwanker, J.H., Gerhart, J., Freeman, R.M. and Lowe, C.J. (2014). The Fox/Forkhead transcription factor family of the hemichordate Saccoglossus kowalevskii. *EvoDevo*, 5(1). doi:https://doi.org/10.1186/2041-9139-5-17.

Fuglerud, B.M., Ledsaak, M., Rogne, M., Eskeland, R. and Gabrielsen, O.S. (2018). The pioneer factor activity of c-Myb involves recruitment of p300 and induction of histone acetylation followed by acetylation-induced chromatin dissociation. *Epigenetics & Chromatin*, 11(1). doi:https://doi.org/10.1186/s13072-018-0208-y.

Fursova, N.A., Blackledge, N.P., Nakayama, M., Ito, S., Koseki, Y., Farcas, A.M., King, H.W., Koseki, H. and Klose, R.J. (2019). Synergy between Variant PRC1 Complexes Defines

Polycomb-Mediated Gene Repression. *Molecular Cell*, 74(5), pp.1020-1036.e8. doi:https://doi.org/10.1016/j.molcel.2019.03.024.

Gao, J., Li, P., Zhang, W., Wang, Z., Wang, X. and Zhang, Q. (2015a). Molecular Cloning, Promoter Analysis and Expression Profiles of the sox3 Gene in Japanese Flounder, Paralichthys olivaceus. *International Journal of Molecular Sciences*, 16(11), pp.27931–27944. doi:https://doi.org/10.3390/ijms161126079.

Gao, J., Wang, Z., Shao, K., Fan, L., Yang, L., Song, H., Liu, M., Wang, Z., Wang, X. and Zhang, Q. (2014). Identification and characterization of a Sox2 homolog in the Japanese flounder Paralichthys olivaceus. *Gene*, 544(2), pp.165–176. doi:https://doi.org/10.1016/j.gene.2014.04.062.

Gao, L., Zhu, X., Chen, G., Ma, X., Zhang, Y., Khand, A.A., Shi, H., Gu, F., Lin, H., Chen, Y., Zhang, H., He, L. and Tao, Q. (2015b). A novel role for ASCL1 in the regulation of mesendoderm formation via HDAC-dependent antagonism of VegT function. *Development*. [online] doi:https://doi.org/10.1242/dev.126292.

Gao, M., Veil, M., Rosenblatt, M., Riesle, A.J., Gebhard, A., Hass, H., Buryanova, L., Yampolsky, L.Y., Grüning, B., Ulianov, S.V., Timmer, J. and Onichtchouk, D. (2022). Pluripotency factors determine gene expression repertoire at zygotic genome activation. *Nature Communications*, [online] 13(1), p.788. doi:https://doi.org/10.1038/s41467-022-28434-1.

Gao, Y., Tan, D.S., Mathias Girbig, Hu, H., Zhou, X., Xie, Q., Yeung, S.W., Lee, K.S., Ho, S.Y., Cojocaru, V., Yan, J., Hochberg, G.K.A., Mendoza, A. de and Jauch, R. (2024). The emergence of Sox and POU transcription factors predates the origins of animal stem cells. *Nature Communications*, [online] 15(1). doi:https://doi.org/10.1038/s41467-024-54152-x.

Garner, S., Zysk, I., Byrne, G., Kramer, M., Moller, D., Taylor, V. and Burke, R.D. (2015). Neurogenesis in sea urchin embryos and the diversity of deuterostome neurogenic mechanisms. *Development*. doi:https://doi.org/10.1242/dev.124503.

Gasparini, F., Degasperi, V., Shimeld, S.M., Burighel, P. and Manni, L. (2013). Evolutionary conservation of the placodal transcriptional network during sexual and asexual development in chordates. *Developmental Dynamics*, 242(6), pp.752–766. doi:https://doi.org/10.1002/dvdy.23957.

Gentsch, G.E., Spruce, T., Nick D.L. Owens and Smith, J.A. (2019). Maternal pluripotency factors initiate extensive chromatin remodelling to predefine first response to inductive signals. *Nature Communications*, 10(1). doi:https://doi.org/10.1038/s41467-019-12263-w.

Graham, V., Khudyakov, J., Ellis, P. and Pevny, L. (2003). SOX2 Functions to Maintain Neural Progenitor Identity. *Neuron*, 39(5), pp.749–765. doi:https://doi.org/10.1016/s0896-6273(03)00497-5.

Green, J.B.A. and Smith, J.C. (1990). Graded changes in dose of a Xenopus activin A homologue elicit stepwise transitions in embryonic cell fate. *Nature*, 347(6291), pp.391–394. doi:https://doi.org/10.1038/347391a0.

Groves, A.K. and LaBonne, C. (2014). Setting appropriate boundaries: Fate, patterning and competence at the neural plate border. *Developmental Biology*, 389(1), pp.2–12. doi:https://doi.org/10.1016/j.ydbio.2013.11.027.

Gubbay, J., Collignon, J., Koopman, P., Capel, B., Economou, A., Münsterberg, A., Vivian, N., Goodfellow, P. and Lovell-Badge, R. (1990). A gene mapping to the sex-determining region of the mouse Y chromosome is a member of a novel family of embryonically expressed genes. *Nature*, [online] 346(6281), pp.245–250. doi:https://doi.org/10.1038/346245a0.

Gupta, R., Wills, A., Ucar, D. and Baker, J. (2014). Developmental enhancers are marked independently of zygotic Nodal signals in Xenopus. *Developmental biology*, [online] 395(1), pp.38–49. doi:https://doi.org/10.1016/j.ydbio.2014.08.034.

Gurdon, J.B., Elsdale, T.R. and Fischberg, M. (1958). Sexually mature individuals of Xenopus laevis from the transplantation of single somatic nuclei. *Nature*, [online] 182(4627), pp.64–65. doi:https://doi.org/10.1038/182064a0.

Gurdon, J.B., Fairman, S., Mohun, T.J. and Brennan, S. (1985). Activation of muscle-specific actin genes in xenopus development by an induction between animal and vegetal cells of a blastula. *Cell*, 41(3), pp.913–922. doi:https://doi.org/10.1016/s0092-8674(85)80072-6.

Hans, S., Irmscher, A. and Brand, M. (2013). Zebrafish Foxi1 provides a neuronal ground state during inner ear induction preceding the Dlx3b/4b-regulated sensory lineage. *Development*, 140(9), pp.1936–1945. doi:https://doi.org/10.1242/dev.087718.

Hao, Y., Hao, S., Andersen-Nissen, E., Mauck, W.M., Zheng, S., Butler, A., Lee, M.J., Wilk, A.J., Darby, C., Zager, M., Hoffman, P., Stoeckius, M., Papalexi, E., Mimitou, E.P., Jain, J., Srivastava, A., Stuart, T., Fleming, L.M., Yeung, B. and Rogers, A.J. (2021). Integrated analysis of multimodal single-cell data. *Cell*, 184(13). doi:https://doi.org/10.1016/j.cell.2021.04.048.

Harris, C.R., Millman, K.J., van der Walt, S.J., Gommers, R., Virtanen, P., Cournapeau, D., Wieser, E., Taylor, J., Berg, S., Smith, N.J., Kern, R., Picus, M., Hoyer, S., van Kerkwijk, M.H., Brett, M., Haldane, A., del Río, J.F., Wiebe, M., Peterson, P. and Gérard-Marchant, P. (2020). Array Programming with NumPy. *Nature*, [online] 585(7825), pp.357–362. doi:https://doi.org/10.1038/s41586-020-2649-2.

Hau, A.-C., Mommaerts, E., Laub, V., Müller, T., Dittmar, G. and Schulte, D. (2021). Transcriptional cooperation of PBX1 and PAX6 in adult neural progenitor cells. *Scientific Reports*, [online] 11(1), p.21013. doi:https://doi.org/10.1038/s41598-021-99968-5.

Heintzman, N.D., Hon, G.C., Hawkins, R.D., Kheradpour, P., Stark, A., Harp, L.F., Ye, Z., Lee, L.K., Stuart, R.K., Ching, C.W., Ching, K.A., Antosiewicz-Bourget, J.E., Liu, H., Zhang, X.,

Green, R.D., Lobanenkov, V.V., Stewart, R., Thomson, J.A., Crawford, G.E. and Kellis, M. (2009). Histone modifications at human enhancers reflect global cell-type-specific gene expression. *Nature*, 459(7243), pp.108–112. doi:https://doi.org/10.1038/nature07829.

Heinz, S., Benner, C., Spann, N., Bertolino, E., Lin, Y.C., Laslo, P., Cheng, J.X., Murre, C., Singh, H. and Glass, C.K. (2010). Simple Combinations of Lineage-Determining Transcription Factors Prime cis-Regulatory Elements Required for Macrophage and B Cell Identities. *Molecular Cell*, [online] 38(4), pp.576–589. doi:https://doi.org/10.1016/j.molcel.2010.05.004.

Hendrickson, C.L., Blitz, I.L., Hussein, A., Paraiso, K.D., Cho, J., Klymkowsky, M.W., Kofron, M.J. and Cho, K.W.Y. (2025). Foxi2 and Sox3 are master regulators controlling ectoderm germ layer specification. *bioRxiv : the preprint server for biology*, [online] p.2025.01.09.632114. doi:https://doi.org/10.1101/2025.01.09.632114.

Hickey, G.J., Wike, C.L., Nie, X., Guo, Y., Tan, M., Murphy, P.J. and Cairns, B.R. (2022). Establishment of developmental gene silencing by ordered polycomb complex recruitment in early zebrafish embryos. *eLife*, 11. doi:https://doi.org/10.7554/elife.67738.

Hiroki Sugishita, Kondo, T., Ito, S., Nakayama, M., Nayuta Yakushiji-Kaminatsui, Kawakami, E., Haruhiko Koseki, Yasuhide Ohinata, Sharif, J., Mio Harachi, Blackledge, N.P. and Klose, R.J. (2021). Variant PCGF1-PRC1 links PRC2 recruitment with differentiation-associated transcriptional inactivation at target genes. *Nature Communications*, 12(1). doi:https://doi.org/10.1038/s41467-021-24894-z.

Hong, C.-S. and Saint-Jeannet, J.-P. (2007). The Activity of Pax3 and Zic1 Regulates Three Distinct Cell Fates at the Neural Plate Border. *Molecular Biology of the Cell*, 18(6), pp.2192–2202. doi:https://doi.org/10.1091/mbc.e06-11-1047.

Hontelez, S., van Kruijsbergen, I., Georgiou, G., van Heeringen, S.J., Bogdanovic, O., Lister, R. and Veenstra, G.J.C. (2015). Embryonic transcription is controlled by maternally defined chromatin state. *Nature Communications*, 6(1). doi:https://doi.org/10.1038/ncomms10148.

Horb, M.E., Shen, C.-N., Tosh, D. and Slack, J.M.W. (2003). Experimental Conversion of Liver to Pancreas. *Current Biology*, 13(2), pp.105–115. doi:https://doi.org/10.1016/s0960-9822(02)01434-3.

Hou, L., Srivastava, Y. and Jauch, R. (2017). Molecular basis for the genome engagement by Sox proteins. *Seminars in Cell & Developmental Biology*, 63, pp.2–12. doi:https://doi.org/10.1016/j.semcdb.2016.08.005.

Hsiao, C.-D., You, M.-S., Ying-Jey Guh, Ma, M., Jiang, Y.-J. and Hwang, P. (2007). A Positive Regulatory Loop between foxi3a and foxi3b Is Essential for Specification and Differentiation of Zebrafish Epidermal Ionocytes. *PLOS ONE*, 2(3), pp.e302–e302. doi:https://doi.org/10.1371/journal.pone.0000302.

Hu, Y., Wang, Y., He, Y., Ye, M., Yuan, J., Ren, C., Wang, X., Wang, S., Guo, Y., Cao, Q., Zhou, S., Wang, B., He, A., Hu, J., Guo, X., Shu, W. and Huo, R. (2024). Maternal KLF17 controls zygotic genome activation by acting as a messenger for RNA Pol II recruitment in mouse embryos. *Developmental Cell*, 59(5), pp.613-626.e6. doi:https://doi.org/10.1016/j.devcel.2024.01.013.

Hug, C.B., Grimaldi, A.G., Kruse, K. and Vaquerizas, J.M. (2017). Chromatin Architecture Emerges during Zygotic Genome Activation Independent of Transcription. *Cell*, 169(2), pp.216-228.e19. doi:https://doi.org/10.1016/j.cell.2017.03.024.

Hulander, M., Kiernan, A.E., Blomqvist, S.R., Carlsson, P., Samuelsson, E.-J., Johansson, B.R., Steel, K.P. and EnerbäckS. (2003). Lack of pendrin expression leads to deafness and expansion of the endolymphatic compartment in inner ears of Foxi1 null mutant mice. *Development*, 130(9), pp.2013–2025. doi:https://doi.org/10.1242/dev.00376.

Hulander, M., Wurst, W., Carlsson, P. and Enerbäck, S. (1998). The winged helix transcription factor Fkh10 is required for normal development of the inner ear. *Nature genetics*, [online] 20(4), pp.374–6. doi:https://doi.org/10.1038/3850.

Hunter, J.D. (2007). Matplotlib: A 2D Graphics Environment. *Computing in Science & Engineering*, [online] 9(3), pp.90–95. Available at: https://ieeexplore.ieee.org/document/4160265.

Hwang, J.-Y. and Zukin, R.S. (2018). REST, a master transcriptional regulator in neurodegenerative disease. *Current Opinion in Neurobiology*, [online] 48, pp.193–200. doi:https://doi.org/10.1016/j.conb.2017.12.008.

Ikuo Nobuhisa, Gerel Melig and Taga, T. (2024). Sox17 and Other SoxF-Family Proteins Play Key Roles in the Hematopoiesis of Mouse Embryos. *Cells*, 13(22), pp.1840–1840. doi:https://doi.org/10.3390/cells13221840.

Itin, P.H. (2014). Etiology and pathogenesis of ectodermal dysplasias. *American Journal of Medical Genetics Part A*, 164(10), pp.2472–2477. doi:https://doi.org/10.1002/ajmg.a.36550.

Iurlaro M, Ficz G, Oxley D, Raiber EA, Bachman M, Booth MJ, Andrews S, Balasubramanian S, Reik W. A screen for hydroxymethylcytosine and formylcytosine binding proteins suggests functions in transcription and chromatin regulation. Genome Biol. 2013;14(10):R119. doi: 10.1186/gb-2013-14-10-r119. PMID: 24156278; PMCID: PMC4014808.

Jacobs, C.T. and Huang, P. (2019). Notch signalling maintains Hedgehog responsiveness via a Gli-dependent mechanism during spinal cord patterning in zebrafish. *eLife*, 8. doi:https://doi.org/10.7554/elife.49252.

Jansen, C., Paraiso, K.D., Zhou, J.J., Blitz, I.L., Fish, M.B., Charney, R.M., Cho, J.S., Yasuoka, Y., Sudou, N., Bright, A.R., Wlizla, M., Veenstra, G.J.C., Taira, M., Zorn, A.M., Mortazavi, A. and Cho, K.W.Y. (2022). Uncovering the mesendoderm gene regulatory network through multi-omic

data integration. *Cell Reports*, [online] 38(7), p.110364. doi:https://doi.org/10.1016/j.celrep.2022.110364.

Jayasena, C.S., Ohyama, T., Segil, N. and Groves, A.K. (2008). Notch signaling augments the canonical Wnt pathway to specify the size of the otic placode. *Development*, 135(13), pp.2251–2261. doi:https://doi.org/10.1242/dev.017905.

Jeschonek, S.P. and Mowry, K.L. (2018). Whole-Mount Immunofluorescence for Visualizing Endogenous Protein and Injected RNA in *Xenopus* Oocytes. *Cold Spring Harbor Protocols*, [online] 2018(10), pp.pdb.prot097022–pdb.prot097022. doi:https://doi.org/10.1101/pdb.prot097022.

Jiang, P., Nelson, J.D., Leng, N., Collins, M., Swanson, S., Dewey, C.N., Thomson, J.A. and Stewart, R. (2017). Analysis of embryonic development in the unsequenced axolotl: Waves of transcriptomic upheaval and stability. *Developmental Biology*, 426(2), pp.143–154. doi:https://doi.org/10.1016/j.ydbio.2016.05.024.

Jnicke, M., Bjrn Renisch and Hammerschmidt, M. (2009). Zebrafish grainyhead-like1 is a common marker of different non-keratinocyte epidermal cell lineages, which segregate from each other in a Foxi3-dependent manner. *The International Journal of Developmental Biology*, 54(5), pp.837–850. doi:https://doi.org/10.1387/ijdb.092877mj.

Jones, E.A. and Woodland, H.R. (1987). The development of animal cap cells in Xenopus: a measure of the start of animal cap competence to form mesoderm. *Development*, 101(3), pp.557–563. doi:https://doi.org/10.1242/dev.101.3.557.

Jussila M, Aalto AJ, Sanz Navarro M, Shirokova V, Balic A, Kallonen A, Ohyama T, Groves AK, Mikkola ML, Thesleff I. Suppression of epithelial differentiation by Foxi3 is essential for molar crown patterning. Development. 2015 Nov 15;142(22):3954-63. doi: 10.1242/dev.124172. Epub 2015 Oct 8. PMID: 26450968; PMCID: PMC6517835.

Kahn, T.G., Dorafshan, E., Schultheis, D., Zare, A., Stenberg, P., Reim, I., Pirrotta, V. and Schwartz, Y.B. (2016). Interdependence of PRC1 and PRC2 for recruitment to Polycomb Response Elements. *Nucleic Acids Research*, p.gkw701. doi:https://doi.org/10.1093/nar/gkw701.

Kamimoto, K., Stringa, B., Hoffmann, C.M., Jindal, K., Solnica-Krezel, L. and Morris, S.A. (2023a). Dissecting cell identity via network inference and in silico gene perturbation. *Nature*, 614(7949), pp.742–751. doi:https://doi.org/10.1038/s41586-022-05688-9.

Karaiskos, N., Wahle, P., Alles, J., Boltengagen, A., Ayoub, S., Kipar, C., Kocks, C., Rajewsky, N. and Zinzen, R.P. (2017). TheDrosophilaembryo at single-cell transcriptome resolution. *Science*, [online] 358(6360), pp.194–199. doi:https://doi.org/10.1126/science.aan3235.

Kenji Kamimoto, Hoffmann, C. and Morris, S.A. (2020). CellOracle: Dissecting cell identity via network inference and in silico gene perturbation. doi:https://doi.org/10.1101/2020.02.17.947416.

Kenji Kamimoto, Mohd Tayyab Adil, Jindal, K., Hoffmann, C.M., Kong, W., Yang, X. and Morris, S.A. (2023b). Gene regulatory network reconfiguration in direct lineage reprogramming. *Stem cell reports*, 18(1), pp.97–112. doi:https://doi.org/10.1016/j.stemcr.2022.11.010.

Kenny, A.P., Oleksyn, D.W., Newman, L.A., Angerer, R.C. and Angerer, L.M. (2003). Tight regulation of SpSoxB factors is required for patterning and morphogenesis in sea urchin embryos. *Developmental Biology*, 261(2), pp.412–425. doi:https://doi.org/10.1016/s0012-1606(03)00331-2.

Keramari, M., Razavi, J., Ingman, K.A., Patsch, C., Edenhofer, F., Ward, C.M. and Kimber, S.J. (2010). Sox2 Is Essential for Formation of Trophectoderm in the Preimplantation Embryo. *PLoS ONE*, 5(11), p.e13952. doi:https://doi.org/10.1371/journal.pone.0013952.

Khatri, S.B., Edlund, R.K. and Groves, A.K. (2014). Foxi3 is necessary for the induction of the chick otic placode in response to FGF signaling. *Developmental Biology*, 391(2), pp.158–169. doi:https://doi.org/10.1016/j.ydbio.2014.04.014.

Khatri, S.B. and Groves, A.K. (2013). Expression of the Foxi2 and Foxi3 transcription factors during development of chicken sensory placodes and pharyngeal arches. *Gene Expression Patterns*, 13(1-2), pp.38–42. doi:https://doi.org/10.1016/j.gep.2012.10.001.

Kishi, M., Mizuseki, K., Sasai, N., Yamazaki, H., Shiota, K., Nakanishi, S. and Sasai, Y. (2000). Requirement of Sox2-mediated signaling for differentiation of early Xenopus neuroectoderm. *Development*, 127(4), pp.791–800. doi:https://doi.org/10.1242/dev.127.4.791.

Kobak, D. and Linderman, G.C. (2021). Initialization is critical for preserving global data structure in both t-SNE and UMAP. *Nature Biotechnology*, 39(2), pp.156–157. doi:https://doi.org/10.1038/s41587-020-00809-z.

Kojima, M.L., Hoppe, C. and Giraldez, A.J. (2024). The maternal-to-zygotic transition: reprogramming of the cytoplasm and nucleus. *Nature Reviews Genetics*. [online] doi:https://doi.org/10.1038/s41576-024-00792-0.

Kotov, A., Seal, S., Mansour Alkobtawi, Kappès, V., Sofia Medina Ruiz, Arbès, H., Harland, R.M., Leonid Peshkin and Monsoro-Burq, A.H. (2024). A time-resolved single-cell roadmap of the logic driving anterior neural crest diversification from neural border to migration stages. *Proceedings of the National Academy of Sciences*, 121(19). doi:https://doi.org/10.1073/pnas.2311685121.

Kruijsbergen, I. van, Saartje Hontelez and Veenstra, J.C. (2015). Recruiting polycomb to chromatin. *The International Journal of Biochemistry & Cell Biology*, 67, pp.177–187. doi:https://doi.org/10.1016/j.biocel.2015.05.006.

Kubo, N., Chen, P.B., Hu, R., Ye, Z., Sasaki, H. and Ren, B. (2024). H3K4me1 facilitates promoter-enhancer interactions and gene activation during embryonic stem cell differentiation. *Molecular Cell*, [online] 84(9), pp.1742-1752.e5. doi:https://doi.org/10.1016/j.molcel.2024.02.030.

Kudryavtseva, E.I., Sugihara, T.M., Wang, N., Lasso, R.J., Gudnason, J.F., Lipkin, S.M. and Andersen, B. (2003). Identification and characterization of Grainyhead-like epithelial transactivator (GET-1), a novel mammalian Grainyhead-like factor. *Developmental Dynamics*, 226(4), pp.604–617. doi:https://doi.org/10.1002/dvdy.10255.

Lake, B.B., Chen, S., Sos, B.C., Fan, J., Kaeser, G.E., Yung, Y.C., Duong, T.E., Gao, D., Chun, J., Kharchenko, P.V. and Zhang, K. (2017). Integrative single-cell analysis of transcriptional and epigenetic states in the human adult brain. *Nature Biotechnology*, 36(1), pp.70–80. doi:https://doi.org/10.1038/nbt.4038.

Lan, X., Wen, L., Li, K., Liu, X., Luo, B., Chen, F., Xie, D. and Kung, H. (2011). Comparative analysis of duplicated *sox21* genes in zebrafish. *Development Growth & Differentiation*, 53(3), pp.347–356. doi:https://doi.org/10.1111/j.1440-169x.2010.01239.x.

Langmead, B. and Salzberg, S.L. (2012). Fast gapped-read alignment with Bowtie 2. *Nature Methods*, 9(4), pp.357–359. doi:https://doi.org/10.1038/nmeth.1923.

Larroux, C., Fahey, B., Liubicich, D., Hinman, V.F., Gauthier, M., Gongora, M., Green, K., Worheide, G., Leys, S.P. and Degnan, B.M. (2006). Developmental expression of transcription factor genes in a demosponge: insights into the origin of metazoan multicellularity. *Evolution Development*, 8(2), pp.150–173. doi:https://doi.org/10.1111/j.1525-142x.2006.00086.x.

Larroux, C., Luke, G.N., Koopman, P., Rokhsar, D.S., Shimeld, S.M. and Degnan, B.M. (2008). Genesis and Expansion of Metazoan Transcription Factor Gene Classes. *Mol Biol Evol*, [online] 25(5), pp.980–996. doi:https://doi.org/10.1093/molbev/msn047.

Lee, M.-K. (2021). PRC1, PRC2 and BAP1 : Three tightly-linked chromatin modifiers involved in transcriptional regulation. *Hal.science*. [online] doi:https://pastel.hal.science/tel-04842227.

Lee, M.T., Bonneau, A.R., Takacs, C.M., Bazzini, A.A., DiVito, K.R., Fleming, E.S. and Giraldez, A.J. (2013). Nanog, Pou5f1 and SoxB1 activate zygotic gene expression during the maternal-to-zygotic transition. *Nature*, [online] 503(7476), pp.360–364. doi:https://doi.org/10.1038/nature12632.

Lee, S.A. (2003). The zebrafish forkhead transcription factor Foxi1 specifies epibranchial placode-derived sensory neurons. *Development*, 130(12), pp.2669–2679. doi:https://doi.org/10.1242/dev.00502.

Lef, J., Clement, J.H., Oschwald, R., Manfred Köster and Knöchel, W. (1994). Spatial and temporal transcription patterns of the forkhead related XFD-2/XFD-2′ genes in Xenopus laevis

embryos. *Mechanisms of Development*, 45(2), pp.117–126. doi:https://doi.org/10.1016/0925-4773(94)90025-6.

Leichsenring, M., Maes, J., Mössner, R., Driever, W. and Onichtchouk, D. (2013). Pou5f1 Transcription Factor Controls Zygotic Gene Activation In Vertebrates. *Science*, 341(6149), pp.1005–1009. doi:https://doi.org/10.1126/science.1242527.

Li, B. and Dewey, C.N. (2011). RSEM: accurate transcript quantification from RNA-Seq data with or without a reference genome. *BMC Bioinformatics*, 12(1). doi:https://doi.org/10.1186/1471-2105-12-323.

Li, J., Zhang, T., Ramakrishnan, A., Fritzsch, B., Xu, J., Wong, E.Y.M., Loh, Y.-H.E., Ding, J., Shen, L. and Xu, P.-X. (2020). Dynamic changes in cis-regulatory occupancy by Six1 and its cooperative interactions with distinct cofactors drive lineage-specific gene expression programs during progressive differentiation of the auditory sensory epithelium. *Nucleic Acids Research*, [online] 48(6), pp.2880–2896. doi:https://doi.org/10.1093/nar/gkaa012.

Li, L., Lai, F., Hu, X., Liu, B., Lu, X., Lin, Z., Liu, L., Xiang, Y., Frum, T., Halbisen, M.A., Chen, F., Fan, Q., Ralston, A. and Xie, W. (2023). Multifaceted SOX2-chromatin interaction underpins pluripotency progression in early embryos. *Science*, 382(6676). doi:https://doi.org/10.1126/science.adi5516.

Li, L., Lai, F., Liu, L., Lu, X., Hu, X., Liu, B., Lin, Z., Fan, Q., Kong, F., Xu, Q. and Xie, W. (2024). Lineage regulators TFAP2C and NR5A2 function as bipotency activators in totipotent embryos. *Nature structural & molecular biology*, [online] 31(6), pp.950–963. doi:https://doi.org/10.1038/s41594-023-01199-x.

Li, Q., Brown, J.B., Huang, H. and Bickel, P.J. (2011). Measuring reproducibility of high-throughput experiments. *The Annals of Applied Statistics*, 5(3), pp.1752–1779. doi:https://doi.org/10.1214/11-aoas466.

Liao, Y., Ma, L., Guo, Q., E, W., Fang, X., Yang, L., Ruan, F., Wang, J., Zhang, P., Sun, Z., Chen, H., Lin, Z., Wang, X., Wang, X., Sun, H., Fang, X., Zhou, Y., Chen, M., Shen, W. and Guo, G. (2022). Cell landscape of larval and adult Xenopus laevis at single-cell resolution. *Nature Communications*, [online] 13(1), p.4306. doi:https://doi.org/10.1038/s41467-022-31949-2.

Lilly, A.J., Lacaud, G. and Kouskoff, V. (2017). SOXF transcription factors in cardiovascular development. *Seminars in Cell & Developmental Biology*, [online] 63, pp.50–57. doi:https://doi.org/10.1016/j.semcdb.2016.07.021.

Lin, Y., Chen, D., Fan, Q. and Zhang, H. (2009). Characterization of SoxB2 and SoxC genes in amphioxus (Branchiostoma belcheri): Implications for their evolutionary conservation. *Science in China Series C Life Sciences*, 52(9), pp.813–822. doi:https://doi.org/10.1007/s11427-009-0111-7.

Liu, Y., Luo, X., Sun, Y., Chen, K., Hu, T., You, B., Xu, J., Zhang, F., Cheng, Q., Meng, X., Yan, T., Li, X., Qi, X., He, X., Guo, X., Li, C. and Su, B. (2025). Comparative single-cell multiome identifies evolutionary changes in neural progenitor cells during primate brain development. *Developmental cell*, [online] 60(3), pp.414-428.e8. doi:https://doi.org/10.1016/j.devcel.2024.10.005.

Livak, K.J. and Schmittgen, T.D. (2001). Analysis of Relative Gene Expression Data Using Real-Time Quantitative PCR and the 2−ΔΔCT Method. *Methods*, 25(4), pp.402–408. doi:https://doi.org/10.1006/meth.2001.1262.

Longobardi, E., Penkov, D., Mateos, D., Florian, G., Torres, M. and Blasi, F. (2013). Biochemistry of the tale transcription factors PREP, MEIS, and PBX in vertebrates. *Developmental Dynamics*, 243(1), pp.59–75. doi:https://doi.org/10.1002/dvdy.24016.

Lorente-Cánovas, B., Ingham, N., Norgett, E.E., Golder, Z.J., Karet, F.E. and Steel, K.P. (2012). Mice deficient in the H+-ATPase a4 subunit have severe hearing impairment associated with enlarged endolymphatic compartments within the inner ear. *Disease models & mechanisms*. doi:https://doi.org/10.1242/dmm.010645.

Loupe, J.M., Anderson, A.G., Rizzardi, L.F., Rodriguez-Nunez, I., Moyers, B., Trausch-Lowther, K., Jain, R., Bunney, W.E., Bunney, B.G., Cartagena, P., Sequeira, A., Watson, S.J., Akil, H., Cooper, G.M. and Myers, R.M. (2024). Multiomic profiling of transcription factor binding and function in human brain. *Nature Neuroscience*, 27(7), pp.1387–1399. doi:https://doi.org/10.1038/s41593-024-01658-8.

Love, M.I., Huber, W. and Anders, S. (2014). Moderated estimation of fold change and dispersion for RNA-seq data with DESeq2. *Genome Biology*, 15(12), p.550. doi:https://doi.org/10.1186/s13059-014-0550-8.

Luo, T., Lee, Y.-H., Jean-Pierre Saint-Jeannet and Sargent, T.D. (2003). Induction of neural crest in *Xenopus* by transcription factor AP2α. *Proceedings of the National Academy of Sciences*, 100(2), pp.532–537. doi:https://doi.org/10.1073/pnas.0237226100.

Ma, L., Gao, Z., Wu, J., Zhong, B., Xie, Y., Huang, W. and Lin, Y. (2021). Co-condensation between transcription factor and coactivator p300 modulates transcriptional bursting kinetics. *Molecular Cell*, 81(8), pp.1682-1697.e7. doi:https://doi.org/10.1016/j.molcel.2021.01.031.

Maharana, S.K. and Schlosser, G. (2018). A gene regulatory network underlying the formation of pre-placodal ectoderm in Xenopus laevis. *BMC Biology*, 16(1). doi:https://doi.org/10.1186/s12915-018-0540-5.

Manni, L., Lane, N.J., Joly, J., Gasparini, F., Stefano Tiozzo, Caicci, F., Zaniolo, G. and Paolo Burighel (2004). Neurogenic and non-neurogenic placodes in ascidians. *Journal of Experimental Zoology Part B Molecular and Developmental Evolution*, 302B(5), pp.483–504. doi:https://doi.org/10.1002/jez.b.21013.

Matsuo-Takasaki, M., Matsumura, M. and Sasai, Y. (2005). An essential role of *Xenopus Foxi1a* for ventral specification of the cephalic ectoderm during gastrulation. *Development*, 132(17), pp.3885–3894. doi:https://doi.org/10.1242/dev.01959.

Matsuwaka, M., Kumon, M. and Inoue, A. (2024). H3K27 dimethylation dynamics reveal stepwise establishment of facultative heterochromatin in early mouse embryos. *Nature Cell Biology*, [online] 27(1), pp.28–38. doi:https://doi.org/10.1038/s41556-024-01553-1.

Mazet, F., Hutt, J.A., Milloz, J., Millard, J., Graham, A. and Shimeld, S.M. (2005). Molecular evidence from Ciona intestinalis for the evolutionary origin of vertebrate sensory placodes. *Developmental Biology*, 282(2), pp.494–508. doi:https://doi.org/10.1016/j.ydbio.2005.02.021.

Mazet, F., Yu, J.-K., Liberles, D.A., Holland, L.Z. and Shimeld, S.M. (2003). Phylogenetic relationships of the Fox (Forkhead) gene family in the Bilateria. *Gene*, 316, pp.79–89. doi:https://doi.org/10.1016/s0378-1119(03)00741-8.

McInnes, L., Healy, J. and Melville, J. (2018). *UMAP: Uniform Manifold Approximation and Projection for Dimension Reduction*. [online] arXiv.org. Available at: https://arxiv.org/abs/1802.03426.

McKinney, W. (2010). Data Structures for Statistical Computing in Python. *Proceedings of the 9th Python in Science Conference*, 445. doi:https://doi.org/10.25080/majora-92bf1922-00a.

Mehta, R.J., Jain, R.K., Leung, S., Choo, J., Nielsen, T., Huntsman, D., Nakshatri, H. and Badve, S. (2011). FOXA1 is an independent prognostic marker for ER-positive breast cancer. *Breast Cancer Research and Treatment*, 131(3), pp.881–890. doi:https://doi.org/10.1007/s10549-011-1482-6.

Mei, H., Kozuka, C., Hayashi, R., Kumon, M., Koseki, H. and Inoue, A. (2021). H2AK119ub1 guides maternal inheritance and zygotic deposition of H3K27me3 in mouse embryos. *Nature Genetics*, 53(4), pp.539–550. doi:https://doi.org/10.1038/s41588-021-00820-3.

Miao, L., Tang, Y., Bonneau, A.R., Chan, S.H., Kojima, M.L., Pownall, M.E., Vejnar, C.E., Gao, F., Krishnaswamy, S., Hendry, C.E. and Giraldez, A.J. (2022). The landscape of pioneer factor activity reveals the mechanisms of chromatin reprogramming and genome activation. *Molecular Cell*, [online] 82(5), pp.986-1002.e9. doi:https://doi.org/10.1016/j.molcel.2022.01.024.

Millard, C.J., Varma, N., Saleh, A., Morris, K., Watson, P.J., Bottrill, A.R., Fairall, L., Smith, C.J. and Schwabe, J.W. (2016). The structure of the core NuRD repression complex provides insights into its interaction with chromatin. *eLife*, 5. doi:https://doi.org/10.7554/elife.13941.

Mir, A., Kofron, M., Heasman, J., Mogle, M., Lang, S., Birsoy, B. and Wylie, C. (2008). Long- and short-range signals control the dynamic expression of an animal hemisphere-specific gene in Xenopus. *Developmental Biology*, 315(1), pp.161–172. doi:https://doi.org/10.1016/j.ydbio.2007.12.022.

Mir, A., Kofron, M., Zorn, A.M., Bajzer, M., Haque, M., Heasman, J. and Wylie, C.C. (2007). Foxl1e activates ectoderm formation and controls cell position in the Xenopus blastula. *Development*, [online] 134(4), pp.779–788. doi:https://doi.org/10.1242/dev.02768.

Mitsuhiro Endoh, Endo, T.A., Jun Shinga, Hayashi, K., Farcas, A., Ma, K.-W., Ito, S., Sharif, J., Endoh, T., Onaga, N., Nakayama, M., Tomoyuki Ishikura, Masui, O., Kessler, B.M., Suda, T., Ohara, O., Okuda, A., Klose, R. and Haruhiko Koseki (2017). PCGF6-PRC1 suppresses premature differentiation of mouse embryonic stem cells by regulating germ cell-related genes. *eLife*, 6. doi:https://doi.org/10.7554/elife.21064.

Mochizuki, K., Sharif, J., Shirane, K., Uranishi, K., Bogutz, A.B., Janssen, S.M., Suzuki, A., Okuda, A., Koseki, H. and Lorincz, M.C. (2021). Repression of germline genes by PRC1.6 and SETDB1 in the early embryo precedes DNA methylation-mediated silencing. *Nature Communications*, [online] 12(1). doi:https://doi.org/10.1038/s41467-021-27345-x.

Mogollón, I., Niko Kangasniemi, Moustakas-Verho, J.E. and Ahtiainen, L. (2022). Foxi3 Suppresses Signaling Center Fate and is Necessary for the Early Development of Mouse Teeth. *bioRxiv (Cold Spring Harbor Laboratory)*. doi:https://doi.org/10.1101/2022.07.18.500404.

Mok, C.H., Hu, D., Losa, M., Maurizio Risolino, Licia Selleri and Marcucio, R.S. (2024). PBX1 and PBX3 transcription factors regulate SHH expression in the Frontonasal Ectodermal Zone through complementary mechanisms. *bioRxiv (Cold Spring Harbor Laboratory)*. [online] doi:https://doi.org/10.1101/2024.06.04.597450.

Moody, S.A. and LaMantia, A.-S. (2015). Transcriptional Regulation of Cranial Sensory Placode Development. *Current Topics in Developmental Biology*, [online] pp.301–350. doi:https://doi.org/10.1016/bs.ctdb.2014.11.009.

Moriguchi, T. and Yamamoto, M. (2014). A regulatory network governing Gata1 and Gata2 gene transcription orchestrates erythroid lineage differentiation. *International Journal of Hematology*, 100(5), pp.417–424. doi:https://doi.org/10.1007/s12185-014-1568-0.

Mortazavi, A., Williams, B.A., McCue, K., Schaeffer, L. and Wold, B. (2008). Mapping and quantifying mammalian transcriptomes by RNA-Seq. *Nature Methods*, 5(7), pp.621–628. doi:https://doi.org/10.1038/nmeth.1226.

Nakagawa, M., Koyanagi, M., Tanabe, K., Takahashi, K., Ichisaka, T., Aoi, T., Okita, K., Mochiduki, Y., Takizawa, N. and Yamanaka, S. (2007). Generation of induced pluripotent stem cells without Myc from mouse and human fibroblasts. *Nature Biotechnology*, 26(1), pp.101–106. doi:https://doi.org/10.1038/nbt1374.

Nakayama, T., Roubroeks, J.A.Y., Veenstra, G.J.C. and Grainger, R.M. (2022). Preparation of Intact Nuclei for Single-Nucleus Omics Using Frozen Cell Suspensions from Mutant Embryos of *Xenopus tropicalis*. *Cold Spring Harbor protocols*, [online] 2022(12), pp.641–652. doi:https://doi.org/10.1101/pdb.prot107825.

Newton, F., Petra zur Lage, Somdatta Karak, Moore, D.R., Göpfert, M.C. and Jarman, A.P. (2012). Forkhead Transcription Factor Fd3F Cooperates with Rfx to Regulate a Gene Expression Program for Mechanosensory Cilia Specialization. 22(6), pp.1221–1233. doi:https://doi.org/10.1016/j.devcel.2012.05.010.

Nguyen, T., Costa, E.J., Deibert, T., Reyes, J., Keber, F.C., Tomschik, M., Stadlmeier, M., Gupta, M., Kumar, C.K., Cruz, E.R., Amodeo, A., Gatlin, J.C. and Wühr, M. (2022). Differential nuclear import sets the timing of protein access to the embryonic genome. *Nature Communications*, [online] 13(1), p.5887. doi:https://doi.org/10.1038/s41467-022-33429-z.

Nissen, R.M., Yan, J., Amsterdam, A., Hopkins, N. and Burgess, S.M. (2003). Zebrafish foxi one modulates cellular responses to Fgf signaling required for the integrity of ear and jaw patterning. *Development*, 130(11), pp.2543–54. doi:https://doi.org/10.1242/dev.00455.

Oak, M.S., Stock, M., Matthias Mezes, Straub, T., Hynes-Allen, A.M., van, Ignasi Forne, Ettinger, A., Imhof, A., Scialdone, A. and Hoermanseder, E.B. (2025). H3K4 methylation-promoted transcriptional memory ensures faithful zygotic genome activation and embryonic development. *bioRxiv (Cold Spring Harbor Laboratory)*. doi:https://doi.org/10.1101/2025.01.20.633863.

Ohyama, T. (2006). Wnt signals mediate a fate decision between otic placode and epidermis. *Development*, 133(5), pp.865–875. doi:https://doi.org/10.1242/dev.02271.

Okuda, Y., Ogura, E., Kondoh, H. and Kamachi, Y. (2010). B1 SOX Coordinate Cell Specification with Patterning and Morphogenesis in the Early Zebrafish Embryo. *PLoS Genetics*, 6(5), p.e1000936. doi:https://doi.org/10.1371/journal.pgen.1000936.

Okuda, Y., Yoda, H., Uchikawa, M., Furutani-Seiki, M., Takeda, H., Kondoh, H. and Kamachi, Y. (2006). Comparative genomic and expression analysis of group B1*sox*genes in zebrafish indicates their diversification during vertebrate evolution. *Developmental Dynamics*, 235(3), pp.811–825. doi:https://doi.org/10.1002/dvdy.20678.

Ossipova, O., Tabler, J., Green, J.B.A. and Sokol, S.Y. (2007). PAR1 specifies ciliated cells in vertebrate ectoderm downstream of aPKC. *Development*, 134(23), pp.4297–4306. doi:https://doi.org/10.1242/dev.009282.

Otero, L.J., Devaux, A. and Standart, N. (2001). A 250-nucleotide UA-rich element in the 3' untranslated region of Xenopus laevis Vg1 mRNA represses translation both in vivo and in vitro. *RNA (New York, N.Y.)*, [online] 7(12), pp.1753–67. Available at: http://www.ncbi.nlm.nih.gov/pubmed/11780632.

Owens, Nick D.L., Blitz, Ira L., Lane, Maura A., Patrushev, I., Overton, John D., Gilchrist, Michael J., Cho, Ken W.Y. and Khokha, Mustafa K. (2016). Measuring Absolute RNA Copy Numbers at High Temporal Resolution Reveals Transcriptome Kinetics in Development. *Cell Reports*, 14(3), pp.632–647. doi:https://doi.org/10.1016/j.celrep.2015.12.050.

Packer, J.S., Zhu, Q., Huynh, C., Sivaramakrishnan, P., Preston, E., Dueck, H., Stefanik, D., Tan, K., Trapnell, C., Kim, J., Waterston, R.H. and Murray, J.I. (2019). A lineage-resolved molecular atlas of C. elegans embryogenesis at single-cell resolution. *Science*, 365(6459), p.eaax1971. doi:https://doi.org/10.1126/science.aax1971.

Pálfy, M., Schulze, G., Valen, E. and Vastenhouw, N.L. (2020). Chromatin accessibility established by Pou5f3, Sox19b and Nanog primes genes for activity during zebrafish genome activation. *PLOS Genetics*, 16(1), p.e1008546. doi:https://doi.org/10.1371/journal.pgen.1008546.

Paraiso, K. (2020). *Early Xenopus gene regulatory programs, chromatin states, and the role of maternal transcription factors*. [online] Available at: https://www.bohrium.com/paper-details/early-xenopus-gene-regulatory-programs-chromatin-states-and-the-role-of-maternal-transcription-factors/812655534959230978-5010 [Accessed 20 Aug. 2023].

Paraiso, K.D., Blitz, I.L. and Cho, K.W.Y. (2025). Maternal and zygotic contributions to H3K4me1 chromatin marking during germ layer formation. *Developmental biology*, [online] 518, pp.8–19. doi:https://doi.org/10.1016/j.ydbio.2024.11.006.

Paraiso, K.D., Blitz, I.L., Coley, M., Cheung, J., Sudou, N., Taira, M. and Cho, K.W.Y. (2019). Endodermal Maternal Transcription Factors Establish Super-Enhancers during Zygotic Genome Activation. *Cell Reports*, 27(10), pp.2962-2977.e5. doi:https://doi.org/10.1016/j.celrep.2019.05.013.

Park, J.T., Shih, I.-M. and Wang, T.-L. (2008). Identification of *Pbx1*, a Potential Oncogene, as a Notch3 Target Gene in Ovarian Cancer. *Cancer Research*, [online] 68(21), pp.8852–8860. doi:https://doi.org/10.1158/0008-5472.can-08-0517.

Pastor, W.A., Liu, W., Chen, D., Ho, J., Kim, R., Hunt, T.J., Lukianchikov, A., Liu, X., Polo, J.M., Jacobsen, S.E. and Clark, A.T. (2018). TFAP2C regulates transcription in human naive pluripotency by opening enhancers. *Nature Cell Biology*, 20(5), pp.553–564. doi:https://doi.org/10.1038/s41556-018-0089-0.

Penzel, R., Oschwald, R., Chen, Y., Tacke, L. and Grunz, H. (1997). Characterization and early embryonic expression of a neural specific transcription factor xSOX3 in Xenopus laevis. *The International journal of developmental biology*, [online] 41(5), pp.667–77. Available at: https://pubmed.ncbi.nlm.nih.gov/9415486/.

Phelps, W.A., Hurton, M.D., Ayers, T.N., Carlson, A.E., Rosenbaum, J.C. and Lee, M.T. (2023). Hybridization led to a rewired pluripotency network in the allotetraploid Xenopus laevis. *eLife*, 12. doi:https://doi.org/10.7554/elife.83952.

Pieper, M., Ahrens, K., Rink, E., Peter, A. and Schlosser, G. (2012). Differential distribution of competence for panplacodal and neural crest induction to non-neural and neural ectoderm. *Development*, 139(6), pp.1175–1187. doi:https://doi.org/10.1242/dev.074468.

Pijuan-Sala, B., Griffiths, J.A., Guibentif, C., Hiscock, T.W., Jawaid, W., Calero-Nieto, F.J., Mulas, C., Ibarra-Soria, X., Tyser, R.C.V., Ho, D.L.L., Reik, W., Srinivas, S., Simons, B.D., Nichols, J., Marioni, J.C. and Göttgens, B. (2019). A single-cell molecular map of mouse gastrulation and early organogenesis. *Nature*, [online] 566(7745), pp.490–495. doi:https://doi.org/10.1038/s41586-019-0933-9.

Pla, P. and Monsoro-Burq, A.H. (2018). The neural border: Induction, specification and maturation of the territory that generates neural crest cells. *Developmental Biology*, [online] 444, pp.S36–S46. doi:https://doi.org/10.1016/j.ydbio.2018.05.018.

Pliner, H.A., Packer, J.S., McFaline-Figueroa, J.L., Cusanovich, D.A., Daza, R.M., Aghamirzaie, D., Srivatsan, S., Qiu, X., Jackson, D., Minkina, A., Adey, A.C., Steemers, F.J., Shendure, J. and Trapnell, C. (2018). Cicero Predicts cis-Regulatory DNA Interactions from Single-Cell Chromatin Accessibility Data. *Molecular Cell*, 71(5), pp.858-871.e8. doi:https://doi.org/10.1016/j.molcel.2018.06.044.

Pohl, B.S., Rossner, A. and Knochel, W. (2005). The Fox gene family in Xenopus laevis:FoxI2, FoxM1 and FoxP1 in early development. *The International Journal of Developmental Biology*, 49(1), pp.53–58. doi:https://doi.org/10.1387/ijdb.051977bp.

Pohl, B.S., Sigrun Knöchel, Dillinger, K. and Knöchel, W. (2002). Sequence and expression of FoxB2 (XFD-5) and FoxI1c (XFD-10) in Xenopus embryogenesis. *Mechanisms of Development*, 117(1-2), pp.283–287. doi:https://doi.org/10.1016/s0925-4773(02)00184-3.

Popovic, J. and Stevanovic, M. (2009). Remarkable evolutionary conservation of SOX14 orthologues. *Journal of Genetics*, 88(1), pp.15–24. doi:https://doi.org/10.1007/s12041-009-0003-4.

Quigley, I.K. and Kintner, C. (2017). Rfx2 Stabilizes Foxj1 Binding at Chromatin Loops to Enable Multiciliated Cell Gene Expression. *PLoS Genetics*, 13(1), pp.e1006538–e1006538. doi:https://doi.org/10.1371/journal.pgen.1006538.

Raas, M.W.D., Zijlmans, D.W., Vermeulen, M. and Marks, H. (2022). There is another: H3K27me3-mediated genomic imprinting. *Trends in Genetics*, 38(1), pp.82–96. doi:https://doi.org/10.1016/j.tig.2021.06.017.

Radek Sindelka, Pavel Abaffy, Qu, Y., Silvie Tomankova, Sidova, M., Naraine, R., Kolar, M., Peuchen, E., Sun, L., Dovichi, N. and Kubista, M. (2018). Asymmetric distribution of biomolecules of maternal origin in the Xenopus laevis egg and their impact on the developmental plan. *Scientific Reports*, 8(1). doi:https://doi.org/10.1038/s41598-018-26592-1.

Raft, S., Andrade, L.R., Shao, D., Akiyama, H., Henkemeyer, M. and Wu, D.K. (2014). Ephrin-B2 governs morphogenesis of endolymphatic sac and duct epithelia in the mouse inner ear. *Developmental Biology*, 390(1), pp.51–67. doi:https://doi.org/10.1016/j.ydbio.2014.02.019.

Ramírez, F., Dündar, F., Diehl, S., Grüning, B.A. and Manke, T. (2014). deepTools: a flexible platform for exploring deep-sequencing data. *Nucleic Acids Research*, 42(W1), pp.W187–W191. doi:https://doi.org/10.1093/nar/gku365.

Ramsköld, D., Luo, S., Wang, Y.-C., Li, R., Deng, Q., Faridani, O.R., Daniels, G.A., Khrebtukova, I., Loring, J.F., Laurent, L.C., Schroth, G.P. and Sandberg, R. (2012). Full-length mRNA-Seq from single-cell levels of RNA and individual circulating tumor cells. *Nature Biotechnology*, 30(8), pp.777–782. doi:https://doi.org/10.1038/nbt.2282.

Ray, H.J. and Niswander, L.A. (2016). Grainyhead-like 2 downstream targets act to suppress epithelial-to-mesenchymal transition during neural tube closure. *Development*, 143(7), pp.1192–1204. doi:https://doi.org/10.1242/dev.129825.

Richards, G.S. and Rentzsch, F. (2014). Transgenic analysis of a SoxB gene reveals neural progenitor cells in the cnidarian Nematostella vectensis. *Development*, 141(24), pp.4681–4689. doi:https://doi.org/10.1242/dev.112029.

Richards, G.S. and Rentzsch, F. (2015). Regulation of*Nematostella*neural progenitors by SoxB, Notch and bHLH genes. *Development*, 142(19), pp.3332–3342. doi:https://doi.org/10.1242/dev.123745.

Rogers, C.D., Harafuji, N., Archer, T., Cunningham, D.D. and Casey, E.S. (2009). Xenopus Sox3 activates sox2 and geminin and indirectly represses Xvent2 expression to induce neural progenitor formation at the expense of non-neural ectodermal derivatives. *Mechanisms of Development*, 126(1-2), pp.42–55. doi:https://doi.org/10.1016/j.mod.2008.10.005.

Roellig, D., Tan-Cabugao, J., Sevan Esaian and Bronner, M.E. (2017). Dynamic transcriptional signature and cell fate analysis reveals plasticity of individual neural plate border cells. 6. doi:https://doi.org/10.7554/elife.21620.

Sackville, M. (2020). Ions before oxygen : ancestral origins of vertebrate gill function. doi:https://doi.org/10.14288/1.0394140.

Saeid Mohammad Parast, Yu, D., Chen, C., Dickinson, A.J., Chang, C. and Wang, H. (2023). Recognition of H2AK119ub plays an important role in RSF1-regulated early Xenopus development. *Frontiers in Cell and Developmental Biology*, 11. doi:https://doi.org/10.3389/fcell.2023.1168643.

Saint-Jeannet, J.-P. and Moody, S.A. (2014). Establishing the pre-placodal region and breaking it into placodes with distinct identities. *Developmental Biology*, 389(1), pp.13–27. doi:https://doi.org/10.1016/j.ydbio.2014.02.011.

Sanulli, S., Justin, N., Aurélie Teissandier, Ancelin, K., Portoso, M., Caron, M., Michaud, A., Lombard, B., Teixeira, S., Offer, J., Loew, D., Servant, N., Wassef, M., Fabienne Burlina, Gamblin, S.J., Heard, E. and Raphaël Margueron (2015). Jarid2 Methylation via the PRC2

Complex Regulates H3K27me3 Deposition during Cell Differentiation. *Molecular Cell*, 57(5), pp.769–783. doi:https://doi.org/10.1016/j.molcel.2014.12.020.

Sarma, A. and Pruthi, S. (2022). Congenital Brain Malformations- Update on Newer Classification and Genetic Basis. *Seminars in Roentgenology*. doi:https://doi.org/10.1053/j.ro.2022.11.004.

Satija, R., Farrell, J.A., Gennert, D., Schier, A.F. and Regev, A. (2015). Spatial reconstruction of single-cell gene expression data. *Nature Biotechnology*, 33(5), pp.495–502. doi:https://doi.org/10.1038/nbt.3192.

Sato, Y., Hilbert, L., Oda, H., Wan, Y., Heddleston, J.M., Chew, T.-L., Zaburdaev, V., Keller, P., Lionnet, T., Vastenhouw, N. and Kimura, H. (2019). Histone H3K27 acetylation precedes active transcription during zebrafish zygotic genome activation as revealed by live-cell analysis. *Development (Cambridge, England)*, [online] 146(19), p.dev179127. doi:https://doi.org/10.1242/dev.179127.

Scelfo, A., Fernández-Pérez, D., Tamburri, S., Zanotti, M., Lavarone, E., Soldi, M., Bonaldi, T., Karin Johanna Ferrari and Pasini, D. (2019). Functional Landscape of PCGF Proteins Reveals Both RING1A/B-Dependent-and RING1A/B-Independent-Specific Activities. 74(5), pp.1037-1052.e7. doi:https://doi.org/10.1016/j.molcel.2019.04.002.

Scheucher, M., Dege, P., Lef, J., Hille, S. and Kn□chel, W. (1995). Transcription patterns of four different fork head/HNF-3 related genes (XFD-4, 6, 9 and 10) in Xenopus laevis embryos. *Roux's Archives of Developmental Biology*, 204(3), pp.203–211. doi:https://doi.org/10.1007/bf00241274.

Schlosser, G. (2008). Do vertebrate neural crest and cranial placodes have a common evolutionary origin? *BioEssays*, 30(7), pp.659–672. doi:https://doi.org/10.1002/bies.20775.

Schlosser, G. (2014). Early embryonic specification of vertebrate cranial placodes. 3(5), pp.349–363. doi:https://doi.org/10.1002/wdev.142.

Schmetz, A., Amiel, J. and Wieczorek, D. (2021). Genetics of craniofacial malformations. *Seminars in Fetal and Neonatal Medicine*, [online] 26(6), p.101290. doi:https://doi.org/10.1016/j.siny.2021.101290.

Schock, E.N., York, J.R. and LaBonne, C. (2022). The developmental and evolutionary origins of cellular pluripotency in the vertebrate neural crest. *Seminars in Cell & Developmental Biology*. doi:https://doi.org/10.1016/j.semcdb.2022.04.008.

Schoeftner, S., Sengupta, A.K., Kubicek, S., Mechtler, K., Spahn, L., Koseki, H., Jenuwein, T. and Wutz, A. (2006). Recruitment of PRC1 function at the initiation of X inactivation independent of PRC2 and silencing. *The EMBO Journal*, 25(13), pp.3110–3122. doi:https://doi.org/10.1038/sj.emboj.7601187.

Shen, Y.-A., Jung, J., Shimberg, G.D., Hsu, F.-C., Rahmanto, Y.S., Gaillard, S.L., Hong, J., Bosch, J., Shih, I.-M., Chuang, C.-M. and Wang, T.-L. (2021). Development of small molecule inhibitors targeting PBX1 transcription signaling as a novel cancer therapeutic strategy. *iScience*, [online] 24(11), p.103297. doi:https://doi.org/10.1016/j.isci.2021.103297.

Shimeld, S.M., Degnan, B. and Luke, G.N. (2010). Evolutionary genomics of the Fox genes: Origin of gene families and the ancestry of gene clusters. *Genomics*, 95(5), pp.256–260. doi:https://doi.org/10.1016/j.ygeno.2009.08.002.

Shinzato, C., Iguchi, A., Hayward, D.C., Technau, U., Ball, E.E. and Miller, D.J. (2008). Sox genes in the coral Acropora millepora: divergent expression patterns reflect differences in developmental mechanisms within the Anthozoa. *BMC Evolutionary Biology*, 8(1). doi:https://doi.org/10.1186/1471-2148-8-311.

Simon, Akkers, R.C., Ila van Kruijsbergen, Arif, M., Hanssen, L., Sharifi, N. and Veenstra, J.C. (2013). Principles of nucleation of H3K27 methylation during embryonic development. *Genome Research*, 24(3), pp.401–410. doi:https://doi.org/10.1101/gr.159608.113.

Sladitschek, H.L., Fiuza, U.-M., Pavlinic, D., Benes, V., Hufnagel, L. and Neveu, P.A. (2020). MorphoSeq: Full Single-Cell Transcriptome Dynamics Up to Gastrulation in a Chordate. *Cell*, [online] 181(4), pp.922-935.e21. doi:https://doi.org/10.1016/j.cell.2020.03.055.

Smith, J.C., Price, B.M.J., Nimmen, K.V. and Huylebroeck, D. (1990). Identification of a potent Xenopus mesoderm-inducing factor as a homologue of activin A. *Nature*, 345(6277), pp.729–731. doi:https://doi.org/10.1038/345729a0.

Snape, A., Wylie, C.C., Smith, J.C. and J. Heasman (1987). Changes in states of commitment of single animal pole blastomeres of Xenopus laevis. *Developmental Biology*, 119(2), pp.503–510. doi:https://doi.org/10.1016/0012-1606(87)90053-4.

Solomon, K.S. (2003). Zebrafish foxi1 mediates otic placode formation and jaw development. *Development*, 130(5), pp.929–940. doi:https://doi.org/10.1242/dev.00308.

Solomon, K.S., Logsdon, J.M. and Fritz, A. (2003). Expression and phylogenetic analyses of three zebrafish FoxI class genes. *Developmental Dynamics*, 228(3), pp.301–307. doi:https://doi.org/10.1002/dvdy.10373.

Sonam, S., Bangru, S., Perry, K.J., Chembazhi, U.V., Kalsotra, A. and Henry, J.J. (2022). Cellular and molecular profiles of larval and adult Xenopus corneal epithelia resolved at the single-cell level. *Developmental Biology*, [online] 491, pp.13–30. doi:https://doi.org/10.1016/j.ydbio.2022.08.007.

Stasiulewicz, M., Gray, S.D., Mastromina, I., Silva, J.C., Bjorklund, M., Seymour, P.A., Booth, D., Thompson, C., Green, R.J., Hall, E.A., Serup, P. and Dale, J.K. (2015). A conserved role for Notch signaling in priming the cellular response to Shh through ciliary localisation of the key Shh transducer Smo. *Development*, 142(13), pp.2291–2303. doi:https://doi.org/10.1242/dev.125237.

Stielow, B., Finkernagel, F., Stiewe, T., Nist, A. and Suske, G. (2018). MGA, L3MBTL2 and E2F6 determine genomic binding of the non-canonical Polycomb repressive complex PRC1.6. *PLoS genetics*, [online] 14(1), p.e1007193. doi:https://doi.org/10.1371/journal.pgen.1007193.

Stundl, J. (2021). *Evolution of new cell types at the lateral neural border.* [online] Europepmc.org. Available at: https://europepmc.org/article/MED/33602488 [Accessed 20 Mar. 2024].

Suri, C., Tomomi Haremaki and Weinstein, D.C. (2005). *Xema*, a*foxi*-class gene expressed in the gastrula stage*Xenopus*ectoderm, is required for the suppression of mesendoderm. *Development*, 132(12), pp.2733–2742. doi:https://doi.org/10.1242/dev.01865.

Taguchi, S., Tagawa, K., Humphreys, T. and Nori Satoh (2002). Group B*Sox*Genes That Contribute to Specification of the Vertebrate Brain are Expressed in the Apical Organ and Ciliary Bands of Hemichordate Larvae. 19(1), pp.57–66. doi:https://doi.org/10.2108/zsj.19.57.

Takahashi, K. and Yamanaka, S. (2006). Induction of Pluripotent Stem Cells from Mouse Embryonic and Adult Fibroblast Cultures by Defined Factors. *Cell*, [online] 126(4), pp.663–676. Available at: https://pubmed.ncbi.nlm.nih.gov/16904174/.

Takahiro Ohyama and Groves, A.K. (2004). Expression of mouse Foxi class genes in early craniofacial development. *Developmental Dynamics*, 231(3), pp.640–646. doi:https://doi.org/10.1002/dvdy.20160.

Takashi Ariizumi, Tatsuo Michiue and Makoto Asashima (2017). In Vitro Induction of*Xenopus*Embryonic Organs Using Animal Cap Cells. *Cold Spring Harbor Protocols*, 2017(12), pp.pdb.prot097410–pdb.prot097410. doi:https://doi.org/10.1101/pdb.prot097410.

Tang, F., Barbacioru, C., Wang, Y., Nordman, E., Lee, C., Xu, N., Wang, X., Bodeau, J., Tuch, B.B., Siddiqui, A., Lao, K. and Surani, M.A. (2009). mRNA-Seq whole-transcriptome analysis of a single cell. *Nature Methods*, 6(5), pp.377–382. doi:https://doi.org/10.1038/nmeth.1315.

Tao, J. (2005). BMP4-dependent expression of Xenopus Grainyhead-like 1 is essential for epidermal differentiation. *Development*, 132(5), pp.1021–1034. doi:https://doi.org/10.1242/dev.01641.

Tassano, E., Jagannathan, V., Cord Drögemüller, Leoni, M., Hytönen, M.K., Severino, M., Gimelli, S., Cuoco, C., Maja Di Rocco, Kirsi Sanio, Groves, A.K., Leeb, T. and Giorgio Gimelli (2015). Congenital aural atresia associated with agenesis of internal carotid artery in a girl with a*FOXI3*deletion. *American Journal of Medical Genetics*, 167(3), pp.537–544. doi:https://doi.org/10.1002/ajmg.a.36895.

Tharindumala Abeywardana, Wu, X., Huang, S.-T., Masangkay, G.A., Rodin, A.S., Branciamore, S., Grigoriy Gogoshin, Li, A., Du, L., Neranjan Tharuka, Tomaino, R. and Chen, Y. (2024). Regulation of Enhancers by SUMOylation Through TFAP2C Binding and Recruitment of

HDAC Complex to the Chromatin. *Research Square (Research Square)*. [online] doi:https://doi.org/10.21203/rs.3.rs-4201913/v1.

Thawani, A. and Groves, A.K. (2020). Building the Border: Development of the Chordate Neural Plate Border Region and Its Derivatives. *Frontiers in Physiology*, 11. doi:https://doi.org/10.3389/fphys.2020.608880.

Thiery, A., Buzzi, A.L. and Streit, A. (2020). Cell fate decisions during the development of the peripheral nervous system in the vertebrate head. [online] Academic Press, pp.127–167. doi:https://doi.org/10.1016/bs.ctdb.2020.04.002.

Thiery, A.P., Buzzi, A.L., Hamrud, E., Cheshire, C., Luscombe, N.M., Briscoe, J. and Streit, A. (2023). scRNA-sequencing in chick suggests a probabilistic model for cell fate allocation at the neural plate border. *eLife*, 12. doi:https://doi.org/10.7554/elife.82717.

Ting, S.B. (2005). A Homolog of Drosophila grainy head Is Essential for Epidermal Integrity in Mice. *Science*, 308(5720), pp.411–413. doi:https://doi.org/10.1126/science.1107511.

TING, S.B., Tomasz WILANOWSKI, CERRUTI, L., ZHAO, L.-L., CUNNINGHAM, J.M. and JANE, S.M. (2003). The identification and characterization of human Sister-of-Mammalian Grainyhead (SOM) expands the grainyhead-like family of developmental transcription factors. *Biochemical Journal*, [online] 370(3), pp.953–962. doi:https://doi.org/10.1042/bj20021476.

Tomasz Wilanowski, Tuckfield, A., Cerruti, L., Sinead O'Connell, Saint, R., Parekh, V., Tao, J., Cunningham, J.M. and Jane, S.M. (2002). A highly conserved novel family of mammalian developmental transcription factors related to Drosophila grainyhead. *Mechanisms of Development*, 114(1-2), pp.37–50. doi:https://doi.org/10.1016/s0925-4773(02)00046-1.

Traag, V.A., Waltman, L. and van Eck, N.J. (2019). From Louvain to Leiden: guaranteeing well-connected communities. *Scientific Reports*, 9(1). doi:https://doi.org/10.1038/s41598-019-41695-z.

Trevers, K.E., Lu, H.-C., Yang, Y., Thiery, A.P., Strobl, A.C., Anderson, C., Božena Pálinkášová, Nidia, Irene, Khan, M.A.F., Moncaut, N., Luscombe, N.M., Dale, L., Streit, A. and Stern, C.D. (2023). A gene regulatory network for neural induction. *eLife*, 12. doi:https://doi.org/10.7554/elife.73189.

Tu, Q., Brown, C.T., Davidson, E.H. and Oliveri, P. (2006). Sea urchin Forkhead gene family: Phylogeny and embryonic expression. *Developmental Biology*, 300(1), pp.49–62. doi:https://doi.org/10.1016/j.ydbio.2006.09.031.

Urness, L. (2010). FGF signaling regulates otic placode induction and refinement by controlling both ectodermal target genes and hindbrain Wnt8a. *Developmental Biology*, [online] 340(2), pp.595–604. doi:https://doi.org/10.1016/j.ydbio.2010.02.016.

Ushey, K. (2025). *Authors and Citation*. [online] Github.io. Available at: https://rstudio.github.io/reticulate/authors.html [Accessed 19 Aug. 2025].

van Boxtel, R., Gomez-Puerto, C., Mokry, M., Eijkelenboom, A., van der Vos, K.E., Nieuwenhuis, E.E., Burgering, B.M., Lam, E.W.-F. and Coffer, P.J. (2013). FOXP1 acts through a negative feedback loop to suppress FOXO-induced apoptosis. *Cell Death & Differentiation*, 20(9), pp.1219–1229. doi:https://doi.org/10.1038/cdd.2013.81.

van den Eijnden-Van Raaij, A.J.M., van Zoelent, E.J.J., van Nimmen, K., Koster, C.H., Snoek, G.T., Durston, A.J. and Huylebroeck, D. (1990). Activin-like factor from a Xenopus laevis cell line responsible for mesoderm induction. *Nature*, 345(6277), pp.732–734. doi:https://doi.org/10.1038/345732a0.

van der Maaten, L. and Hinton, G. (2008). Visualizing Data using t-SNE Laurens van der Maaten. *Journal of Machine Learning Research*, [online] 9, pp.2579–2605. Available at: https://www.jmlr.org/papers/volume9/vandermaaten08a/vandermaaten08a.pdf.

Vernes, S.C., Oliver, P.L., Spiteri, E., Lockstone, H.E., Puliyadi, R., Taylor, J.M., Ho, J., Mombereau, C., Brewer, A., Lowy, E., Nicod, J., Groszer, M., Baban, D., Sahgal, N., Cazier, J.-B., Ragoussis, J., Davies, K.E., Geschwind, D.H. and Fisher, S.E. (2011). Foxp2 Regulates Gene Networks Implicated in Neurite Outgrowth in the Developing Brain. *PLoS Genetics*, 7(7), p.e1002145. doi:https://doi.org/10.1371/journal.pgen.1002145.

Vidarsson, H., Westergren, R., Heglind, M., Blomqvist, S.R., Breton, S. and Enerbäck, S. (2009). The Forkhead Transcription Factor Foxi1 Is a Master Regulator of Vacuolar H+-ATPase Proton Pump Subunits in the Inner Ear, Kidney and Epididymis. *PLoS ONE*, 4(2), p.e4471. doi:https://doi.org/10.1371/journal.pone.0004471.

Vij, S., Rink, J.C., Ho, H.K., Babu, D., Eitel, M., Narasimhan, V., Tiku, V., Westbrook, J., Schierwater, B. and Roy, S. (2012). Evolutionarily Ancient Association of the FoxJ1 Transcription Factor with the Motile Ciliogenic Program. *PLoS Genetics*, 8(11), p.e1003019. doi:https://doi.org/10.1371/journal.pgen.1003019.

Wagner, D.A., Weinreb, C., Collins, Z.M., Briggs, J.M., Megason, S.G. and Klein, A.M. (2018). Single-cell mapping of gene expression landscapes and lineage in the zebrafish embryo. *Science*, 360(6392), pp.981–987. doi:https://doi.org/10.1126/science.aar4362.

Wakamatsu, Y. and Uchikawa, M. (2021). The many faces of *Sox2* function in neural crest development. *Development, Growth & Differentiation*, 63(1), pp.93–99. doi:https://doi.org/10.1111/dgd.12705.

Wallmeier, J. (2019). De Novo Mutations in FOXJ1 Result in a Motile Ciliopathy with Hydrocephalus and Randomization of Left/Right Body Asymmetry. *The American Journal of Human Genetics*, [online] 105(5), pp.1030–1039. doi:https://doi.org/10.1016/j.ajhg.2019.09.022.

Wang, M., Chen, Z. and Zhang, Y. (2022). CBP/p300 and HDAC activities regulate H3K27 acetylation dynamics and zygotic genome activation in mouse preimplantation embryos. *The EMBO Journal*, [online] 41(22). doi:https://doi.org/10.15252/embj.2022112012.

Wei, L., Yang, C., Tao, W. and Wang, D. (2016). Genome-Wide Identification and Transcriptome-Based Expression Profiling of the Sox Gene Family in the Nile Tilapia (Oreochromis niloticus). *International Journal of Molecular Sciences*, 17(3), p.270. doi:https://doi.org/10.3390/ijms17030270.

Weigel, D., Jürgens, G., Küttner, F., Seifert, E. and Jäckle, H. (1989). The homeotic gene fork head encodes a nuclear protein and is expressed in the terminal regions of the Drosophila embryo. *Cell*, 57(4), pp.645–658. doi:https://doi.org/10.1016/0092-8674(89)90133-5.

White, R.J., Collins, J.E., Sealy, I.M., Wali, N., Dooley, C.M., Digby, Z., Stemple, D.L., Murphy, D.N., Billis, K., Hourlier, T., Füllgrabe, A., Davis, M.P., Enright, A.J. and Busch-Nentwich, E.M. (2017). A high-resolution mRNA expression time course of embryonic development in zebrafish. *eLife*, [online] 6, p.e30860. doi:https://doi.org/10.7554/eLife.30860.

Whyte, W.A., Orlando, D.A., Hnisz, D., Abraham, B.J., Lin, C.Y., Kagey, M.H., Rahl, P.B., Lee, T.I. and Young, R.A. (2013). Master Transcription Factors and Mediator Establish Super-Enhancers at Key Cell Identity Genes. *Cell*, [online] 153(2), pp.307–319. doi:https://doi.org/10.1016/j.cell.2013.03.035.

Wijchers, P.J.E.C., Hoekman, M.F.M., Burbach, J.P.H. and Smidt, M.P. (2005). Cloning and analysis of the murine Foxi2 transcription factor. *Biochimica et biophysica acta*, [online] 1731(2), pp.133–8. doi:https://doi.org/10.1016/j.bbaexp.2005.09.003.

Williams, R.M., Lukoseviciute, M., Sauka-Spengler, T. and Bronner, M.E. (2022). Single-cell atlas of early chick development reveals gradual segregation of neural crest lineage from the neural plate border during neurulation. *eLife*, 11. doi:https://doi.org/10.7554/elife.74464.

Wilhelm, J.E., Vale, R.D. and Hegde, R.S. (2000). Coordinate control of translation and localization of Vg1 mRNA in Xenopus oocytes. *Proceedings of the National Academy of Sciences of the United States of America*, [online] 97(24), pp.13132–7. doi:https://doi.org/10.1073/pnas.97.24.13132.

Wolf, F.A., Angerer, P. and Theis, F.J. (2018). SCANPY: large-scale single-cell gene expression data analysis. *Genome Biology*, 19(1). doi:https://doi.org/10.1186/s13059-017-1382-0.

Wolffe, A.P. (1989). Dominant and specific repression of Xenopus oocyte 5S RNA genes and satellite I DNA by histone H1. *The EMBO Journal*, 8(2), pp.527–537. doi:https://doi.org/10.1002/j.1460-2075.1989.tb03407.x.

Wolock, S.L., Lopez, R. and Klein, A.M. (2019). Scrublet: Computational Identification of Cell Doublets in Single-Cell Transcriptomic Data. *Cell Systems*, 8(4), pp.281-291.e9. doi:https://doi.org/10.1016/j.cels.2018.11.005.

Wormington, W.Michael. and Brown, D.D. (1983). Onset of 5 S RNA gene regulation during Xenopus embryogenesis. *Developmental Biology*, 99(1), pp.248–257. doi:https://doi.org/10.1016/0012-1606(83)90273-7.

Wu, K., Fan, D., Zhao, H., Liu, Z., Hou, Z., Tao, W., Yu, G., Yuan, S., Zhu, X., Kang, M., Tian, Y., Chen, Z., Liu, J. and Gao, L. (2023). Dynamics of histone acetylation during human early embryogenesis. *Cell Discovery*, 9(1). doi:https://doi.org/10.1038/s41421-022-00514-y.

Xie, Z., Sokolov, I., Osmala, M., Yue, X., Bower, G., Pett, J.P., Chen, Y., Wang, K., Cavga, A.D., Popov, A., Teichmann, S.A., Morgunova, E., Kvon, E.Z., Yin, Y. and Taipale, J. (2025). DNA-guided transcription factor interactions extend human gene regulatory code. *Nature*. doi:https://doi.org/10.1038/s41586-025-08844-z.

Yan, B., Neilson, K.M., Ranganathan, R., Maynard, T., Streit, A. and Moody, S.A. (2015). Microarray identification of novel genes downstream of Six1, a critical factor in cranial placode, somite, and kidney development. *Developmental dynamics : an official publication of the American Association of Anatomists*, [online] 244(2), pp.181–210. doi:https://doi.org/10.1002/dvdy.24229.

Yan, J., Xu, L., Crawford, G., Wang, Z. and Burgess, S.M. (2005). The Forkhead Transcription Factor Foxl1 Remains Bound to Condensed Mitotic Chromosomes and Stably Remodels Chromatin Structure. *Molecular and Cellular Biology*, 26(1), pp.155–168. doi:https://doi.org/10.1128/mcb.26.1.155-168.2006.

Yanagi, N., Kato, S., Taro Fukazawa and Kubo, T. (2022). Cellular responses in the FGF10-mediated improvement of hindlimb regenerative capacity in *Xenopus laevis* revealed by single-cell transcriptomics. *Development Growth & Differentiation*, [online] 64(6), pp.266–278. doi:https://doi.org/10.1111/dgd.12795.

Yang, M., Xu, F., Liu, J., Que, H., Li, L. and Zhang, G. (2014). Phylogeny of forkhead genes in three spiralians and their expression in Pacific oyster Crassostrea gigas. *Chinese Journal of Oceanology and Limnology*, 32(6), pp.1207–1223. doi:https://doi.org/10.1007/s00343-015-4009-x.

Yang, X., Xie, B., Shen, P., Chen, Y., Li, C., Tan, F., Yang, Y., Yang, Y., Song, R., Mi, P., Liu, Z., Wen, M., Tam, P.P.L., Suo, S. and Jing, N. (2024). Spatiotemporal Regulatory Logics of Mouse Gastrulation. doi:https://doi.org/10.1101/2024.12.22.630012.

York, J.R., Rao, A., Huber, P.B., Schock, E.N., Montequin, A., Rigney, S. and LaBonne, C. (2024). Shared features of blastula and neural crest stem cells evolved at the base of vertebrates. *Nature Ecology & Evolution*, [online] 8(9), pp.1680–1692. doi:https://doi.org/10.1038/s41559-024-02476-8.

Yu, L., Sun, Q., Huang, Z., Bu, G., Yu, Z., Wu, L., Zhang, J., Zhang, X., Zhou, J., Liu, X. and Miao, Y.-L. (2023). Arsenite exposure disturbs maternal-to-zygote transition by attenuating

H3K27ac during mouse preimplantation development. *Environmental Pollution*, [online] 331, p.121856. doi:https://doi.org/10.1016/j.envpol.2023.121856.

Yu, M., Mazor, T., Kang, Z., Huang, H.-T., Kathrein, K.L., Woo, A.J., Chouinard, C.R., Cole, P.A., Akie, T.E., Moran, T., Xie, H., Zacharek, S., Ichiro Taniuchi, Roeder, R.G., Kim, C.F., Zon, L.I., Fraenkel, E. and Cantor, A.B. (2012). Direct Recruitment of Polycomb Repressive Complex 1 to Chromatin by Core Binding Transcription Factors. 45(3), pp.330–343. doi:https://doi.org/10.1016/j.molcel.2011.11.032.

Zenk, F., Loeser, E., Schiavo, R., Kilpert, F., Bogdanović, O. and Iovino, N. (2017). Germ line–inherited H3K27me3 restricts enhancer function during maternal-to-zygotic transition. *Science*, [online] 357(6347), pp.212–216. doi:https://doi.org/10.1126/science.aam5339.

Zhang, B., Wu, X., Zhang, W., Shen, W., Sun, Q., Liu, K., Zhang, Y., Wang, Q., Li, Y., Meng, A. and Xie, W. (2018). Widespread Enhancer Dememorization and Promoter Priming during Parental-to-Zygotic Transition. *Molecular Cell*, [online] 72(4), pp.673-686.e6. doi:https://doi.org/10.1016/j.molcel.2018.10.017.

Zhang, C., Basta, T., Jensen, E.D. and Klymkowsky, M.W. (2003). The β-catenin/VegT-regulated early zygotic gene *Xnr5* is a direct target of SOX3 regulation. *Development*, 130(23), pp.5609–5624. doi:https://doi.org/10.1242/dev.00798.

Zhang, C., Wang, M., Li, Y. and Zhang, Y. (2022). Profiling and functional characterization of maternal mRNA translation during mouse maternal-to-zygotic transition. *Science Advances*, 8(5). doi:https://doi.org/10.1126/sciadv.abj3967.

Zhang, Y., Liu, T., Meyer, C.A., Eeckhoute, J., Johnson, D.S., Bernstein, B.E., Nussbaum, C., Myers, R.M., Brown, M., Li, W. and Liu, X.S. (2008). Model-based Analysis of ChIP-Seq (MACS). *Genome Biology*, [online] 9(9), p.R137. doi:https://doi.org/10.1186/gb-2008-9-9-r137.

Zheng Wen-ling, Angerer, R.C. and Angerer, L.M. (2011). Direct development of neurons within foregut endoderm of sea urchin embryos. *Proceedings of the National Academy of Sciences of the United States of America*, 108(22), pp.9143–9147. doi:https://doi.org/10.1073/pnas.1018513108.

Zhou, B.-R., Feng, H., Huang, F., Zhu, I., Portillo-Ledesma, S., Shi, D., Zaret, K.S., Schlick, T., Landsman, D., Wang, Q. and Bai, Y. (2024). Structural insights into the cooperative nucleosome recognition and chromatin opening by FOXA1 and GATA4. *Molecular Cell*, 84(16), pp.3061-3079.e10. doi:https://doi.org/10.1016/j.molcel.2024.07.016.

Zhou, J.J., Cho, J.S., Han, H., Blitz, I.L., Wang, W. and Cho, K.W.Y. (2023). Histone deacetylase 1 maintains lineage integrity through histone acetylome refinement during early embryogenesis. *eLife*, [online] 12, p.e79380. doi:https://doi.org/10.7554/eLife.79380.